Editors
Michael Cunliffe
Oliver Wurl

Guide to best practices to study the ocean's surface

International Council for Science
SCOR
Scientific Committee on Oceanic Research

PREFACE

Scientific Committee on Oceanic Research (SCOR)

The Scientific Committee on Oceanic Research (SCOR) was founded 1957 by the International Council for Science (ICSU) to develop an interdisciplinary approach to ocean science. SCOR is the leading international non-governmental organisation for the promotion and coordination of international oceanographic activities, with the aim to solve conceptual and methodological problems that hinder marine research.

SCOR activities include the setup and facilitation of scientific working groups, which are formed from small and focused international groups that address specific scientific topics. All SCOR working groups have defined objectives that must be fulfilled within the period of the working group and that deliver significant advancements to the science field.

SCOR Sea Surface Microlayer (SML) Working Group

The SCOR SML working group (WG 141) was approved in October 2012 and is sponsored by SCOR and the National Science Foundation (NSF). The working group includes scientists from various chemical, biological and physical disciplines, and is focused on understanding the governing mechanisms that underlie SML processes, including the role of the SML in the earth system. The SCOR SML working group is comprised of 22 full and associate members from 10 different countries (United Kingdom, Germany, Croatia, Brazil, USA, Malaysia, Sweden, China, Finland, and Canada).

Terms of Reference of the SCOR Sea Surface Microlayer (SML) Working Group;

- Review sampling techniques and provide best practice sampling protocols.
- Create a consensus definition of the SML in terms of physical, chemical and biological perspectives for a better understanding within the ocean science

community, and discuss the SML's role in a changing ocean. This will be delivered as an opinion/position paper in a peer-reviewed journal and will support future international projects concerning the SML and ocean change.

- Initiate sessions on SML research during major meetings to increase the awareness of the importance of the SML within the general ocean science community.
- Summarise and publish the latest advances in microlayer research in a special issue of a peer-reviewed journal, including consolidation of existing sea surface microlayer datasets among different disciplines (chemistry, biology, atmospheric, physics).

Purpose of this guide

This guide is a deliverable of the SCOR SML working group. It reviews the most widely used SML sampling techniques and provides best practice sampling protocols for studying the ocean's surface. This guide is a source of practical knowledge in the sampling and analysis of the ocean's surface that is communicated in a logical manner with step-by-step guidelines. It should help new researchers to implement SML sampling techniques and in situ monitoring into new projects, and to apply them quickly and reliably. The guide includes standard designs and handling of microlayer samplers and other devices, but also includes related sub-surface sampling techniques and the use of subsurface (water column) reference samples. The guide promotes the standardisation of sample collection and the use of descriptive parameters, including standard parameters to describe certain surface condition of the ocean, i.e. meteorology, chemical and biological indicators, and slick conditions.

This guide is available for free download from the National Marine Biological Library website (http://www.mba.ac.uk/NMBL/) from the "Download Occasional Publications of the MBA" section.

Photograph on cover page by M. Shinki (with permission).

Citation

Cunliffe, M & Wurl, O (2014) Guide to best practices to study the ocean's surface. Occasional Publications of the Marine Biological Association of the United Kingdom, Plymouth, UK. 118 pp.

ISSN 0260-2784

CONTENTS

CONTRIBUTORS 7
INTRODUCTION 9
Air-Ocean gas transfer 9
Aerosol formation 10
Neuston ecosystems 10
Marine Pollution 10
Summary of previous sea surface microlayer sampling reviews 11
What is different about this guide? 14

1. SELECTION OF SAMPLING SITES AND SUITABLE SAMPLING PLATFORMS 16
1.1. Selecting and characterising a sampling site 16
1.2. Selection of suitable sampling platforms 17

2. SAMPLING TECHNIQUE: SCREEN SAMPLER 19
2.1. Design and characteristics 19
2.2. Procedures for handling 22
2.2.1. Sampling prerequisites 22
2.2.2. Sampling procedure 23
2.2.3. Cleaning 26
2.2.4. Transport and storage 27
2.3. Advantages and disadvantages 28
2.3.1. Advantages 28
2.3.2. Disadvantages 30

3. SAMPLING TECHNIQUE: GLASS PLATE SAMPLER 32
3.1. Design and characteristics 32
3.2. Procedures for handling 33
3.2.1. Sampling prerequisites 33
3.2.2. Sampling procedure 34
3.2.3. Cleaning 34
3.2.3. Transport and storage 34
3.3. Advantages and disadvantages 35
2.3.1. Advantages 35
2.3.2. Disadvantages 36

4. SAMPLING TECHNIQUE: MEMBRANE SAMPLER 40
4.1. Design and characteristics 40
4.2. Procedures for handling 40
4.3. Advantages and disadvantages 42
4.3.1. Advantages 42
4.3.2. Disadvantages 42

5. AUTONOMOUS SAMPLING DEVICES 44
5.1. Introduction 44
5.2. Autonomous microlayer sampler design criteria 45
5.3. Multi-sensor autonomous microlayer sampler, an example 46
5.4. Deployment and sampling operation 49

6. NEUSTON NET SAMPLING 51
6.1. Introduction 51
6.2. Design and characteristics of neuston nets 52
6.2.1. Surface sampling nets 53
6.2.2. Multiple layer plankton-neuston samplers 54
6.3. Procedure for handling 55
6.4. Advantages and disadvantages 57

7. SUBSURFACE SAMPLING 59
7.1. Introduction 59
7.2. Subsurface sampling strategies 60
7.2.1. Overview of subsurface sampling techniques 60
7.2.2. Prevention of sample contamination 60
7.2.3. Multilayer surface sampling 63
7.3. Hand-dip sampling and pump systems 64
7.3.1. Advantages and disadvantages 67
7.4. Niskin and GO-FLO samplers 69
7.4.1. Advantages and disadvantages 70
7.5. Rosette/carousel sampling devices 72
7.5.1. Advantages and disadvantages 73

8. PHYSICAL AND IN-SITU TECHNIQUES 75
8.1. Meteorological fluxes 75
8.1.1. Techniques 75
8.1.2. Instruments 76
8.1.3. Platforms 78
8.2. Ocean wave characterization 82
8.2.1. Polarimetric ocean wave slope sensing 82
8.2.2. Fixed and linear scanning laser altimeters 84
8.2.3. Marine wave radar (X-Band) 85
8.3. Ocean surface and near-surface characterization 86
8.3.1. Ocean skin temperature 86
8.3.2. Ocean wave breaking characterization 86
8.3.3. Ocean surface thermography 87
8.3.4. Ocean near-surface turbulence 90
8.4. Additional platforms and sensors 93
8.4.1. Saildrone 93
8.4.2. Wave Glider from Liquid Robotics 94
8.4.3. Air-Sea Interaction Profiler (ASIP) 94

9. DESCRIPTIVE INDICATORS FOR SURFACE CONDITIONS 96
9.1. How to describe and differentiate slick conditions 96
9.2. Defining microlayer enrichment 97
9.3. Standardization of descriptive physical, chemical and biological indicators 98
9.4. Reporting metorological data 100

REFERENCES 102

CONTRIBUTORS

Michael Cunliffe Marine Biological Association of the United Kingdom, The Laboratory, Citadel Hill, Plymouth, PL1 2PB, UNITED KINGDOM micnli@mba.ac.uk

Oliver Wurl Institute for Chemistry and Biology of the Marine Environment, Carl-von-Ossietzky University Oldenburg, Emsstrasse 20, 26382 Wilhelmshaven, GERMANY oliver.wurl@uni-oldenburg.de

Anja Engel Biologische Ozeanographie GEOMAR Helmholtz-Zentrum für Ozeanforschung Kiel, Düsternbrooker Weg 20, 24105 Kiel, GERMANY aengel@geomar.de

Sanja Frka Ruđer Bošković Institute, Institute for Marine and Environmental Research, Bijenička c. 54, 10000 Zagreb, CROATIA sanja.frka@irb.hr

William Landing Department of Earth, Ocean, and Atmospheric Science, Florida State University, Tallahassee, Florida 32306-4320, USA wlanding@fsu.edu

Mohd T. Latif School of Environmental and Natural Resource Sciences, Faculty of Science and Technology, Universiti Kebangsaan Malaysia, 43600 Bangi, Selangor MALAYSIA talib@ukm.my

Gui-Peng Yang Key Laboratory of Marine Chemistry Theory and Technology, Ocean University of China, No. 238, Song Ling Road, Qingdao, CHINA gpyang@ouc.edu.cn

Christopher Zappa Lamont-Doherty Earth Observatory, 204E Oceanography, P.O. Box 1000, Palisades, NY 10964-8000, USA zappa@ldeo.columbia.edu

Robert Upstill-Goddard School of Marine Science and Technology, Newcastle University Newcastle upon Tyne, NE1 7RU, UNITED KINGDOM rob.goddard@ncl.ac.uk

Blaženka Gašparović Ruđer Bošković Institute, Institute for Marine and Environmental Research, Bijenička 54, 10000 Zagreb, CROATIA Blazenka.Gasparovic@irb.hr

Anna Lindroos Finnish Environment Institute, Marine Research Centre, Mechelininkatu 34a P.O.Box 140, FI-00251 Helsinki, FINLAND anna.lindroos@utu.fi

Miguel Leal Universidade de aveiro, Centro de estudos do ambiente e do mar Campus Uuniversitario de Santiago, 3810-193 Aveiro, PORTUGAL miguelcleal@gmail.com

Svein Vagle Ocean Sciences Division Institute of Ocean Sciences, 9860 West Saanich Road, Sidney, BC, V8L 4B2, CANADA svein.Vagle@dfo-mpo.gc.ca

Christian Stolle Leibniz-Institute for Baltic Sea Research, Seestrasse 15, 18119 Rostock, GERMANY christian.stolle@io-warnemuende.de

Werner Ekau Leibniz Center for Tropical Marine Ecology, Fahrenheitstr. 6, D-28359 Bremen GERMANY werner.ekau@zmt-bremen.de

Alexander Soloviev Oceanographic Center , Nova Southeastern University , 8000 North Ocean Drive, Dania Beach, FL 33004, USA soloviev@nova.edu

Kristian Laß Institut für Physikalische Chemie, Christian-Albrechts-Universität Kiel, Max-Eyth-Str. 2, 24118 Kiel, GERMANY lass@phc.uni-kiel.de

INTRODUCTION

The sea surface microlayer (SML) is the boundary interface between the atmosphere and ocean, covering 70% of the Earth's surface. Many studies have shown that the SML typically has measurably distinct physical, chemical and biological properties from underlying waters (Cunliffe et al., 2013). Because the SML has a unique position at the interface between the marine environment and the atmosphere, the SML plays a central role in a diverse range of global biogeochemical cycles and climate-related processes. It is not within the scope of this guide to fully review SML processes. Below is a brief summary of selected key topics that highlight the global scale significance of the SML.

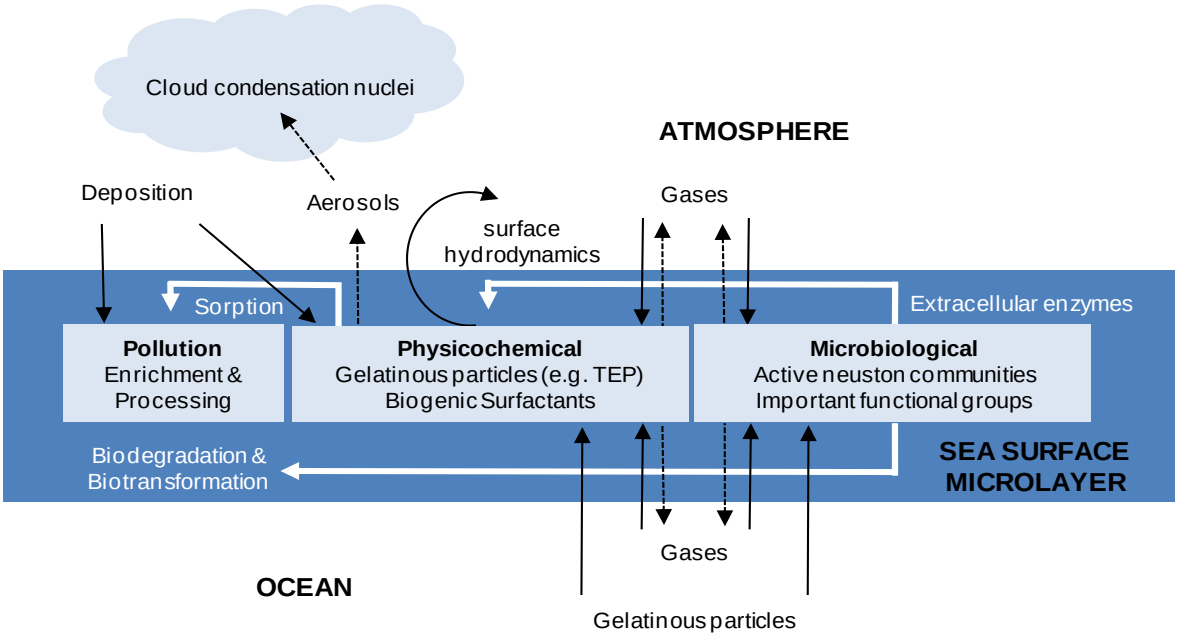

Figure 1: Diagram illustrating some of the key topics that highlight the global scale significance of the SML (modified from Cunliffe et al., 2013).

Air-Ocean gas transfer

The SML modifies the transfer of dissolved gases in seawater to the atmosphere, and atmospheric gases into the ocean (Upstill-Goddard, 2006). Surface active (surfactant) material is a major component that is enriched in the SML, and is dominated by biogenic material, such as polysaccharides (Wurl and Holmes, 2008) and amino acids (Kattner et al., 1983; Kutznetsova et al., 2004). SML surfactants can act as a physical barrier to gas transfer, and modify sea surface hydrodynamics, which subsequently alter turbulent energy transfer (Upstill-Goddard, 2006). Artificial release of surfactant to the SML in the North Atlantic caused up to 55% suppression of gas transfer velocity, even at high wind speeds (Salter et al., 2011).

Biological processes that are active in the SML can also directly modify air-sea gas transfer by changing concentrations of gases, such as methane, in the SML (Cunliffe et al., 2011). The net balance of general community metabolism (i.e. heterotrophy or autotrophy dominating) can control carbon dioxide transfer (Calleja et al., 2005). Specific functional groups within neuston communities, such as methane-oxidising bacteria, may also potentially modify gas transfer rates (Upstill-Goddard et al., 2003).

Aerosol formation

Carbohydrate-enriched particles, including gels, accumulating in the SML can be injected into the marine boundary layer during bubble bursting (Russell et al., 2010). Subsequently, SML derived organics may be an important source of aerosols that lead to the production of cloud condensation nuclei (CCN) (Orellana et al., 2011, Quinn and Bates, 2011).

Neuston ecosystems

The SML is a novel ecosystem, often referred to as the neuston, which can be distinct from those found in underlying waters (Cunliffe and Murrell, 2009). Most research has focused on microbial communities in the neuston, and in particular bacterioneuston communities using molecular-based approaches (Cunliffe et al., 2011). Bacterioneuston communities are equally as complex as bacterioplankton communities, and have many potential functional roles in SML biogeochemical processes, such as air-sea gas transfer, gelatinous particle cycling and pollution degradation (Cunliffe et al., 2013). Neustons also harbour distinct eukaryote communities that can be very dissimilar to those in underlying waters, resulting in different food web structures compared to the plankton (Cunliffe and Murrell, 2010).

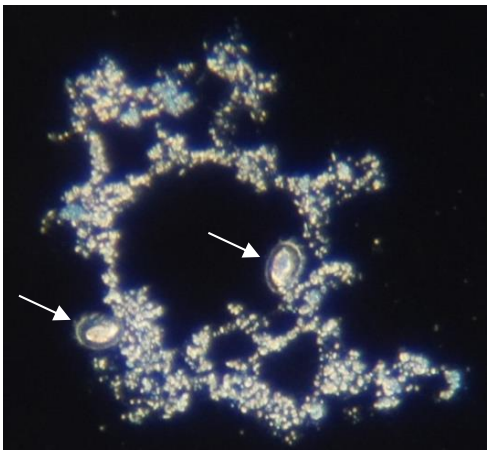

Figure 2: Neustonic ciliates feeding on biogenic aggregates in the SML isolated from coastal UK waters.

Marine Pollution

A diverse range of pollutants are found in the SML that are typically enriched in concentration compared to underlying waters and that can impact upon neuston ecosystems (Wurl and Obbard, 2004). SML pollutant concentrations are generally higher in the coastal zone where they occur via direct inputs, however pollutants can also entire the SML by wet and dry deposition (Cunliffe et al., 2013, Guitart et al., 2007).

Summary of previous sea surface microlayer sampling reviews

The interest to study the sea-surface microlayer (SML) has driven the development of diverse SML sampling techniques, often designed to carry out certain criteria in the applied research field. Sampling techniques that are based on the deployment of either screens, plates or membranes - originally described by Garrett (1965), Harvey and Burzell (1972) and Crow et al. (1975), respectively - have been used and reported most often.

These sampling techniques differ substantially in their operational mode as well as the material used for construction of the sampler. The result is the collection of different SML samples regarding layer thickness and composition (as highlighted in the following chapters and intensively discussed in Garrett and Duce, 1980, Hühnerfuss, 1981a and Hühnerfuss, 1981b). This limits considerably an inter-comparison between studies (Carlson, 1982). Moreover, such comparisons have to account for other factors, such as the depth of the respective bulk water sample (Agogue et al., 2004) and bias introduced by the sampling technique to the parameters of interest (Stolle et al., 2009).

Due to these limitations, many studies aimed to compare the different sampling techniques with respect to their application potential for specific scientific questions. These range, for example, from the retrieval of surface-active monolayers under laboratory conditions (e.g. Kjelleberg et al., 1979) to a characterization of complex biological and chemical SML components in bogs (Estep et al., 1985). Table 1 summarizes these comparative studies, illustrating the diversity of sampling techniques, the measured parameters and the outcome and conclusions drawn.

As can be seen in Table 1, several authors recommend the screen for SML sampling. One main argument is the amount of sample retrieved in a relatively short amount of time, making it favourable for multi-parameter studies (Guitart et al., 2004; Momzikoff et al., 2004). Moreover, it was found to be well suited to broadly characterize suspended particles (Falkowska, 1999b) and organisms of different size classes, i.e. ranging from viruses to phytoplankton (Agogue et al., 2004). Other authors argue for sampling techniques that collect thinner SML samples, such as the glass plate, Teflon sheet or membranes. These suggestions are derived from experiments studying a variety of SML aspects. Examples are retrieval efficiencies of artificial surface films (Hatcher and Parker, 1974a; Kjelleberg et al., 1979; VanVleet and Williams, 1980) or observations of higher enrichments of hydrophobic dissolved material (Momzikoff et al., 2004). Furthermore, investigations of bacterial cell counts (Kjelleberg et al., 1979) or the specificity of bacterioneuston communities (Cunliffe et al., 2009) argued in favour of the “thin-layer” samplers.

Reference	Samplers				Parameters			Conclusions/Suggestions
	Metal Screen	Glass plate	Mem-brane	Other	Biological	Chemical	Physical	
Hatcher & Parker, 1974a	x	x		Drum sampler Tray sampler		Surface-active/ unsoluble lab model substances	Sample thickness	Glass plate is most efficient. *Study has been criticised in Garrett, 1974.*
Daumas et al., 1976	x			Drum sampler	Seston (as pATP)	Proteins, Org. C, Org. N, Carbohydrates, Fatty acids, Alkanes	Sample thickness	Drum shows higher enrichment factors than screen.
Kjelleberg et al., 1979			x (1, 2)	Teflon sheet Teflon plate	Counts of bacteria, yeasts, fungi	Fatty acids, ~ glycerides	Sample thickness	Teflon sheet is recommended.
VanVleet&Williams, 1980	x	x (3)	x (1)	diverse other screens, slides and filters		artificial surface film (carbohydrates, proteins, lipids)		Teflon screen and glass fiber filters not recommended. General sampling efficiency: filters > screens > slides.
Carlson, 1982		x		Nylon screen	Chl.A	DOC, CDOM (UV absorbing material), ATP, POC, PON	Sample thickness	Sample thickness of glass plate depends on environmental conditions - screen does not. Comparison of different sampling methods (=different sample thickness) inadvisable.
Estep et al., 1985	x	x			Chl.A, Phaeo	NO3-, NH4+, NO2-, soluble reactive silica, soluble reactive phosphorous, TN, TP, pATP, pGTP	Sample thickness	"Surface microlayer" of nutrient-rich water considerably more complex than just one monolayer of material
Falkowska, 1999a		x		Polyethylene Screen, Teflon plate			Sample thickness	Layer thickness decreases with wind speed. Chemical properties of surfactants govern effectivity of the Teflon plate. Screen sample thickness varies with temperature. Teflon plate is not suitable for sampling large quantities of water.
Falkowska, 1999b		x		Polyethylene Screen, Teflon plate	Chl.A, Phaeo, algae (counts and community composition)	NO3-, NH4+, CO43-, TP, DOC, POC, ATP	Particle size distribution	Concentrations of dissolved substances depend on layer/sample thickness. Selectivity of every sampling method to specific parameters. No general preference, but screen gives good characterisation of SPM.
Agogue et al., 2004	x	x	x (1, 2)		Bacteria (abundance, activity, community composition), Counts of viruses, protists, Chl. A/B/C, Phaeo			Screen recommended for analysing organisms of different sizes. Membranes show high bias for bacterial cell counts. Caution when comparing literature: this should take the sampling depth of bulk water (i.e. the basis for enrichment factor calculations) into account.
Guitart et al., 2004	x	x		Drum sampler, commercial "slick sampler"		14 polycyclic aromatic hydrocarbons		Screen recommended in terms of volume per time
Momzikoff et al., 2004	x	x		Nylon screen	Chl.A, Phaeo	SPM, POC, DOC, NO3-, NO2-, PO43-, amino acids, carbohydrates, lipids		Metal screen better for multiparametric studies (higher sample volume). Glass plate better for dissolved hydrophobic matter, particulate matter and nutrients
García-Flor et al., 2005	x	x		commercial "slick sampler"		SPM, POC, DOC, polychlorinated biphenyls (PCB)		No significance difference between screen and glass plate. "Slick sampler" is less effective.
Cunliffe et al., 2009	x	x	x (1, 2)		Bacteria (community composition)		Sample thickness	Membrane is recommended for analysing bacterioneuston community (thinnest layer).
Stolle et al., 2009	x	x		Drum sampler	Bacteria (abundance, activity, community composition)		Sample thickness	Need to evaluate potential bias introduced by sampling device for parameters of interest.

Table Legend

1 hydrophilic membrane
2 hydrophobic membrane
3 used glass slide (dimensions 76x25x1 mm)

LITERATURE

Hatcher & Parker, 1974a — Hatcher R.F. and Parker B.C., 1974a. Laboratory comparisons of four surface microlayer samplers. Limnology and Oceanography, 19(1): 162-165.

Garrett, 1974 — Garrett W.D., 1974. Comments on "Laboratory comparisons of four surface microlayer samplers". Limnology and Oceanography, 19(1): 166-167.

Daumas et al., 1976 — Daumas R.A., Laborde P.L., Marty J.C. and Saliot A., 1976. Influence of sampling method on the chemical composition of water surface film. Limnology and Oceanography, 21(2): 319-326.

Kjelleberg et al., 1979 — Kjelleberg S., Stenström T.A. and Odham G., 1979. Comparative study of different hydrophobic devices for sampling lipid surface films and adherent microorganisms. Marine Biology, 53(1): 21-25.

VanVleet&Williams, 1980 — VanVleet&Williams, 1980, Sampling sea surface films: A laboratory evaluation of techniques and collecting materials, Limnol. Oceanogr., 25(4), 764-770

Carlson, 1982 — Carlson D.J., 1982. A field evaluation of plate and screen microlayer sampling techniques. Marine Chemistry, 11(3): 189-208.

Estep et al., 1985 — Estep K.W., Maki J.S., Danos S.C. and Remsen C.C., 1985. The retrieval of material from the surface micro layer with screen and plate samplers and its implications for partitioning of material within the micro layer. Freshwater Biology, 15(1): 15-19.

Falkowska, 1999a — Falkowska L., 1999. Sea surface microlayer: a field evaluation of teflon plate, glass plate and screen sampling techniques. Part 1. Thickness of microlayer samples and relation to wind speed. Oceanologia, 41(2): 211-221.

Falkowska, 1999b — Falkowska L., 1999. Sea surface microlayer: a field evaluation of teflon plate, glass plate and screen sampling techniques. Part 2. Dissolved and suspended matter. Oceanologia, 41(2): 223-240.

Agogue et al., 2004 — Agogue te al., 2004, Comparison of samplers for the biological characterization of the sea surface microlayer, Limnol. Ocean. Methods, 2: 213-225

Guitart et al., 2004 — Guitart et al., 2004, Evaluation of sampling devices for the determination of polycyclic aromatic hydrocarbons in surface microlayer coastal waters, Marine Pollution Bulletin, 48, 961-968

Momzikoff et al., 2004 — Momzikoff A. et al., 2004. Field study of the chemical characterization of the top ocean surface using various samplers. Limnology and Oceanography: Methods, 2: 374-386.

García-Flor et al., 2005 — García-Flor N. et al., 2005. Comparison of sampling devices for the determination of polychlorinated biphenyls in the sea surface microlayer. Marine Environmental Research, 59(3): 255-275.

Cunliffe et al., 2009 — Cunliffe et al., 2009, Comparison and validation of sampling strategies for the molecular microbial analysis of surface microlayers, Aquat. Microb. Ecol., 57: 69-77

Stolle et al., 2009 — Stolle et al., 2009, Bacterial activity in the sea-surface microlayer: in situ investigations in the Baltic Sea and the influence of sampling devices, Aquat. Microb. Ecol., 58: 67-78

ABBREVIATIONS

pATP	particulate Adenosine-triphosphate
pGTP	particulate Guanosine-5'-triphosphate
DOC	dissolved organic carbon
POC	particulate organic carbon
PON	particulate organic nitrogen
Chl.A/B/C	Chlorphyll A/B/C
Phaeo	Phaeophytin A
TN	total nitrogen
TP	total phosphorous
SPM	suspended particulate matter

Overall, Table 1 clearly shows that the question of the most suitable sampling technique cannot be answered easily. Elucidating this challenge, however, is one main prerequisite to standardize future SML research. The following chapters will provide a detailed description of frequently used SML sampling techniques, including their design, the procedure for handling as well as their (dis)advantages.

What is different about this guide?

The different SML sampling devices that are available to study the ocean surface tend to sample different microlayer depths or selectively sample specific microlayer components (e.g. hydrophobic only). In addition, sampling techniques used by individual researchers (e.g. withdraw speed of the glass plate sampler) can also influence the depth of microlayer sample collected. Because the SML is most commonly operationally defined by the sampling device and technique used, variation in sampling procedure can limit the potential for the inter-comparison of data.

- *This guide identifies specific SML sampling devices that could be used by scientists from multiple disciplines, and standardises the sampling techniques for each device. This will improve the potential for data interpretation and the intercomparison between studies.*

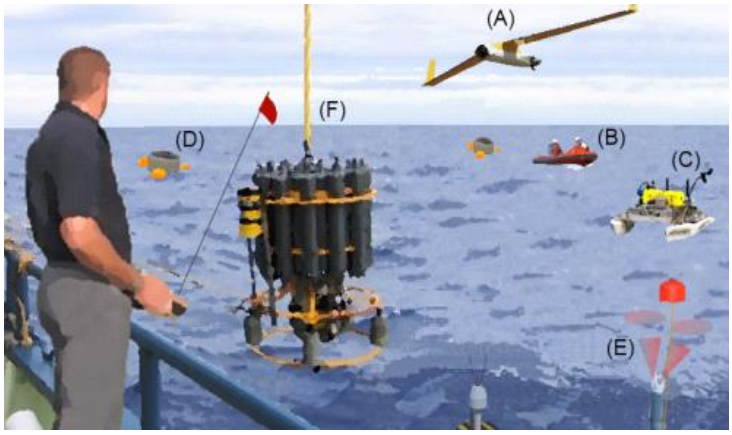

Figure 3: Illustration showing examples of the diverse range of sampling equipment and approaches used to study the surface ocean. Including, unmanned airborne systems (A), small boats for manual sampling using mesh screens and glass plates (B), remote controlled catamaran with surface skimmer (C), free-floating gas exchange chambers (D), sensor arrays (E) and CTD profilers for reference samples.

Interdisciplinary approaches to scientific research are the key to establishing a comprehensive understanding of the marine environment, however such approaches depend upon the legitimate inter-comparison of data from different disciplines and across changing oceanographic systems. To achieve this, there is a requirement for both the improved standardisation of analytical procedures and the widespread use of standard parameters that are routinely measured by all scientists studying the SML.

- *This guide proposes a set of standard parameters that SML scientists should try to quantify, and suggests which analytical procedures to follow.*

1. SELECTION OF SAMPLING SITES AND SUITABLE SAMPLING PLATFORMS

Oliver Wurl and Alexander Soloviev

1.1. Selecting and characterising a sampling site

The sea-surface microlayer (SML) is a highly dynamic and heterogeneous layer with numerous environmental influences. The sampling site should be selected to allow the collection of representative samples. It is very important to describe the sampling site and environmental conditions well to further understand processes on the sea's surface. Many marine and meteorological processes and characteristics of the sea's surface can influence the sampling site as indicated in Table 1.

Table 1: Environmental conditions typically influencing the sampling site

Force	Effects	Observations to be made
Land	Creating wind-sheltered areas, i.e. in bays	Record distance from shore, shape of coastline, sampling position and wind direction.
	Dry deposition of terrestrial material, i.e. dust, pines and leaves	Avoid sampling unless it is related to the scientific question. Record the type of visible material and measure particulate organic carbon (POC) and lignin as a proxy.
	River run-offs	Record river flow rate, season and measurement of terrestrial proxies, i.e. POC and lignin.
Wind	Temporarily disrupts the SML by forcing waves to break	Record wind speed and direction, preferably the wind history (last 6 hours) prior sampling.
Precipitation	Wet deposition of atmospheric material on the SML	Record any precipitation and its intensity in the 24 hours prior to sampling through the local weather service. Precipitation can create slicks (see below).
Solar radiation	Triggers photochemical reactions in the SML	Record UV and light intensities.
Internal waves, gyres and fronts	Physical phenomena creating slicks, e.g. excessive accumulation of a surface-active substance on damp capillary waves	Visual observation of slick coverage. Slicks are easily observed as bright spots or streaks on the sea's surface. Sea-surface temperature (SST) changes rapidly across slicks. For example, mesoscale gyres and fronts can be seen on satellite images of SST.
Primary productivity	Production of surface-active substances susceptible to accumulation in the SML	Measurement of primary productivity, or alternatively chlorophyll-a as a proxy. Pigment or microscopic analysis supports the identification of major primary producers.

The wind is one of the primary factors that determines the enrichment and fate of material in the SML. For example, in the selection of a sampling site, it should be considered that the distribution of the SML and its enrichment may differ significantly between the wind-sheltered and the wind-exposed area of a bay. Wind forces waves to break and temporarily disrupt the SML, but the dispersed SML material may rise to the surface on ascending air bubbles. Dry and wet depositions are other meteorological phenomena influencing the characteristics of the sea's surface. Adding to the complexity, physical and biological processes in the upper ocean affect the sea's surface as outlined in Table 1. The selection of a sampling site requires the consideration of the abovementioned forces in relation to the scientific question. Many of the above forces are relatively easy to measure or record and they could explain some of the variability in observed SML data.

1.2 Selection of suitable sampling platforms

The sea's surface is very susceptible to dynamic changes and contamination caused by sampling platforms and gear. Any artificial disturbance due to sampling should be minimized. For this reason, it is recommended to perform the SML sampling from a smaller boat (i.e. 3 to 7 m in length), a fixed platform or by using an autonomous sampling device (see chapter 5). A boat should move slowly forward while collecting the samples from the bow, and a glass plate sampler (see Chapter 3) works best in this scenario. It is very helpful to have a second person holding the sample container on the hull as shown in Figure 1.

Figure 1: Sampling with a glass plate from a Zodiac boat.

Sampling of completely undisturbed SML is not possible with the available techniques (see chapter 2-6) due to the need of a platform. Best scientific judgement is required to decide if representative samples at a given conditions can be collected. Collection of representative samples is possible from a suitable platform and experienced crew and science team (Carlson, 1983; Kuznetsova et al., 2004; Reinthaler et al., 2008; Wurl et al., 2011a). For example, using a 7 meter rigged-hull boat and experienced crew member artificial disruptions of the SML can be minimized on the leeward side of the boat. If conditions allow, the boat should move slowly into

the wind and ride on the waves. A dip with the glass plate can be performed (chapter 3) while moving from one wave crest to the other, but wiping adhered water from glass plate should be completed before reaching the next crest. Due to time constraints, the glass plate may need to be withdrawn quicker as the standard rate of 5 cm s^{-1} (chapter 3) causing a thicker SML being collected. Recording details on weather condition (chapter 9) and sampling procedure is therefore very important. Sampling should never be performed from the stern of the boat or a moving larger vessel due to unpreventable turbulences and the risk of contamination. Sampling from a platform (pier, jetty or wharf) should be performed from the upcurrent edge or edge to allow ambient water to flow constantly to the sampling site. In this way, interferences, such as contamination from the platform and restricted water flow, are minimized.

2. SAMPLING TECHNIQUE: SCREEN SAMPLER

Blaženka Gašparović, Kristian Laß, Sanja Frka, Anna Reunamo, Gui–Peng Yang and Robert Upstill–Goddard

The screen sampler exploits the surface tension of the water to retain it within the mesh of a wire grid. The first screen sampler was described by Garrett (1965) as a means of rapidly collecting SML samples for chemical analysis. Figure 1a shows the basic mesh screen design, and Figures 1b–1e show some variations on this basic design that are all currently in use.

2.1. Design and characteristics

Garrett's (1965) original model was similar to that shown in Figure 1a. It was a rectangular ASTM[1] MESH 16 screen of 1.4 mm mesh opening constructed from 0.14 mm diameter Monel metal wire; Monel metal is an alloy comprising predominantly nickel and copper, with some iron and other trace elements. The screen had dimensions of 75 x 60 cm, contained 60.2% open space and was held in a rectangular aluminium frame with two 75 cm aluminium handles. The same basic design was adopted by the Intergovernmental Oceanographic Commission (IOC, 1985) as the standard sampling technique for surface films in the context of oil pollution monitoring. This design remains in routine use.

The principle of operation involves lowering the screen through the water surface, either vertically or horizontally and then slowly withdrawing it horizontally (parallel to the water surface). The SML entrapped in the mesh spaces is then drained immediately into a sample bottle, often facilitated by a groove along one side (Figure 1a). The procedure is repeated until the desired volume is obtained. The optimal screen size is often a compromise between the desire to acquire as large a volume of the SML as is possible in a single dip and the force required to compensate surface tension and adhesion forces when lifting the screen. In practice a screen size of about 60 x 80 cm is usually optimal. With Garrett's (1965) original prototype approximately 20 to 30 surface contacts were required to collect a 1 litre SML sample. The typical sampling depth of a mesh screen is 150 to 400 µm (Cunliffe et al., 2013).

In addition to Monel metal, screen materials have included stainless steel, polyethylene and nylon, the choice of material being largely dependent on the proposed downstream analyses. For example, SML samples for trace metal analysis should be sampled with polyethylene or

[1] American Society For Testing and Materials: http://www.astm.org/

nylon screens to preclude sample contamination with metals from the screen or frame. There is also some variability in handle design; for example a single handle, a handle bar, three–point suspension, and a floating frame have all been used. Some investigators have used round wire mesh screens of given mesh sizes, welded or soldered into a round stainless–steel frame (e.g. Laß et al., 2010). Such devices may be manufactured as standard equipment and thus can be bought off–the–shelf, requiring only the attachment of a suitable suspension mechanism (Figures 1d and e). The mounting frames of these devices tend to be rather bulky in comparison to the traditional rectangular screen sampler.

Calculating the thickness of the sampled SML:

The thickness of the SML recovered with a screen sampler depends on screen wire diameter and mesh size and can be calculated from the surface area of the screen and the collected sample volume. At least 20 repeated single dips are recommended for precisely and accurately estimating the sampling volume.

The total open mesh area, A_{To} (mm^2), is given by Eq. 1 for a rectangular screen sampler:

$$A_{To} = \left(\frac{d}{a_o + d_w} \times a_o\right) \times \left(\frac{w}{a_o + d_w} \times a_o\right) \quad (1)$$

where d and w are the length and width of mesh sides (mm), d_w is the wire diameter (mm); a_o is the length of the sides of the mesh opening (mm) ($a_o = \sqrt{A_o}$, where A_0 is open area of an individual mesh square (mm^2)). $\frac{d}{a_o + d_w}$ and $\frac{w}{a_o + d_w}$ represent the total number of mesh squares for the mesh length and width, respectively. A_0 and d_w are supplied by the mesh manufacturer.

The SML thickness (d_{SML}) is then determined from Eq. 2:

$$d_{SML} = \frac{V_{one\ dip}}{A_{To}} \quad (2)$$

where $V_{one\ dip}$ is the volume collected from a single screen deployment.

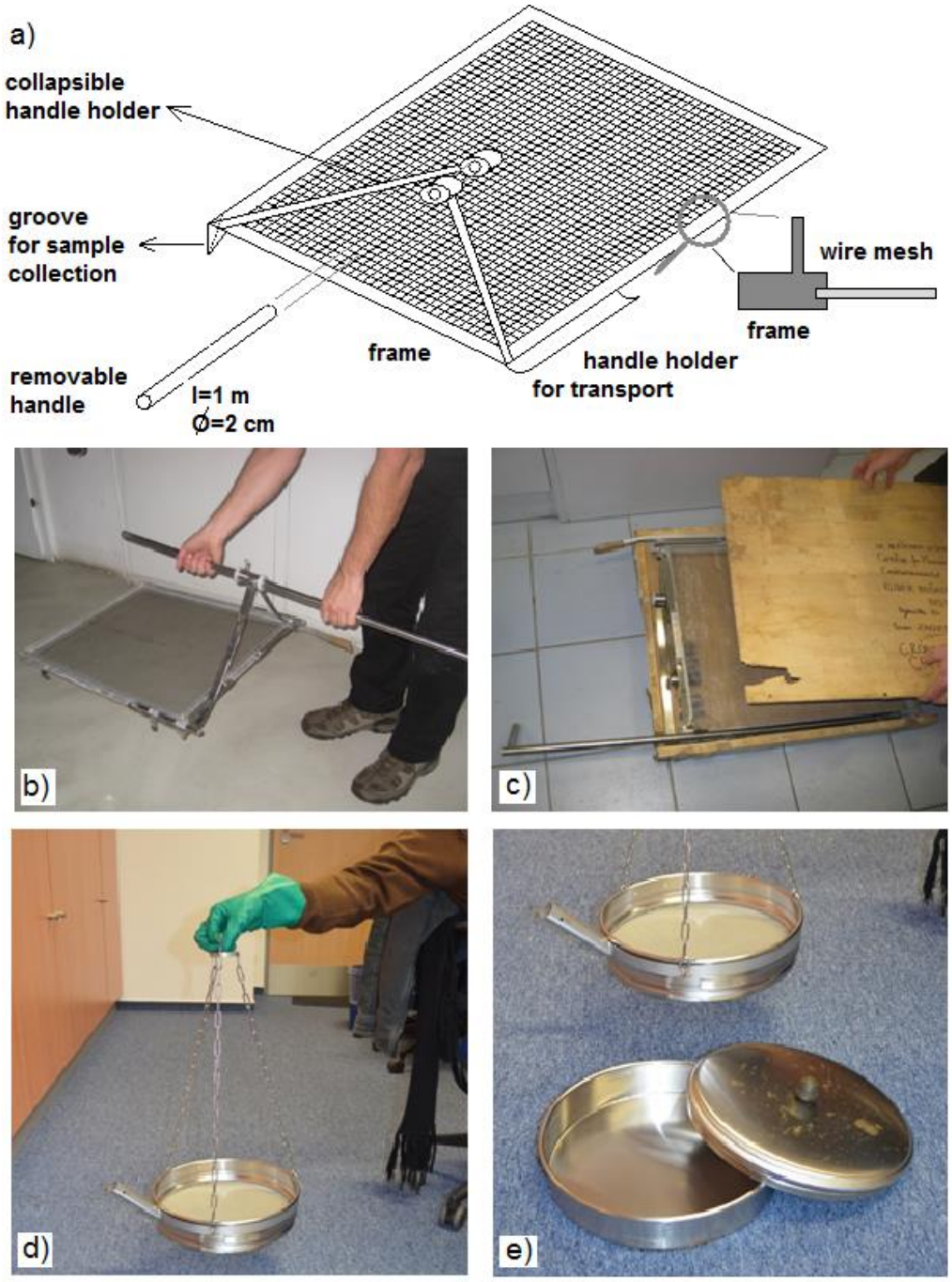

Figure 1: Screen sampling devices. a) Drawing of a typical screen sampler; b) Rectangular screen sampler equipped with a handle for working close to the water surface; c) Rectangular screen sampler in a protective cover for transportation; d) Round screen sampler, factory–welded into a frame (Linker Industrietechnik No. 553055222056, originally manufactured for grain size classification, according to ASTM MESH 16), with lid, bottom and three–point chain suspension. The sampler is operated by rope; e) Round screen sampler and transportation covers.

The mesh screen grid size is chosen in such a way that the surface tension retains a water film between the meshes as long as the screen is kept horizontal. When the screen is tilted the film

is able to run off for collection. Where the mesh size is too large, for example with a 4–mesh screen (opening 4.76 mm), water cannot be effectively trapped and will run out of the sampler before it can be collected in a sample bottle. Where the mesh is too small, for example a 30–mesh screen (0.595 mm), the sampling efficiency is reduced due to the comparatively small fractional area of open mesh. Garrett (1965) established the 16–mesh (1.4 mm) screen as the optimal choice with respect to sampling efficiency.

Table 1 summarises the key properties of a selection of mesh screens used by various investigators. Of note is the variability in SML thickness routinely obtained with these devices, which prompted to underscore the need for a unified sampler specification (Cunliffe et al., 2013), a need that was originally recognised some time earlier in a SML sampling report of the Intergovernmental Oceanographic Commission (IOC) (1985).

Table 1: Key properties of a selection of mesh screens used in the literature.

Reference	Form	Size	Mesh size	Wire diameter (mm)	Material	thickness (µm)
Lechtenfeld et al., 2013	Rectangular	76x60 cm	1.03 mm^2	0.24	Stainless steel	110
Laß et al., 2010	Round on chain	30 cm diameter	16 mesh		Stainless steel	~500
García–Flor et al., 2005a			1000 μm^2		Metal	200–400
Momzikoff et al., 2004	Rectangular	60x80 cm 72x50 cm	1.25 mm^2 100 μm^2	0.36 0.32	Stainless steel Nylon	440 n.a.
Carlson, 1982		900 cm^2	3.32 mm^2 1.19 mm^2	0.40 0.55	Nitex net with PVC frame	222 465
Stadler and Schomaker, 1977	Rectangular with floating body	42x30 cm	0.4 mm^2	0.22	Stainless steel	
Garrett, 1965	Rectangular with handles	75x60 cm	16–mesh	0.14	Monel	150

2.2. Procedures for handling

2.2.1. Sampling prerequisites

Sampling can be carried out from a suitable land–based platform such as a bridge or a jetty, from a small boat or vessel (see Chapter 1). In the case of sampling during a research cruise, it

is important to eliminate as much as is practical, any potential for contamination by the ship's propulsion, exhaust and domestic waste systems. If it is at all possible the IOC (1985) recommends deployment from a small boat away from the mother ship and "upstream" of any such emissions. In this case it is important to also bear in mind the hydrocarbon release potential of small boat engines; switching these off during sampling is also highly recommended. If it is not possible to sample from the ship's bow, using a triangular–shaped sampling frame mounted on a three–point suspension, is recommended (IOC, 1985). Immediately before deployment the integrity and attachment of the screen sampler should be checked. Securing the frame to the sampling platform using a rope is also recommended.

2.2.2. Sampling procedure

Prior to sampling the mesh screen should be rinsed in seawater at the sample site. This will avoid potential contamination from previous samples or during storage. Washing also saturates the sampler surface by adsorbing surfactant material to the metal structure in order to avoid surfactants from the actual sample being (irreversibly) adsorbed to the mesh during sampling. This is achieved by completely submersing the screen for a few seconds prior to removing it and then repeating the procedure several times. This can also be done for any funnels etc. used for draining the screen.

Figure 2 shows examples of the sampling procedure using two different screen configurations. Initially, the screen should be submersed completely in the water at an angle but once submerged it should be kept horizontal. As the action of submersion locally disturbs the SML, the operator should either wait a few seconds before sampling (IOC, 1985) or move the sampler laterally below the water surface to an undisturbed spot. The sampler can be deployed in coastal as well as oceanic stations, depending on the platform available. However, if a small boat is available, it should be preferred. The sampler is raised horizontally through the water surface. During this step, water runs through the wire mesh but the topmost layer (*i.e*. the SML) is retained in it due to surface tension. If using a frame construction that has a tendency to retain some unwanted subsurface water below the wire mesh (standard analysis sieves factory–mounted in stacking frames tend to show this behaviour, e.g. Fig. 1d), the operator should tilt the screen *very* slightly (i.e. only by a few degrees) to allow this subsurface water to run–off, while still maintaining the SML within the wire mesh.

Following recovery and the removal of any unwanted subsurface water as described above, the screen should be immediately tilted in order to collect the SML sample (Fig. 2d and f), either

directly into a clean amber sample bottle or via a suitable funnel (e.g. stainless steel) that has been pre–cleaned and washed in sample as described above for the screen. Samples should ideally be stored cool (~4°C) and in the dark during transport (Schneider–Zapp et al., 2013). Although not routine, for some applications, specialized techniques have been used for removing samples from the screen, such as extraction with organic solvents (Mackie et al., 1974; Stadler and Schomaker, 1977).

The mesh screen facilitates collecting substantial volumes of SML even in relatively high sea states. Approximately 10 to 50 surface contacts (dips) are typically required to collect one liter sample, depending on the mesh size. This volume can be collected in 1 to 2 hours. Sampling requires experience to collect samples with high reproducibility. Knap et al. (1986) reported a relative standard deviation (RSD) of 15% in the collected SML volume among a group of ten scientists using a screen sampler. This resulted in a significant difference in collected SML thickness, mainly due to a non–uniform withdrawal rate.

Chemical and biological samples should be collected simultaneously to provide quantitative data on the variable activities of organisms. This allows distinction between organic compounds derived from living material and ambient extracellular organic matter.

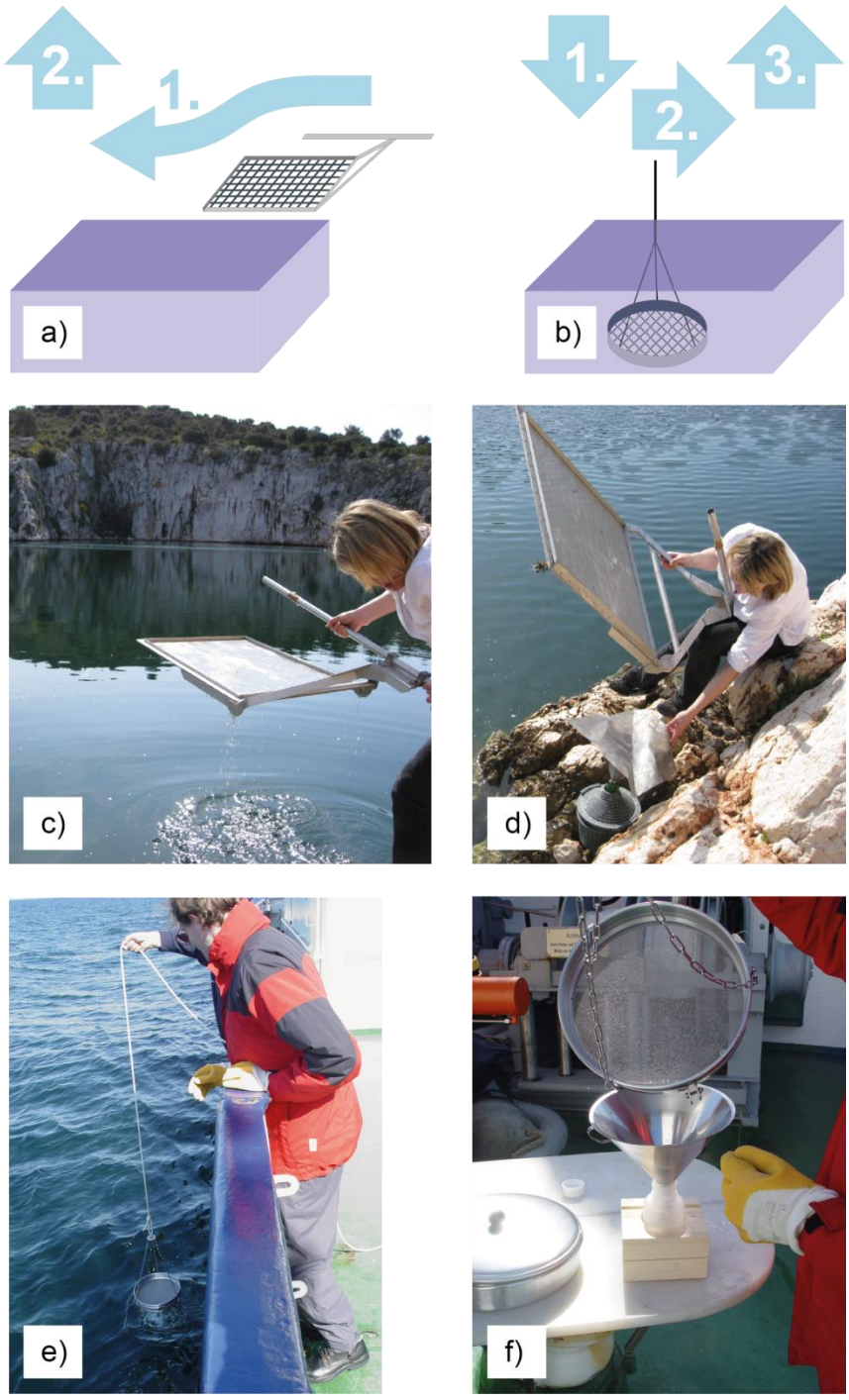

Figure 2: Sampling with a mesh screen: a) sampling using a rectangular sampler with a handle. The sampler is submersed at an angle (1) and raised through the water surface (2); b) sampling with a round suspended sampler. The sampler is submersed (1), moved laterally in order to sample from an undisturbed film (2), and finally drawn through the interface (3). The sampler is finally tilted over a funnel to recover the sample; c) sampling with a rectangular screen sampler; d) collecting a sample from a rectangular screen sampler; e) sampling with a round screen sampler; f) collecting a sample from a round screen sampler.

2.2.3. Cleaning

A screen sampler that is either new or just returned from a workshop most probably has been contaminated by machining or by welding and/or soldering fluids. These sources of contamination must be thoroughly removed prior to use. This usually involves repeated rinsing with organic solvents. The IOC (1985) recommends dichloromethane.

There is no need to use high purity solvents (this can be a cost issue as relatively large amounts are needed), but they should be free from non–volatile components. This can be ensured by the re–distillation of solvent before use in a clean and fat–free distillation apparatus (e. g. rotary evaporator). In any case it should be established that there is no discernable residue after a small sample of the solvent has evaporated.

Cleanliness of the sampler should be checked by rinsing it with high purity water that is free of organic components, especially surface–active material (e.g. Milli–Q water; resistivity typically 18.2 MΩ cm^{-1}; Millipore Corporation, USA). This should be checked for the presence of surface–active material prior to and after cleaning. If surface active material is still present after cleaning the cleaning procedure should be repeated. Finally, the sampler should undergo “routine” cleaning (see below) before use.

Routine cleaning of the screen sampler should take place after use, but also *before* use if the sampler has been stored for a long time or under conditions that risk contamination. If the screen has only been exposed to residues from normal seawater or freshwater (e.g. salt, planktonic material, organic residues) the below procedures should be adequate. If extraordinary contaminants are present, more robust cleaning procedures may be necessary. If, for example, oil spill or tar residues have been sampled, a more thorough cleaning as described above (i.e. “Initial cleaning”) is recommended.

If the screen can fit into a standard laboratory dishwasher, this should be used for standard cleaning. The detergents and cleaning protocols used in such devices (highly basic detergents, high temperatures, cleaning solutions sprayed at high pressure) will readily remove most organic and soluble inorganic contaminants and the final rinsing step, which usually employs de–ionised water, normally is adequate. Care should be taken to fully expose the mesh surface and frame to the dishwasher spraying mechanism. If necessary the sampling mechanism should be dismantled prior to cleaning in order to facilitate this. However, it should be noted that any

aluminium components of the sampler (e. g. serial number plates) may be etched away by the strongly basic cleaning fluids.

If the screen sampler needs to be cleaned by hand (this is often the case for large rectangular screen samplers) and is only slightly or moderately contaminated, a hand–washing detergent for professional use can be employed. “Professional” in this sense means a detergent that is free of additives commonly found in household detergents such as perfumes, lipids added for dermatological reasons, etc. For hard–to–remove residues, more aggressive agents can be used. If a mechanical treatment turns out to be necessary for the removal of ingrained dirt, care should be taken not to deform or damage the wire mesh, which is usually the most sensitive part of the sampler. In general, the sampler should be disassembled before washing, as described above. After wetting the sampler with detergent, the detergent should be washed off using a fast jet of water, which preferably should be warm and clean enough not to leave detectable residues on the sampler. This should be checked as above (“Initial cleaning”). Subsequently, the operator should avoid touching the freshly–cleaned sampler with bare hands. As a final cleaning step, rinsing the sampler with highly purified water (e.g. Milli-Q) is recommended. Again, the water should be applied in the form of a jet. Dipping the sampler into a large water–filled sink or trough for this final cleaning step should be avoided because a surfactant layer often forms on the water surface in such circumstances and this is very difficult to avoid. The sampler will collect this film, as it was designed to do, so leaving it contaminated. Although the initial cleaning phase may be varied somewhat to reflect the nature of any contamination, or availability of facilities, the final steps, i.e. the washing off of detergent and final rinsing are critical and here is where most care should be applied.

2.2.4. Transport and storage

During transport the screen sampler should be protected from mechanical damage and contamination by means of suitable covers or the use of a protective case, as shown in Fig. 1c and e. Any such covers or case should be cleaned to the same standard as the sampler itself, and they should also be cleaned after use.

Prior to storage the screen sampler should be cleaned to preclude corrosion by salt residues. It should be stored in a clean, dry place and be protected from mechanical damage, preferentially in an outer protective box. If the sampler has been stored for a long time, cleaning is recommended to ensure that it is free from dust and dirt that might have accumulated during storage.

2.3. Advantages and disadvantages

2.3.1. Advantages

Screen mesh samplers have important advantages. They can be used at moderate sea states than some other samplers (Falkowska, 1999a, b) and sustaining a surface film across the mesh does not require large surface tension forces; < 1 dyn cm^{-1} is believed to be sufficient (Jarvis, 1967; Jarvis et al., 1967). Considerable effort has focused on the effects of natural SML surfactants collected by mesh screen on surface tension, surface potential, capillary wave damping and surface viscosity, using Langmuir troughs in the laboratory (Jarvis et al., 1967; Barger et al., 1974; Barger and Means, 1985; Bock and Frew, 1993). Such studies have facilitated studying films of accumulated surface active material in a monolayer localized at the air–water interface due to spontaneous delayering of the collected SML in the trough. In this case variable SML "dilution" due to sampler choice is not an issue as the properties of the thin film layer in the trough are closely representative of the true SML. Indeed, hundreds of film samples have shown remarkably similar surface pressure–area isotherms and elasticity coefficients despite the fact that they were collected by various techniques (Barger and Means, 1985; Frew and Nelson, 1992a). The mesh screen is also well suited for studying the adsorption of natural dissolved SML organics onto solid surfaces. A variety of powerful techniques such as electrocapillarity, electrical double–layer capacitance, electrophoresis and ellipsometry have been used in conjunction with mesh screen sampling to study both the progress of adsorption and the nature of the adsorbed layer (Neihof and Loeb, 1972; 1974; Loeb and Neihof, 1975; 1977).

The screen sampler is especially well adapted to multi–parametric studies because of the rapidity with which it can be deployed and the relatively large sample volumes that it can collect relative to some other samplers such as the glass plate (Momzikoff et al., 2004). This is especially important for such SML components as lipids, which typically require a few litres of sample for each analysis. In addition, the ability to collect large water volumes over short time–intervals allows for integrating spatial and temporal variability, thereby making results more representative of the studied area. During sampling, both the composition of the SML and the concentrations of its individual components may change significantly. For example, collection time issues can greatly influence amino acid concentrations and compositions (Kuznetsova et al., 2004). Indeed, it has been shown that SML dissolved free amino acid (DFAA) concentrations can fall to background levels after only a few hours at room temperature, even when incubated in the dark (Kuznetsova and Lee, 2001). The ability of the mesh screen to rapidly collect samples is therefore a distinct advantage. The mesh screen also enables the characterization of

suspended organic matter, although at least some smaller particles may pass through the mesh (Momzikoff et al., 2004). Comparative studies indicated that four out of six of both SML particulate amino acid (PAA) and bacteria and virus–like particle concentrations were lower in rotating drum samples than in mesh screen samples taken at the same locations (Kuznetsova et al., 2004). Sampling the SML for dissolved gases is generally difficult if the air and water are out of equilibrium. Owing to gas volatility, a fraction of any dissolved gas sample is always unavoidably lost during sampling, irrespective of the sampler used. Although Turner and Liss (1985) designed a cryogenic technique to sample SML sulfur gases, they observed no significant difference in dimethylsulfide (DMS) enrichment factors between cryogenically collected and mesh screen collected samples. In addition, it has been shown that mesh screens give much more reproducible results than glass plates when collecting SML samples for DMS; DMS enrichment factors derived from screen–collected samples were essentially constant, whereas those derived from glass plate samples were highly variable depending on SML thickness (Yang et al., 2001). Statistical analysis shows that the variability in mesh screen sampling is very small, which is a clear operational advantage. Guitart et al. (2004) concluded that while both the rotating drum and glass plate samplers gave higher polycyclic aromatic hydrocarbon (PAHs) enrichments than the mesh screen on some occasions, the latter showed no statistical differences in concentrations for all sampling periods and stations. The same authors also detected no significant differences between dissolved phase enrichment factors derived from the glass plate and the mesh screen in samples from Banyuls–sur–Mer (France), probably due to the lower concentration of SML dissolved organic carbon (DOC) in this region (Guitart et al., 2004).

A distinct advantage of the mesh screen sampler is its ability to collect relatively large volumes, which facilitates extensive downstream biological analysis. This makes it amenable to the simultaneous sampling of viruses, bacteria and larger organisms such as flagellates. In the case of bacterioneuston for example, enumeration by flow cytometer, community analysis, colony counting by plating and the detection of functional genes by DNA extraction and amplification are all feasible, at least from a pooled water sample. In this regard it compares favorably with polycarbonate membrane samplers, which although of great value for DNA– based analyses are necessarily limited by the small sample volumes obtained (Lindroos et al., 2011; Cunliffe et al., 2013). An early comparison of SML sampling methods showed the mesh screen to produce the highest enrichment factors for total and culturable bacteria (Tsyban, 1971). Later Agogué et al. (2004) found no significant difference between the mesh screen sampler and the glass plate sampler when measuring the incorporation of thymidine and leucine, in contrast to some earlier

contradictory reports (Albright, 1980, Dietz et al., 1976). Likewise, the mesh screen and glass plate gave comparable results for bacterial community structure; both apparently collected the same dominant bacterial species (Agogué et al., 2004). In contrast the mesh screen performs better than the glass plate with respect to sampling large cells such as diatoms and heterotrophic nanoflagellates; although only a small relative enrichment has been observed for the latter (Agogué et al., 2004). The mesh screen also appears better for the collection of chlorophylls *a*, *b*, and *c*, phaeophytin *a* and photosynthetic nanoeukaryotes, although as a result of cell adsorption to the mesh there may be a potential bias for phaeophytin (Agogué et al., 2004). It has been shown that phytoplankton (chlorophyll *a* and pheophytin *a*) is more efficiently sampled by the mesh screen than by glass plates (Henrichs and Williams, 1985; Agogué et al., 2004).

2.3.2. Disadvantages

The principle disadvantage of the mesh screen sampler is its relatively coarse sampling resolution (typically 150 to 400 µm) relative to both the glass plate and the drum sampler, which leads to an effective dilution of the SML by a factor of six to eight (*i.e*. Yang et al., 2001). Given the work of Zhang et al. (2003) which indicated a "layer of sudden change" in several physico-chemical properties 50±10 µm below the sea surface, such changes would not be resolved. The retention of at least some underlying water on the mesh has the potential to modify/dilute the sampled SML and this should be taken account of as far as is practically possible during sampler construction and deployment. Environmental variables can exert important controls on the thickness of SML samples collected with the mesh screen. Falkowska (1999a) found an inverse relationship between mesh screen SML thickness and water temperature. Increases in wind speed and wave height intensify turbulent mixing and enhance the transfer of organic matter to the SML. Falkowska (1999a) found a direct relationship between wind speed and SML thickness up to a critical wind speed of 8 m s^{-1}, beyond which the thickness of the SML began to decrease. Despite the fact that the mesh screen technique is adequate for studying surface film properties under laboratory conditions in a Langmuir trough, the possibility remains that mechanical collection of the SML may alter the physico-chemical properties of surfactant films naturally occurring at the sea surface. Such surface films may be altered through physical mixing, by the formation of particulate matter and through biological processes.

As a result of its relatively coarse sampling (see above) Guitart et al. (2004) derived lower enrichment factors for dissolved PAHs using a mesh screen than using a glass plate. Conversely, for the particulate phase enrichment factors derived using the mesh screen were

higher than for the glass plate. The collection efficiency of the mesh screen for lipid materials is lower than for Nuclepore or Millipore filters due to a strong preferential adsorption of lipid material onto the screens that can only be removed by rinsing with solvents (Van Vleet and Williams, 1980). Comparisons indicate that a much higher percentage of oleic acid was adsorbed onto the screen than of sucrose, starch, phenylalanine, or albumin. However, two different size stainless steel screens (SS–1: 5×5 cm, 16 mesh, 0.38 mm diameter stainless steel wire, 55% open space and SS–2: 5×5 cm, 16 mesh, 0.38 mm diameter stainless steel wire, 50% open space) did not show significant differences in their collection efficiencies (Van Vleet and Williams, 1980). The efficiency of Garrett's (1965) original Monel metal device for sampling oleic acid monolayers was ~ 75% down to surface film pressures of 10^{-3} N m^{-2} (Garrett,1965). The less than 100% efficiency arises because on the first dip of screen, oleic acid is adsorbed to the screen material. This initial adsorption is thought to deactivate the Monel metal towards further such adsorption, so that on subsequent dipping the screen removes a sample equivalent to its void area. In the case of nitrate and nitrite significantly higher enrichments were derived with the glass plate than the mesh screen, most likely reflecting their upward increasing concentration towards the water surface (Danos et al., 1983; Momzikoff et al., 2004). This enrichment may also reflect a bias arising from interactions with molecules absorbed on the glass plate through mechanisms similar to ion exchange (Kuznetsova and Lee, 2001). In addition, the trend for a higher enrichment of suspended particulate matter in glass plate samples implies that the mesh screen may not be appropriate to study continental inputs, including atmospheric deposition (Momzikoff et al., 2004).

As for physical and chemical measurements, coarse sampling resolution (see above) is an issue for biological sampling. The ability of the mesh screen to effectively sample for organics like ATP, POC and phaeophytin, which are increasingly concentrated towards the air–sea interface (Falkowska, 1999b), is compromised. Estep et al. (1985) and Falkowska (1999b) argued that macroscopic algal filaments can remain trapped on the screen during draining, which may lead to the depletion of algae in the SML relative to the underlying water. Falkowska (1999a) also observed that some phytoplankton cells may transfer from the subsurface to the microlayer during withdrawal of the mesh across the sea surface. A depletion of ciliates may also occur with both the mesh screen and the glass plate. In general larger organisms (e.g. zooplankton) are less likely to attach to the metal screen than to the glass plate (Agogué et al., 2004).

3. SAMPLING TECHNIQUE: GLASS PLATE SAMPLER

William M. Landing, Robert Upstill–Goddard and Christian Stolle

3.1. Design and characteristics

The glass plate sampler was first described by Harvey and Burzell (1972) as a very simple means of efficiently collecting small volume samples of the sea-surface microlayer (SML). Various sizes and designs are currently in use (Fig. 1).

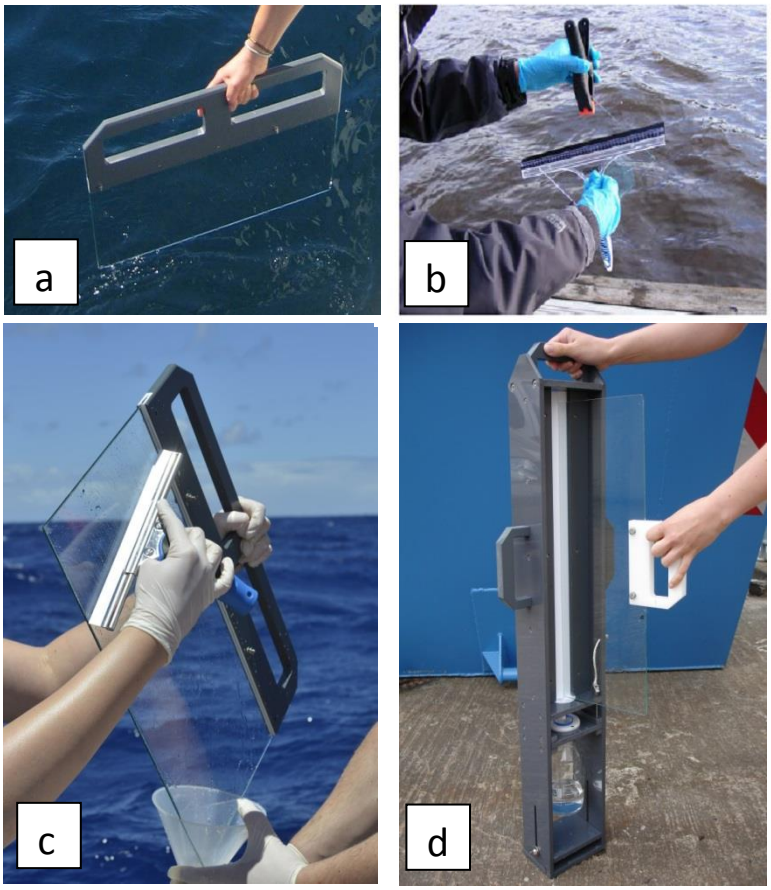

Figure 1: Glass plate samplers. a) glass plate sampler with integral PVC handle showing sample collection (courtesy of Manuela van Pinxteren, TROPOS, Germany). b) squeegeeing a simple plate sampler held with a clean plastic clamp. c) squeegeeing a glass plate sampler using "clean hands/dirty hands" technique (courtesy of Manuela van Pinxteren, TROPOS, Germany). d) a glass plate and sample recovery device containing integral Teflon wiper and funnel, based on the design of Hardy et al. (1985).

The principle of operation is the immersion of a clean, hydrophilic surface (clean glass plate) vertically across, and therefore perpendicular to, the water's surface, followed by its withdrawal at a controlled rate. Harvey and Burzell (1972) originally used a 4 mm thick 20 x 20 cm plate, withdrawn at 20 cm s^{-1}. The SML adheres to the glass plate as it is withdrawn. Typically the uppermost 20–150 μm of the surface is collected (Cunliffe et al., 2013). The sample is then removed from both sides of the plate directly into sampling vials with a non-contaminating wiper such as a neoprene squeegee. The glass plate is held either by hand using clean un-powdered plastic gloves or by a clean plastic, silicone rubber or Teflon clamp (Fig. 1).

For a plate of the original dimensions specified by Harvey and Burzell (1972) the resulting sample volume is therefore ~ 3-12 cm^3 per deployment. The sampled SML thickness *h* (μm) is given by:

$$h = 10^4 * V / (A*N)$$

where V is the sample volume (cm^3), A is the immersed plate area (total of both sides; cm^2) and N is the number of dips per sample.

3.2. Procedures for handling

3.2.1. Sampling prerequisites

While not specific to the use of a glass plate, collecting microlayer samples without contamination requires the sampling conditions to be carefully monitored and rigorous cleaning and handling protocols to be observed. Thorough cleaning prior to use is always necessary to minimize contamination (see also section 2.4.1.2.3). SML samples can be readily collected with a glass plate from a suitable land–based platform such as a pontoon or bridge, or from a small boat or inflatable raft. Sampling during a cruise on a large research ship is also possible if a small boat or raft can be deployed for this purpose. In this case it is important to position the small boat as far upwind of the ship as possible and away from the path taken by the ship as it approached the sampling station, in order to avoid any potential surface contamination by the ship's propulsion, exhaust and domestic waste. It is also important to eliminate contamination from the small boat or raft itself. Where an outboard motor is used it is preferable to switch it off and lift it from the water before commencing sample collection in upstream, clean water. If the motor is left running and/or is not readily removable, it is essential to sample upwind of it to avoid exhaust emissions and any potential oil or fuel leaks. In all cases, it is preferable to sample on the upstream side of the boat while moving slowly into clean, undisturbed water.

It is rather difficult to collect thin SML samples with a glass plate at moderate to high sea states because it is hard to control the rate at which the plate is pulled through the surface. Whatever the sampling conditions, it is convenient to have two people working on SML collection at the same time; one person with clean gloves handles the glass plate while an "assistant" holds the receiving bottle in position, changing it between samples as required. This is an example of the "clean hands/dirty hands" approach to trace element sampling, where the person handling the sampler strives to keep their gloves as clean as possible at all times, while the assistant handles supplies and equipment, for which such care is not quite so critical.

3.2.2. Sampling procedure

The plate should be immersed vertically and thus perpendicular to the water surface several times to remove all remaining traces of final cleaning solutions such as ethanol or ultrapure water before final immersion for sampling. For the precise reproduction of sampling depths the plate should be immersed to a fixed depth indicated by a predetermined mark or line on the plate close to its top edge but below where it is held or clamped. Following sample withdrawal at a controlled rate of ~5 cm s^{-1}, excess water should be allowed to drain for ~20 s by holding the plate vertically. The SML adhering to both sides of the plate should then be immediately removed with a non-contaminating wiper such a Teflon wiper or a neoprene squeegee (Figure 1). This procedure should be repeated two or three times without collecting any sample, in order to remove all traces of cleaning solution and/or previous sample from the equipment. After this cleaning procedure, the sample should be wiped directly into sampling vials that are then sealed for subsequent analysis. The number of dips should be recorded for later calculation of sampling SML thickness. Environmental variables including wind speed /sea state and surface water temperature should be routinely logged (see Chapter 1).

3.2.3. Cleaning

Before first use the glass plate should ideally be cleaned by sonication with a surface active cleaner, followed by extensive rinsing in ultrapure water (resistivity ~18.2MΩ*cm), followed by high purity ethanol. Other cleaning procedures reported include treatments with 0.1 mol L^{-1} hydrochloric acid (Reinthaler et al., 2008) or dichlorodimethylsilane (Gever et al., 1996). Finally it should be dried in a clean oven at 60 ^{o}C and stored in sealable clean plastic bag. Between deployments, the glass plate should be placed in a clean plastic bag or box that can be sealed to avoid airborne contamination. In the field the plate should be thoroughly rinsed with more ethanol followed by ultrapure water prior to each deployment.

3.2.4. Transport and storage of SML samples

When sampling from a small boat or raft away from a larger research vessel, delays of several hours between sample collection and subsequent processing may occur. Therefore, as soon as they are collected SML samples should ideally be stored cool and in the dark (for example in an ice-filled, closed cool box) in order to minimize sample degradation (Schneider–Zapp et al., 2013).

3.3. Advantages and disadvantages

3.3.1. Advantages

Glass plate samplers are relatively cheap to make. Moreover, they are simple to operate and each sample is taken relatively quickly. This makes this sampler more suitable to be employed under rougher sea surface conditions. Additionally, the whole sample collected with the glass plate is retrieved during the sampling procedure when the correct wiping technique is used, which is in contrast to samples retrieved from screen samplers, where water remains adhered to the frame. Therefore, glass plate samplers should collect highly reproducible samples with respect to SML thickness when consistent sampling is assured (retrieval speed, drainage time).

Glass plates appear to be selective for dissolved nitrate and nitrite, which may to some extent reflect their upward increasing concentration towards the water surface (Danos et al., 1983; Momzikoff et al., 2004). They also seem well suited to collecting highly hydrophobic dissolved organic matter such as some lipids and amino acids, although selectivity appears to decrease for less hydrophobic components (Momzikoff et al. 2004). Guitart et al. (2004) found that enrichment factors for dissolved PAHs sampled in coastal waters off Barcelona, Spain, were higher when sampled with a glass plate than with a mesh screen during September 2001 (3.4 ± 3.2 vs 1.3 ± 0.5), although results for the preceding March were not significantly different. Small suspended particles have also been shown to be attracted to the plate surface (Estep et al., 1985), with resultant higher enrichment factors than for mesh screens. Glass plates may thus be well suited to the sampling of atmospheric inputs, especially in coastal waters (Momzikoff et al., 2004).

One advantage of the glass plate sampler as compared to the mesh screen is that because it collects a thinner SML sample (i.e. 20-150 μm vs 150-400 μm) it should theoretically give a better representation of the biological composition of the SML. While the glass plate collects relatively small amounts of the SML (due to the thinner layer collected), these volumes are still sufficient to characterize microbial abundance, activity and community composition in the SML (e.g. viruses, bacteria and archaea), especially given the small volumes needed for cell counting and the sensitivity of molecular techniques for analysing community composition or functional genes involved in biogeochemical processing. The suitability of the glass plate for these analyses has been well documented (Agogue et al., 2004; Stolle et al., 2009). Compared to membranes, glass plate samples might still underrepresent bacterioneuston communities (Cunliffe et al., 2009). However, membranes may be biased due to selective adsorption of bacteria, resulting in a potential overestimation of bacterial abundances (Agogue et al., 2004).

Thus, the glass plate allows combinatory analyses of microbial abundance and community composition, from relatively small volume SML samples. Although Agogué et al. (2004) observed substantial variability among replicates for total and culturable bacteria, bacterial production, and cell numbers of *Synechococcus,* photosynthetic picoeukaryotes and nanoeukaryotes, independent of the sampling device used, overall there were no significant differences between the glass plate and mesh screen samplers, indicating that for these parameters at least, the two samplers perform equally well.

3.3.2. Disadvantages

Glass plate samplers are relatively cheap to make and are simple to operate but due to their comparatively small surface area the collection of large sample volumes can be labour intensive and time consuming; it may take up to 45 min to collect a 1 L sample (Guitart et al. 2004). While alternative SML samplers such as the mesh screen can more easily collect larger volume samples for multi-parameter analyses, the primary reason for this is that a thicker SML layer is sampled, thereby diluting the SML to some extent with underlying bulk water and resulting in lower apparent enrichment factors. However, the automation of glass plate sampling has recently been described (Shinki et al., 2012). If widely adopted, such approaches could help to overcome these restrictions. The number of dips and hence the time for sampling larger volumes can be reduced when glass plates with larger areas are used. However, due to the higher weight additional devices such as manually operated winches are needed for larger plates.

Although the glass plate has a better sampling resolution that some other routinely used samplers such as the mesh screen and should therefore give a more representative SML sample, a study by Zhang et al. (2003) indicated a “layer of sudden change” in several physico-chemical properties including pH, surface tension, chlorophyll-a, NO_3^-, PO_4^{3-} ; dissolved organic carbon (DOC) and dimethylsulfide (DMS), 50±10 μm below the sea surface. Clearly, such changes as these are not always resolved adequately with a glass plate. While the collected SML thickness varies with plate withdrawal rate, the ambient wind speed/wave state, and water temperature, any effect from salinity is apparently insignificant. For a constant withdrawal rate of 5-6 cm s^{-1} the mean sampled SML depth increases approximately linearly with wind speed. Carlson (1982) observed an increase from 33 μm under calm conditions to >60 μm at 7.5-8 m s^{-1}, whereas Falkowska (1999a) reported an increase from ~65 μm to > 100 μm for the same conditions. Above wind speeds of 8 m s^{-1} the sampled SML thickness evidently decreases, as also found for the mesh screen (Falkowska, 1999a). Practical considerations may in any case preclude using the glass plate at higher wind speeds than this (Falkowska, 1999a,b). Taking

account of this, Guitart et al. (2004) recommend using the glass plate only at wind speeds below ~5 m s^{-1}. Decreasing sample thickness with increasing temperature has also been reported, at a rate of ~ 1 μm $^{o}C^{-1}$ for low wind speeds up to ~ 7 m s^{-1} (Carlson, 1982), presumably due to decreasing water viscosity. Such changes are close to earlier laboratory predictions (Hatcher and Parker 1974a; Sieburth 1979). By contrast, evidence for the influence of withdrawal rate is more anecdotal. Hatcher and Parker (1974a) used a plate similar to that of Harvey and Burzell (1972) but their slower withdrawal rate (6-7 cm s^{-1} vs 20 cm s^{-1}) gave an SML thickness of ~22 μm, as compared to the 60-100 μm sampled by Harvey and Burzell (1972).

The observed effects of temperature and withdrawal rate are consistent with earlier theory that considers the effects of viscous forces and gravity on the sampling thickness, *h*, during the immersion and withdrawal of a solid plate from solution (Levich, 1962):

$$h = 0.93\ (\gamma v)^{2/3} / \sigma^{1/6}\ (\rho g)^{1/2}$$

where γ is the dynamic fluid viscosity, σ is the surface tension, v is the plate withdrawal rate, ρ is the fluid density, and *g* is the acceleration due to gravity.

The glass plate sampler is comparatively poorly adapted to multi–parametric studies. Even though it can be deployed quite rapidly the relatively small sample volumes obtained put it at a disadvantage to some other samplers such as the mesh screen, which with multiple dips can more rapidly generate large volumes for several analyses (Momzikoff et al., 2004). Even so, as noted above, the thicker SML layer collected with a mesh screen sampler should result in lower apparent enrichment factors due to dilution of the SML with underlying bulk water. Volume restrictions can impact the ability of the glass plate to integrate spatial and temporal variability and they are especially important for components such as lipids, for which analytical volumes may exceed 1 litre. Collection time issues can greatly influence the concentrations and compositions of reactive compound classes such as amino acids (Kuznetsova et al., 2004). Indeed, at room temperature, SML dissolved free amino acid (DFAA) concentrations can fall to background levels after only a few hours, even when incubated in the dark (Kuznetsova and Lee, 2001). The inability of the glass plate to rapidly collect large volume samples may therefore be a marked disadvantage for some SML components. It has also been shown that some phytoplankton products (chlorophyll *a* and pheophytin *a*) are less efficiently sampled by the glass plate than for example the mesh screen (Henrichs and Williams, 1985; Agogué et al., 2004). Although glass plates seem to be selective for dissolved nutrients (see above) it has been

suggested that the observed enrichment factors may include an element of bias arising from interactions with absorbed molecules, presumably via mechanisms similar to ion exchange (Kuznetsova and Lee, 2001). For dissolved gas sampling, which is generally problematic for the SML due to unavoidable degassing, glass plates do not seem to perform particularly well. Yang et al. (2001) showed glass plates to give less reproducible results than mesh screens when collecting SML samples for DMS. Whereas DMS enrichment factors deriving from mesh screens were essentially constant, those obtained with a glass plate were highly variable and dependent on SML thickness.

The glass plate sampler is also not well-suited to collect uncontaminated samples for trace element analyses. With the exception of pure fused silica (quartz glass), all glass contains trace elements at ppb to ppm levels, and leaching of trace elements during sampling is problematic. Ebling and Landing (2014) describe the use of a fused quartz tube in place of the glass plate (Figure 2). Fused silica quartz is used instead of regular glass because the quartz matrix is less contaminated with trace elements than glass, yet it has the same degree of hydrophilicity to collect the microlayer. A quartz glass tube is also physically more robust and less prone to breakage. The tube is ~9 cm in diameter, 50 cm tall, and has a working surface area of ~2,800 cm^2. A polyethylene handle was fitted to the top of the tube, providing for easier handling. Between uses, the tube is stored safely and conveniently in a large plastic graduated cylinder. The tube is dipped vertically and slowly removed through the sea surface the same way one uses a glass plate. After the tube is removed from the water column, it is allowed to drip into a plastic funnel attached to a polyethylene receiving bottle. Each dip of the tube generates ~10-15mL of sample, equivalent to an SML thickness of ~35-50 µm. A portion of the unfiltered SML sample is then vacuum filtered using 0.4 um PCTE filters held in a polycarbonate filtration rig. This device yields uncontaminated SML samples for dissolved and particulate Al, Mn, Fe, Co, Ni, Cu, Zn, Cd, and Pb.

Even though the glass plate collects a thinner SML layer than for example the mesh screen, it can still underrepresent bacterioneuston community composition, for which membrane techniques appear to be superior, when molecular techniques with a strong sensitivity are used (Cunliffe et al., 2009). Paradoxically however, the relatively coarse sampling of the glass plate in this regard can restrict biological characterisation of the SML because of the relatively small sample volumes obtained, similar to the situation for chemical analyses. This could be especially problematic when aiming to study the full size range of neustonic organisms (from viruses to zooplankton). More important in this respect are observations that the glass plate seems

comparatively poorly suited to sample larger cells for determination of e.g. phytoneuston or ciliates (Carlson et al., 1982, Agogué et al., 2004).

Figure 2: Microlayer sampling with a pure fused silica (quartz) glass tube (Ebling and Landing, 2014).

Comparatively few studies have examined potential glass plate sampling bias for microbiological measurements. An early comparison of SML sampling methods showed enrichment factors for total and culturable bacteria to be lower in glass plate than in mesh screen samples (Tsyban 1971). Later however, Agogué et al. (2004) found no significant difference between the two samplers when measuring the abundances of bacteria and viruses. Evidently both techniques retrieved the same dominant bacterial species (Agogué et al., 2004). Even so, the picture for bacterial activity measurements remains unclear (Hatcher and Parker, 1974b; Agogue et al., 2004; Stolle et al., 2009). An inhibition of bacterial activity by the glass plate may arise during sample removal; bacterial activity measurements were found to be sensitive to the wiping technique used (Stolle et al., 2009).

4. SAMPLING TECHNIQUE: MEMBRANE SAMPLER

Alexander Soloviev[1,2] , Bryan Hamilton[1], Cayla Dean[1], and Aurelin Tartar[3]

[1]Nova Southeastern University Oceanographic Center, 8000 North Ocean Drive, Dania Beach, Florida 33004, USA

[2]University of Miami Rosenstiel School of Marine and Atmospheric Science, 4600 Rickenbacker Causeway, Miami, FL 33149, USA

[3]Nova Southeastern University College of Arts and Science, 3301 College Avenue, Fort Lauderdale, Florida 33314, USA

4.1. Design and characteristics

Membrane filters are disposable and have therefore been used by researchers to help minimize potential cross contamination that may take place using other techniques (Cunliffe et al., 2011). Crow et al. (1975) first used sterile Nuclepore membranes to sample bacteria and fungi in coastal surface films by floating these filters directly on the sea surface before retrieval. Membrane filter sampling methods have been updated to collect microbial life more efficiently.

Membrane filters are commonly 47 mm in diameter with different pore sizes, depending on the materials to be collected. Two types are principally used to sample the sea surface microlayer:

- Polycarbonate filters. Hydrophilic and have an estimated sampling depth of 35 to 42 µm (Franklin et al., 2005).
- Polytetrafluoroethylene (PTFE). Hydrophobic and have an estimated sampling depth of 6 µm (Cunliffe et al., 2009).

4.2. Procedures for handling

Before field work takes place, membrane filters should be transported in a sterile container to avoid contamination. Sampling is performed by carefully placing a filter on the sea surface and then retrieving it. Recent studies have allowed the filter to lay on the surface for a few seconds up to a minute before collection (Agogue et al., 2004, Cunliffe et al., 2008). As with other sampling techniques, when sampling on a research vessel, there should be an emphasis on sampling from an area that is not disturbed or contaminated by the vessel. Sampling should take place in front of the bow and away from the ship wake to avoid this disturbance to the microlayer, as seen in Figure 1a (Kurata et al., 2012). While placing a filter directly on the sea surface using forceps may be too close to the vessel, a recent study has used a fishing rod at least 3 m in length to extend filters away from the vessel using fishing line and a sterilized hook (Figure 1b). This procedure resembles the “fly fishing” technique, where instead of a “fly” a polycarbonate filter is attached to the end of the fishing line. The addition of a fishing rod gives

researchers access to a less disturbed area while making retrieval easier as well. Subsurface water samples can be taken in an undisturbed location (for example from 0.2 m depths) using a peristaltic pump and extension mast. Subsurface water should be pumped into a sterile bag. The polycarbonate filters are then soaked in this water for several seconds and placed into sterile bags (Figure 1d). If possible during sampling, video should be taken in order to analyse suspicious results, possibly from accidental contact of the filters with ship structures.

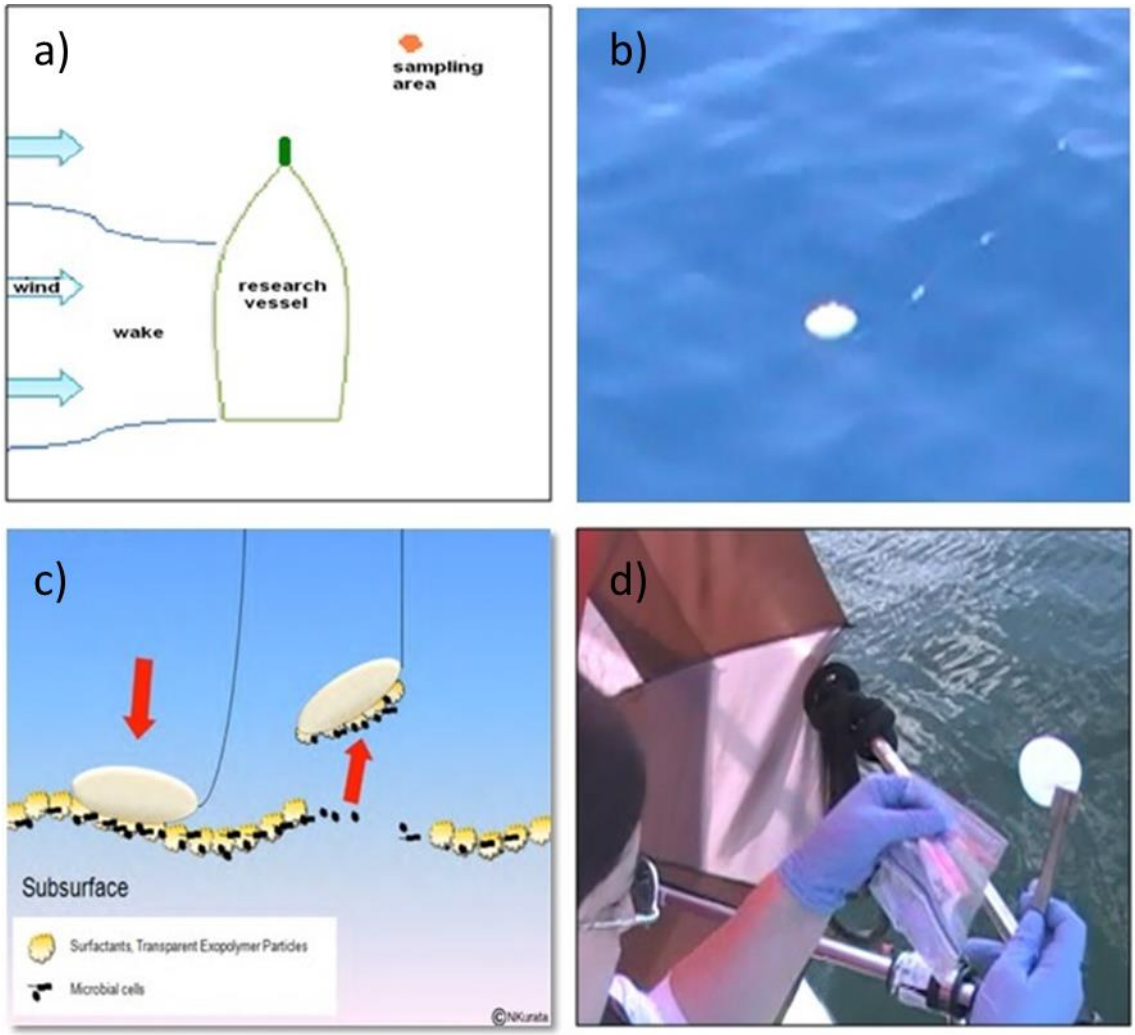

Figure 1: a) Ideal sampling location if on a research vessel. b) To eliminate contamination from the boat, a filter can be attached to hook and line and be extended away from disturbance. c) Image showing a membrane filter picking up materials in the microlayer as it is placed on the water surface. d) Collection of the filter from the fishing hooks using sterile forceps.

4.3. Advantages and disadvantages

4.3.1. Advantages

Membrane filters have a sampling depth range of 6-42 μm (Franklin et al., 2005; Cunliffe et al., 2009). Comparing this range to other sampling techniques, the mesh screen method samples a depth of 150-400 μm and the glass plate technique, also has a larger sampling depth of 20-150 μm (Cunliffe et al., 2009). When using membrane filters, the researcher will get a sample that is only in the sea surface microlayer. Other techniques commonly used potentially collect materials from subsurface waters as well due to their larger depth sampling range. A study by Cunliffe et al. (2009) showed that samples collected by the mesh screen and glass plate method showed a slightly different bacterial makeup than in the comparable membrane filter samples taken at the same location.

Membrane filters are also beneficial in the field due to a minimum of specialized equipment is needed to perform the technique. For other sampling methods, such as the rotating drum technique, heavier equipment is needed to perform the task, which makes sampling and transporting more difficult, especially on a small research vessel. With membrane filters, minimal equipment is needed to deploy and collect each filter, which aids in maneuverability while on the vessel.

Because these filters cannot be reused, preparation and clean up time is minimal compared to other methods. Use of a mesh screen and a glass plate to sample the microlayer requires that each device must be cleaned in between sampling times and locations. If cleaning doesn't occur, contamination issues arise from the previous sample sites. Thorough cleaning must also take place before and after the equipment is used in the field to ensure that contaminants are not building up. This may involve the use of laboratory dishwashers as well as detergents. Using membrane filters avoids these upkeep routines, shortening preparation time as well as the time it takes to sample from area to area during field work.

4.3.2. Disadvantages

The most obvious disadvantage is the sample size that is being obtained per filter at a given sampling site. The surface area of commonly used membrane filters (47 mm diameter) is significantly smaller than the area that other commonly used techniques are able to obtain after one deployment. The small sample size that is obtained can limit the analysis methods only to polymerase chain reaction (PCR) techniques or DNA sequencing (Hamilton et al., 2014).

A recent study has also suggested that there is sampling bias when using membrane filters and that there may be selective surface adsorption taking place, causing the concentration levels of measured parameters to be overestimated (Agogue et al., 2004). However, a more recent study has shown evidence that there is no membrane specific bias regarding bacterial community sampling (Cunliffe et al., 2009).

Weather conditions also play a major role in the efficiency of the sampling procedure. Membrane filters can be fragile in windy conditions, often tearing or flying away before retrieval can take place. High wave conditions affect this sampling technique, making it more difficult to sample the surface without the filter becoming submerged. Rough seas also affect the balance of the researcher on the boat, making it more difficult.

5. AUTONOMOUS SAMPLING DEVICES

Svein Vagle and Oliver Wurl

5.1. Introduction

The need for a better understanding of the role of the microlayer on air-sea exchange processes, has resulted in the search for techniques to be able to study microlayer formation rates and persistence at different wind and wave conditions, film composition and changes to this composition in time and space and spatial patchiness of the microlayer from cm scales to many hundreds of meters. To address these scientific issues the development and use of autonomous and automatic microlayer sampling technologies arise from a number of objectives, including: 1) the desire to reduce potential contamination due to support vessels and platforms, 2) reduce repetitive and tedious tasks, 3) speedup of collection, 4) repeat sampling of fixed stations or tracks, 5) increased spatial coverage, 6) ability to collect microlayer samples in realistic and often higher sea-states, 7) have control over microlayer thickness being sampled, and 8) to allow for sampling of additional enviromental variables and real-time analysis of samples.

The possibility of automating microlayer sampling developed from the suggestion by Harvey in the mid-sixties (Harvey, 1966) of using a rotating hydrophilic cylinder combined with suitable scraper to collect samples. Earlier metal screens and dipping glass disks were rather difficult to automate. In addition, progresses in the field of marine system automation and robotics have led to the development of cost-effective, and small autonomous surface craft for the collection of a whole set of hydrographic, chemical and bathymetric variables, including the microlayer (e.g., Manley, 1997; Manley et al., 2000; Münster et al., 1998; Frew and Nelson, 1999; Caccia et al., 2005). Most autonomous microlayer collection techniques are based on catamarans equipped with a single rotating glass drum for collection of the microlayer (Cincinelli et al, 2001). A more recent design replaces the rotating glass drum with a set of rotating disks (see below) to allow for operation in higher sea-states (Shinki et al. 2012). Also the development of such systems have become more interdisciplinary in nature, concerning both the comprehension of biogeochemical-physical interactions between ocean and atmosphere, and their relations to climatic and environmental change, and the development of the autonomous surface vessels themselves (Stortini et al., 2002).

5.2. Autonomous microlayer sampler design criteria

The choice of sampling method as well as size and complexity of a particular autonomous sampler used will depend on the scientific objectives of a given study. The design criteria for a suitable sampler are:

Environment: The physical environment where the sampler will be used will determine the type of craft, the size of the craft, and the sampling approach being used. For example, a rotating glass disk sampler will be able to operate in larger waves than a glass drum sampler. There will be differences depending on whether the vessel will be used in a harbor environment or for open ocean sampling.

Vessel hull: Decisions will have to be made with regards to the type of vessel shape and size to use. e.g. catamaran, pontoon-boat, single hull. This decision will again depend on the environment in which the sampler will be used, payload, duration of missions etc.

Propulsion: The project objectives will decide whether the sampler will be propelled or operated in one location only, as a passive drifter. If propulsion is required, there will be questions related to the choice of propulsion system. Using combustion engines is possible. However, oils and soot from such engines may contaminate the waters being sampled. Electric motor or motors is normally preferable because of their clean operation. Some sort of sail power is also a possibility. Will there be a single motor or more than one? Two motors can be used to steer the vessel. However, the power consumption is greater. Propellers versus fans are also a decision that has to be made. The size of motor(s) will depend on the size of the vessel and the desirable cruising speed and what sort of currents expected.

Vessel steering: How will the direction of the sampler be controllable while moving through the water? Options include using one or several rudders, turnable outboard motors, jets used to change direction, or the use of two motors that can be controlled separately. Does the vessel need to be able to keep its position against the influence of wind and currents? What sort of turning radius is expected?

Power supply: Assuming electrical propulsion is being used batteries will be needed onboard the sampler. Electrical power is also required to operate the chosen microlayer sampling device (e.g, glass drum or glass disks) and any additional sensors and pumps on the vessel, including radio communication and GPS. The size of batteries required primarily depends on size of propulsion motors and expected mission range and duration. Solar panels can be added to the sampler to increase the duration or reduce batteries required.

Sensors for navigation: Normally a GPS receiver is used onboard the sampler to give the position and for navigation. Additional possible navigation sensors include laser range, radar, and radar transponder. The latter sensors can be used for obstacle avoidance if the sampler is operating in autonomous mode.

Communication: Typically the microlayer sampler will use two-way radio communication with an operator some distance away or to send information about position, speed, microlayer withdrawal speed, battery voltage etc. to the same operator or to a database ashore.

Onboard sensors: In addition to the microlayer skimming device (e.g., glass drum or glass disks), the sampler can be equipped with a number of additional devices and sensors. In the example described below, the sampler has an additional *in-situ* Ocean Optics spectrometer, as well as a small weather station and a small strut with fluorometers, thermistors, acoustic doppler current profiler, and an oxygen sensor. This specific device also has the option of collecting up to 12 separate samples of both microlayer and bulk water.

*Sampling strategy**:*** What is the operating mode of the sampler? Will the vessel be steered remotely by an operator within visual or radio range, or be programmed to steer along a track defined by a number of GPS waypoints? If the latter, will the sampler be able to avoid obstacles in its path? With onboard sampling capabilities, when will the different samples be collected? What microlayer thickness needs to be sampled? Studies of a glass-plate sampler show that the thickness being sampled is dependent on the rotational speed of the glass disks (Shinki et al. 2012). Therefore it is highly desirable that this speed is controllable on the sampler.

5.3. Multi-sensor autonomous microlayer sampler, an example

As part of the Radiance in a Dynamic Ocean (RaDyO) program (Dickey et al. 2011), which had as one of its primary goals to study the problem of underwater visibility and imaging of objects across the air-sea interface, it became apparent that being able to define the microlayer and its temporal and spatial patchiness was important to reaching the objectives of this project. The criteria for a suitable sampler for this project included: 1) The sampler should be capable of sample the microlayer from a range of layer thicknesses between 40 and 80 μm to allow for studies of the layer of sudden physical and chemical change; 2) the sampler should permit quick collection of samples and be automated to allow for up to 12 microlayer and corresponding bulk water (water from approximately 1 m depth) samples at times and locations decided by the

operator of the sampler; 3) the sampler should be autonomous and remotely controllable at ranges up to about 1000 m; 4) the sampler should be able to operate at speeds up to 1 ms^{-1} for missions lasting as long as 1 hour; 5) the sampler should be able to continue operating in open ocean conditions at wind speeds as high as 10 ms^{-1}; 6) the sampler being small enough to allow easy handling from smaller research vessels; 7) be able to be platform for additional integrated sensors, both above and below the air-sea interface.

The resulting microlayer sampler consists of two 1.5 m long by 0.5 m wide, by 0.5 m deep fiberglass hulls connected by an aluminum frame on which propulsion, scientific sensors, control electronics, and a computer are mounted in weather proof housings (Figure 1a,b).

Figure 1: a) Photograph of the radio controlled vessel with rotating disk microlayer sampler and b) R/V Kilo Moana and the microlayer sampler off Santa Barbara, California (courtesy of Masaya Shinki).

The sampler has an onboard computer running a Windows operating system allowing it to execute pre-programmed missions autonomously. A built-in wireless serial connection allows routines to be overridden so that the sampler can be controlled from shore or a research vessel with a range of up to 3 km. The vehicle is propelled by two 12V DC motors and powered by two 12V rechargeable gel cell batteries located in the fiberglass hulls. In its present configuration, these batteries give the vessel a range of approximately 4 km at a maximum speed of 1 m s^{-1}. The sampler is equipped with a set of 10 thin (0.3 cm) glass disks, separated by 5 cm (which is large compared with the thickness of individual disks, minimizing disk-disk interference), for collecting microlayer samples, a GPS receiver (Garmin GPS18), and a fluorescence spectrometer (Ocean Optics USB2000) for real-time spectral analysis. There is also a small weather station (Davis, VantagePro 2) to measure wind speed, wind direction, and air-

temperature. The glass disks are mounted on an axis parallel to the water surface and perpendicular to the direction of travel. To allow for unobstructed access to clean water the module is mounted in front between the hulls. Tests have shown that because of the reduced surface area the sampler can work efficiently even in higher sea states with minimal disruption of the water surface. A stepper motor (VEXTA by Oriental Motor) placed above rotates the disks at a constant speed controllable by the onboard computer and is set to a specified nominal adsorbed layer thickness based on laboratory experiments (Shinki et al. 2012). The microlayer water that adheres to the disks is removed by a set of Teflon wipers mounted on the descending side of the disks. A total of nine wipers are used, each mounted between two adjacent glass disks. Each wiper consists of a piece of Teflon sheet threaded through an aluminum tube. The sheet protrudes on both sides of the tube, thus wiping two disks simultaneously. The slit in the aluminum tube is wide enough to allow microlayer water flowing down the sheet to enter into the tube. Once inside the tube the sample water flows toward an aluminum manifold, which collects the water. From this manifold, the microlayer samples are directed to a 12 mm ID Teflon tube and pumped through the fluorescence spectrometer to a bottle tray. The bottle tray consists of a set of sixteen 250 mL bottles located on a carousel (Figure 2). The bottles are filled in pairs where one bottle is filled with microlayer water collected by the rotating glass disks, while the second bottle is filled by reference bulk water collected through a Teflon tube from a depth of 0.5 m below the vehicle. The start-time of each fill and the duration of filling are user controllable or can be programmed in advance for fixed interval sampling.

Figure 2: Photograph of sample bottles in the programmable rotating carousel. This carousel can accommodate up to 16 sample bottles, eight of which (interior ones) collect microlayer samples from the glass disk array, while the other eight (exterior ones) collect sublayer water from 0.5 m below the surface. The start time of filling and the filling time are independently programmable for each of the eight bottle pairs.

The sampler also is equipped with a 1.8 m long removable leg mounted vertically below for deployment of additional sensors being logged either by the onboard computer or internally to each instrument (Figure 3). During different studies, the sampler leg has been equipped with an array of Wetlabs single angle scattering meters (Wetlabs ECO BB and ECO Triplet B), an array

of thermistors (RBR TR1050) and a dissolved oxygen sensor (JFE Advantech Co. Ltd. RINKO III). The sampler is also capable of carrying a downward pointing 1.2 MHz RDI Acoustic Doppler Current Profiler (ADCP).

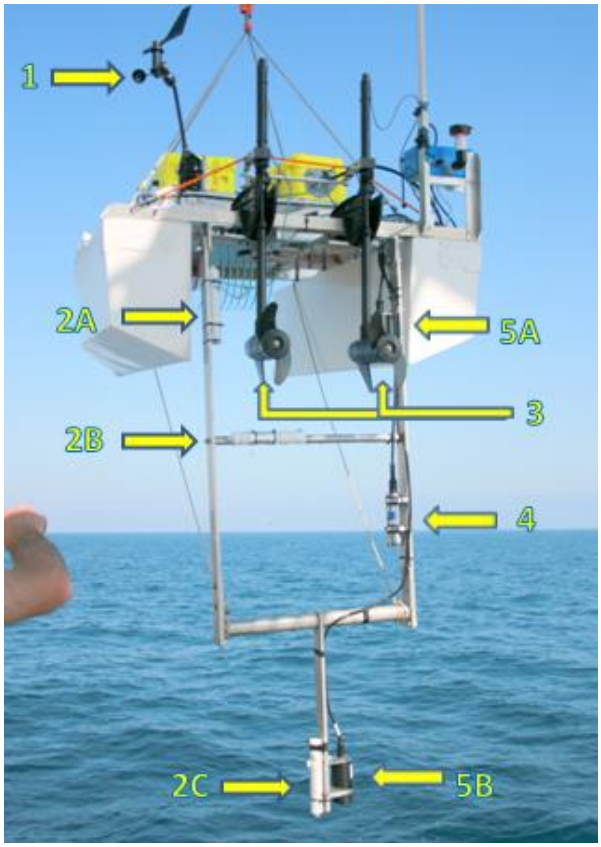

Figure 3: The microlayer sampling vessel in air showing additional sensors on the 1.8 m long instrumented leg deployable from the stern of the vessel. Identifiable components and sensors include: 1) a weather station (Davis instrument Vantage Pro 2), 2A-C) three thermistors (RBR TR1050) , 3) the two 12V independently controllable-DC motors, 4) an optode oxygen sensor (JFE Advantech Co. Ltd. RINKO III), and 5A-B) two Wetlabs optical scattering sensors (Wetlabs ECO BB and ECO Triplet B).

The near-surface temperature field was measured by an array of internally recording temperature loggers (RBR, TR-1050). The skimmer is also designed to carry a downward looking 1.2 MHz Acoustic Doppler Current Profiler (ADCP) (RDI/Teledyne) for upper ocean backscatter measurements and current profiling. The measured microlayer characteristics are related to the optical backscatter, O_2 and temperature measurements with the aid of the flow field observations from the ADCP.

5.4. Deployment and sampling operation

As described above, autonomous microlayer samplers are often one-of-a-kind designs and, therefore, operation and handling will vary somewhat for each vessel. We can therefore only provide some general recommendations with regards to the handling and operation of such samplers. Depending on the technical complexity, a checklist can be used to ensure all systems and sensor packages are working as expected prior to launch. This is especially important when

deploying from a larger vessel because launches and recoveries are often time-consuming and manpower expensive. Also, trouble-shooting from a small boat alongside the sampler is tedious and difficult even in calm seas. From larger vessels, microlayer samplers can be launched with a crane or using an A-frame, depending on the situation and the available equipment. A small boat should be deployed before launching the sampler to tow it away from the mother ship. In sheltered coastal waters, launching and recovery have also been found to be practical from a small landing craft workboat by lowering the ramp (Wurl et al. 2005).

After launch and prior to the actual microlayer/bulk-water sampling the the rotation speed of the glass disks or the glass drum is set to about 8–10 rpm to be consistent with the withdrawal rates of glass plate sampling, or to a speed that gives the desired layer thickness.. Prior to making the actual sample collections, the glass disks or drum should run for about 10 minutes to condition all materials in contact with seawater. During this conditioning the support vessel(s) should be a distance down stream away from the sampler. Binoculars are helpful for observing the operation of the sampler and controlling navigation.

During the actual sampling operation, the water surface should be observed for the appearance of slicks and/or bands of accumulated debris, waste, and oil. This is particularly important in coastal waters. Water sampling while crossing slicks and bands may result in poor representative samples, or provide useful data depending on the scientific objectives of any specific mission. Following the sampling mission, especially if the sampler was in salt water, the vessel and all the components should be rinsed carefully with clean fresh water to avoid salt buildup and clogging of tubes, bearings, and axels.

6. NEUSTON NET SAMPLING

Werner Ekau and Miguel Leal

6.1. Introduction

The early definition of neuston by Naumann (1917) distinguishes between phyto- and zooneuston but reduces the term to the very small organisms directly attached to the surface layer. Neuston nowadays comprises the whole living community closely related and restricted to this thin surface layer (Hempel and Weikert, 1972; Zaitsev, 1997) and covers the whole range of sizes and organism classes from bacteria to metazoa. Phytoneuston mainly consists of diatoms and dinoflagellates and is concentrated in the upper 1 mm at the sea surface layer (Wang et al., 2014). Sampling methods are described in chapters 2 and 3.

Extensive definitions of zooneuston are given e.g. by Zaitsev (1971, 1997). Hardy (1997) classified the neuston into size groups related to different strata of the surface layer. The nanolayer (< 10^{-6} m) and surface microlayer (< 10^{-3} m) are sampled with prisms and screens, membrane filters (chapter 4), glass plates (chapter 3), and the rotating drum technique (chapter 5). Millilayer (<10^{-2} m) and centilayer (<10^{-1} m) are collected using pumps and/or nets. Accordingly he classified the neuston organisms based on their size as piconeuston (< 2 µm), nano/microneuston (2–200 µm), mesoneuston (200 µm–20 mm), and macroneuston (> 20 mm). He also suggested the term macroneuston to be used for large neuston organisms formerly called pleuston, which includes e.g. siphonophores that expose their bodies to the air. These surface dwelling larger species are a kind of exception in the size distribution as shown in Figure 1. The sketch from Hardy (1997) shows an increase in size of organisms with depth. While bacteria and unicellular algae dominate the upper micrometers, larger organisms such as crustaceans or fish eggs and larvae occupy the upper millimeters down to a depth of about five centimeters. Even if winds create turbulences and mix the upper cm or meters up, organisms move back into the microlayer within short times (Champalbert, 1977).

For larger organisms such as phyto- or zooplankton species the layer is important for different reasons. The spectral composition and intensity of light is still similar to sunlight. Inputs of nutrients and micronutrients from the air are enhancing primary production in this shallow layer providing food especially for small organisms. Hardy and Apts (1984) found enrichment ratios (microlayer:bulk water concentrations) for bacteria, microalgae, chlorophyll pigments and photosynthesis of 2444, 380, 12 and 40, respectively.

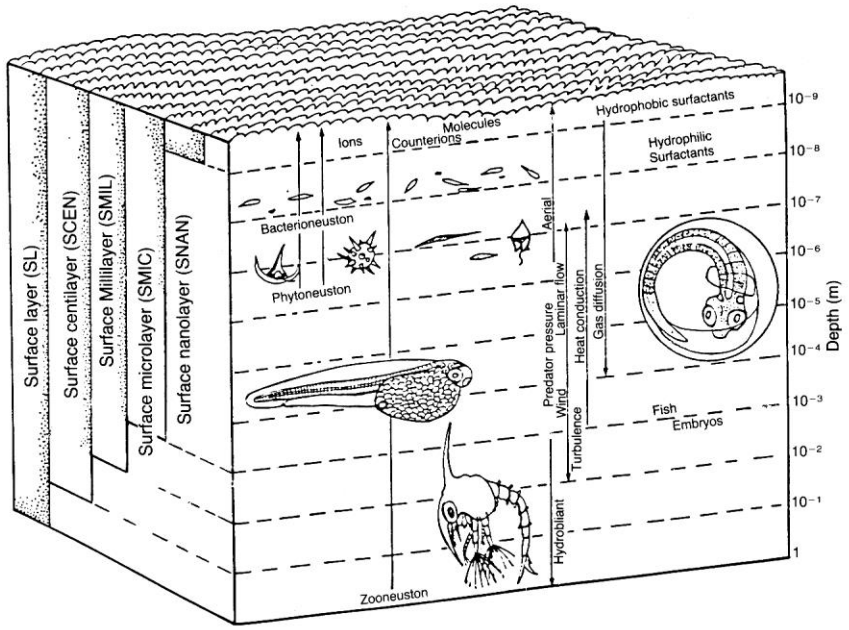

Conceptual model of the sea-surface layer (from Hardy 1997)

Figure 1: A conceptual model of the distribution of organisms in the upper 1 meter of water column (from Hardy 1997).

Above, or better directly on the surface, in the epineuston, many insect species are found. Zaitsev (1997) reports more than 40 species of water striders (Halobates) and some diptera (Clunio marinus and C. ponticus) and springtails (Collembola spp.). Besides these euepineuston species many land-born organisms can be found, that are able to survive substantial time on the sea surface (Ashmole, 1988). Euhyponeuston are those organisms that spend their entire life time in the hyponeuston, the upper 5 cm of the water column, respectively (Zaitsev, 1962, 1964, 1997). It contains a large variety of different taxa (Doyle et al., 1994) specially adapted to this extreme environment and benefiting from the food available near the surface such as mollusks (*Janthina, Glaucus*), copepods (*Pontellidae*), isopods (*Idothea*), decapods (*Planes and Portunus portunus*) (Flores et al., 2002), and fishes.

6.2. Design and characteristics of neuston nets

Design and use of sampling gears for neuston organisms depends strictly on the organism and layers targeted. As shown in Figure 1, meso- and macro neuston such as copepods, fish larvae and eggs occur in a layer of up to 5 cm (hyponeuston). Neuston sampling thus aims to separate this very thin layer from waters below and is usually performed with special nets equipped with floating elements to keep the devices at the surface. Neuston nets are normally non opening/closing designs (see also Wiebe and Benfield, 2003).

The first systematic design of a neuston net and sampling of meso- and macroneuston organisms is going back to Zaitsev and his work in the Black Sea in the 1950s and 1960s (Zaitsev, 1959, 1971). Single and multiple net devices have been developed over time as shown in Figure 2.

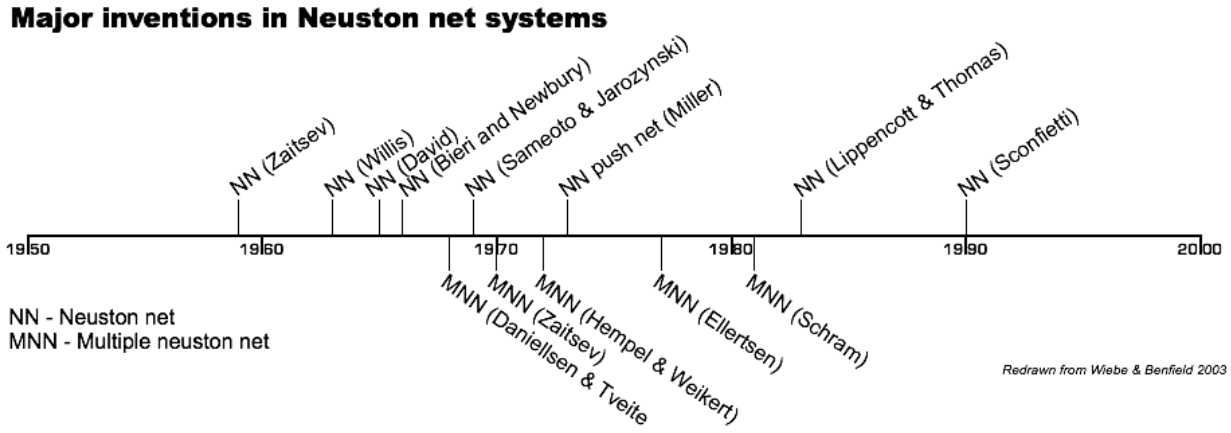

Figure 2: Some milestones in neuston net development as reviewed by Wiebe and Benfield (2003).

6.2.1. Surface sampling nets

First attempts to sample neuston (Figure 3) were performed by means of simple net constructions with small floating elements mounted aside and towed in a way to cut the surface (e.g. Zaitsev, 1959, 1971).

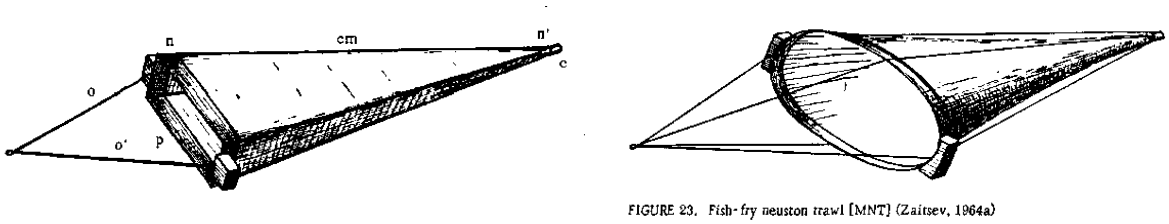

Figure 3: First neuston nets (a, b). b) special version designed for fish-fry (from Zaitsev 1971).

David (1965) constructed a wooden catamaran where he mounted a horizontal net frame in the back between the two floating elements (Figure 4a). Opening of the frame was 30 cm x 15 cm with a net of 365 cm in length. Leal et al. (2009, 2010) used a similar model to sample neuston zooplankton and fish larvae with a mouth size of 100 cm x 20 cm (Figure 4b).

Figure 4: Neuston net mounted in front of the floating elements (picture a) adapted from Bieri and Newbury, 1966; picture b) by Miguel Leal).

6.2.2. Multiple layer plankton-neuston samplers

Zaitsev modified his construction into a multi-layer plankton-neuston net by mounting several of these nets top of each other (Figure 5a). Similarly, multi-layer neuston net has been adapted from the design by David (1965) to a neuston catamaran (Figure 5b). The frames are normally 15 cm high. The upper frame is mounted in a position that it ideally cuts the surface just in the middle and samples the upper ~7.5 cm, which includes the hyponeuston layer. The frames should be equipped with nets of 200 to 500 µm mesh size depending on the target organisms.

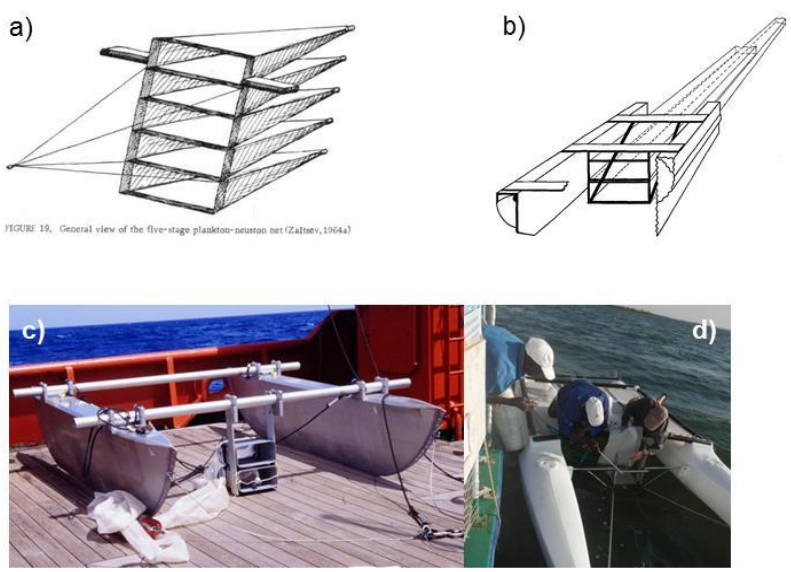

Figure 5: Neuston catamaran with two nets. a) original design by Zaitsev (1964a in Zaitsev 1971). b) Design by Hempel and Weikert (1972). c) Hydro-Bios© commercially mounted neuston catamaran. d) modified catamaran with a surface cutting net working in the Sine Saloum estuary, Senegal.

Other neuston net designs are the push net (Figure 6a) and the manta net (Figure 6b).

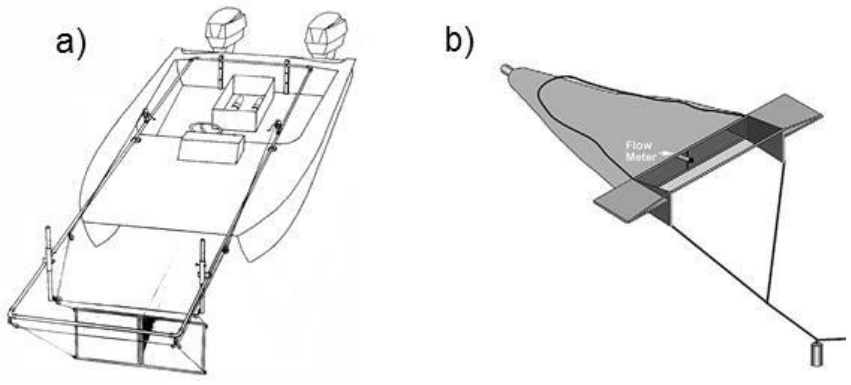

Figure 6: Other neuston net designs. a) push net (Miller, 1973). b) manta net (Brown and Cheng, 1981).

Filtered volume is calculated on the basis of the track or distance (d) through the water and the area of water cut by the upper frame (height (h) x width (w)). The area to be used for the calculation is 50% of the opening area of the frame if the upper frame is perfectly adjusted to the water surface. Filtered volume is then calculated as:

$v_f = d \times h \times w \times 0.5\ (m^3)$

Alteration of the area and the track measured through the water due to rough conditions will ultimately bias the calculated density of the target organisms being sampled.

6.3. Procedure for handling

Depending on the targeted organsims and size groups, mesh size and towing speed have to be adapted. Mesh size of 20 µm is necessary for sampling of microneuston where towing speed should not go beyond 0.5 m s not damaging the nets. A mesh size of 200 µm is common for catching mesoneuston. When targeting highly mobile organisms such as fish larvae the most important factor is towing speed. Neuston nets for fish larvae should be towed through the water with a speed of 2 to 3 knots (1 – 1.5 m s^{-1}; John et al., 2001) and a mesh size of 300 µm to 500 µm. David (1965) suggested a towing speed of 5-6 knots and a mesh size of 500 µm in very calm waters. Low towing speeds may allow organisms to escape and avoid the net, while high towing speed may damage the sampling device (especially when using finer mesh sizes for smaller plankton organisms) and be harmful to collected organisms. Further, in case of rough sea with higher waves, high towing speeds may also impede an accurate sampling, as the sampling device will likely bounce at the water surface and not constantly sample the hyponeuston layer. This will also bias the measurement of the track through the water normally done by means of mechanical flowmeters.

Towing should always be over the side to get the net free of the turbulences created by the ship's propellers (Figure 7). These turbulences will damage the organisms, especially fish larvae. An asymmetric bridle or even better only one fixing point of the towing line at the catamaran keeps the gear free from the towing vessel and guarantees a free inflow of water into the nets and a minimum of dynamic pressure in front of the net.

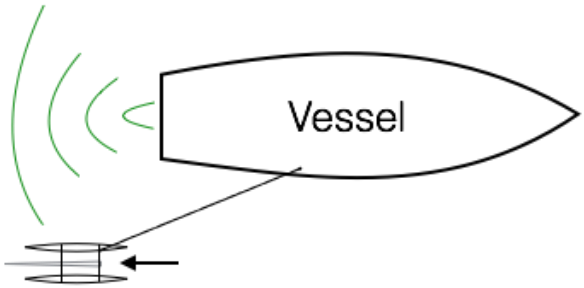

Figure 7: Position of towed nets to avoid turbulences by the moving vessel.

Net clogging may become a problem mainly in coastal waters with high abundance of phytoplankton. It strongly depends on mesh size, filtering area and net form (Smith et al. 1968). After sampling, the neuston net should be thoroughly cleaned using filtered water (sea water if sampling marine environments). This will move the sampled organisms and concentrate them in the cod-end. This should be performed with a relatively reduced water pressure to avoid damaging the sampled organisms. Regular cleaning of the net is mandatory.

The separation of the hyponeuston layer (0-5 cm) requires a very good adjustment of the upper net. Single net versions such as the Manta net provide a good qualitative and quantitative representation of the hyponeuston community. For a more detailed study of the plankton composition near the sea surface, a two- or multi-net version as shown in Figs xx6a and xx6c is required. The abundance of fish larvae in the uppermost 5 cm is significantly higher than in the layer 10 cm below (Lessa et al., 1999; Ekau and Westhaus-Ekau, 1996; Leal et al., 2010; see Figure 8).

Euhyponeuston are those organisms that spend their entire life time in the hyponeuston, the upper 5 cm of the water column, respectively (Zaitsev, 1962, 1964, 1997). It contains a large variety of different taxa (Doyle et al., 1994) specially adapted to this extreme environment and benefiting from the food available near the surface. This community is composed mainly of mollusks (*Janthina; Glaucus*), copepods (*Pontellidae*), isopods (*Idothea*), decapods (*Planes and Portunus portunus*) (Flores et al. 2002), and fishes.

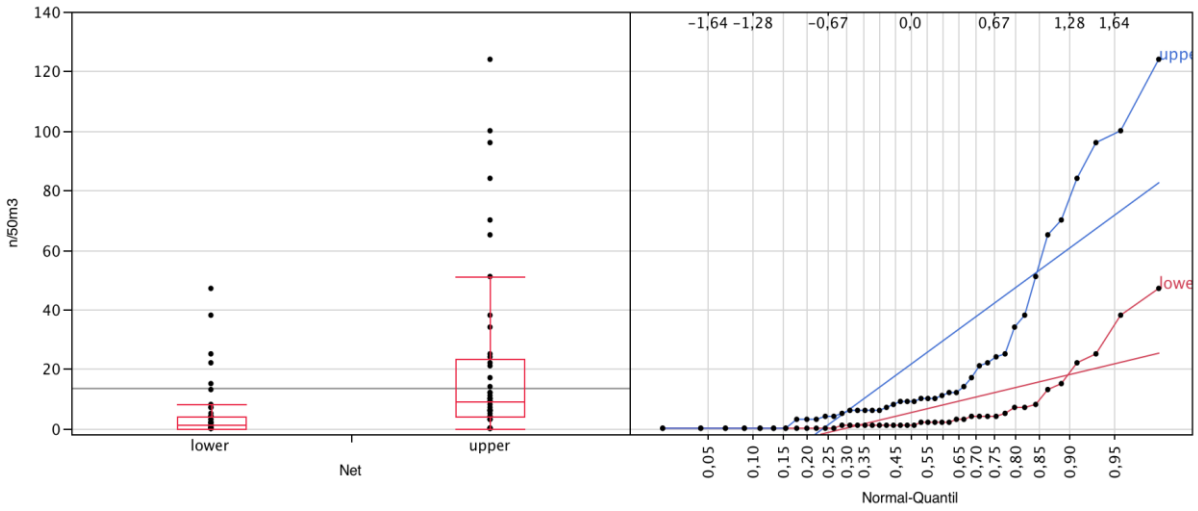

Figure 8: Fish larvae concentrations in individuals per 50 m^3 in the upper (0-7.5 cm) and lower (10-25 cm) net of a neuston catamaran. Concentrations are significantly different with $p<0.001$ (Ekau and Westhaus-Ekau, 1996).

In a study in Northeast Brazilian waters 23 and 17 families occurred in the upper and the lower net of a double-netted neuston catamaran, respectively (Ekau and Westhaus-Ekau, 1996). Total abundance differed significantly between the upper and lower net. Lessa et al. (1999) found a ratio of up to 62 between number of fish larvae of one family in the upper and lower net at open ocean stations around Fernanco da Noronha island. Many groups only occurred in the upper net emphasizing the need for a strict adjustment of the nets to the targeted catching depths.

6.4. Advantages and disadvantages

Lindsay et al. (1978) elaborated on the form of the net for surface tows. The authors argued that a normal ring net of 1m diameter is less than 3% effective in sampling the 5 cm near-surface layer. As can be seen from Figure 9, there is a significant difference between these upper 5 cm layer and the water below. Pumps are frequently used to collect water or plankton samples from discrete water layers to receive very precise vertical locations and volumes. However, targeting generally low abundant fish eggs and larvae requires high sample volumes not achievable with low speed pumps and without biasing the sample with organisms from deeper water layers. Cada and Loar (1982) compared towed nets and pumps finding the former more effective and the letter creating a higher avoidance of the organisms. Pumps also may damage the larvae and thus influence results (King et al., 1981). Taking the disadvantages of ring trawls and pumps into account, constructions such as the manta net or neuston catamarans based on the original design by David (1965) have shown to give the best results.

One main concern when sampling the neuston layer is net avoidance by plankton organisms. This issue may be significant when sampling in clear waters and at low speeds and targeting organisms displaying relatively high-mobility, such as larger fish larvae. The first neuston nets (Figure 3) had the disadvantage of having a bridle in front of the opening, which enhanced net avoidance by larger plankton/neuston organisms. The modifications performed by David (1965) minimized the shooing effect by having a bridle-less entrance. A complete prevention of shooing is only given, if no bridle is used and towing line is fixed asymmetrically at the device.

The development and use of the many different types of neuston nets creates a general problem in comparing the different studies. While in routine ichthyoplankton studies the simple Bongo net has been defined a kind of standard for the collection of fish larvae in the water column (UNESCO, 1975), a standardization of at least meso- and macroneuston sampling has not been achieved. Manta net and neuston catamaran are mostly used in recent studies; a quantitative comparison is not done yet.

7. SUBSURFACE SAMPLING

Sanja Frka, Gui-Peng Yang and William Landing

7.1. Introduction

The sea-surface microlayer (SML), the uppermost layer of the ocean at the air-sea interface, is a very thin layer that is often enriched in different dissolved and particulate species compared to the layers below. The extent of the SML enrichment at any given moment generally results from a combination of different physico-chemical and biological processes and is dependent on the concentration of organics coming from the subsurface water (e. g. Gašparović et al., 2007). Differences due to uncertainties in the SML enrichments come from the variety of samplers used to lift up the most superficial seawater layers as they differ mostly by the thickness of the layer they collect and by the material they are made of. An additional cause of possible uncertainties in the SML enrichments comes from the variety of depths used to sample the reference subsurface water sample beneath the SML (also called underlying water within the SML community). The SML enrichment in a given parameter is quantified by the ratio of analyte in the SML to that in the subsurface, so that the specific depth of the subsurface sample is critical. The subsurface water has been sampled, however, at depths ranging from 0.05 to 20 m, using different sampling devices. A large variety of sampling devices are available for collecting subsurface samples including multilayer sampling of the uppermost meter of the ocean surface as well as discrete samples and profiles of the water column below.

The subsurface sampling strategy is primarily controlled by the objectives of the investigation and by the expected or known spatial and temporal variability of the analyte concentrations in the study area. Based on this information, a sampling scheme can be developed outlining the station grid, the vertical resolution and the frequency of sampling. The sampling program requirements, along with knowledge of individual sampler characteristics, will combine to determine which type of device will provide the best performance. The choice of sampling equipment depends on the physical-chemical properties and expected concentrations of the analytes, on the depth and location of the sampling site, and on the available infrastructure.

This chapter provides an overview and advice on the sampling of representative seawater samples from below the sea surface microlayer. The selection of subsurface sampling devices outlined here focuses on subsurface sampling methods commonly applied within the SML scientific community. The topic of subsurface sampling will be treated in several sections. The

first section summarizes published sampling techniques and equipment, along with the parameters of interest, and discusses the avoidance of contamination artifacts. Other sections describe the advantages and disadvantages of these various sampling techniques moving from the uppermost meter of the ocean below the SML to depths as great as 20 m.

7.2. Subsurface sampling strategies

7.2.1. Overview of subsurface sampling techniques

The subsurface has been sampled from various depths between 0.05 and 20 m using different sampling devices; some of the most common are presented in Table 1. Subsurface samples are perhaps most commonly collected with bottles made of different material using the “hand-dip” method or via attachment to the end of 2-4 m long telescoping poles of non-contaminating material. Hand or powered pumps with an extended inlet tube are also frequently used to collect subsurface water. For collecting seawater profiles, discrete bottles are commonly used (Niskin or GO-FLO type). Multiple bottles may be either sequentially attached to a hydrocable so that several discrete depths can be sampled during one cast, or they may be mounted on a rosette frame, which allows replicate sampling at the same depth in addition to profiling.

7.2.2. Prevention of sample contamination

Contamination for many analytes can be encountered in dissolved, colloidal, and particulate phases, and contaminants may exchange between these phases during sampling and sample processing. Sampling equipment and sample processing techniques therefore need to be rigorously pre-cleaned and tested to minimize or eliminate contamination. The type of material used for sampling equipment (sample containers, tubing, connectors, valves, pumps, filters) will depend on the purpose (target analytes) of the study. Materials such as stainless steel, synthetic polymers such as polypropylene, polyethylene or Teflon (FEP, PFA, or PTFE), borosilicate glass and quartz glass can all be used as long as they neither adsorb nor release the target analytes or any non-target substances that interfere with the chemical analysis. For example, brown glass or stainless steel is suitable for samples containing trace organics, as leaching and adsorption are minimal, but are unsuitable for sampling most trace inorganics because they can release trace elements into samples and because active sites on its surface can bind inorganic ions. Teflon parts are often used for legacy persistent organic pollutants, however they cannot be used for sampling of fluorinated compounds.

Table 1. Overview of some common techniques for sampling the subsurface water beneath the SML.

Technique	Parameter	Sampling depth/m	Sampling volume/L	References
Hand-dip: Glass, amber polypropylene, polyethylene, polycarbonate, Pyrex, FEP-Teflon bottle	particulate and dissolved organic matter, surface active substances, dissolved monosaccharides, polysaccharides, polyaromatic hydrocarbons, proteins, lipids, carbonyls, trace metals, π-A isotherms, optical properties; surface tension, surface potential photochemical processes, hetero- and autotrophic populations (biomass and activities)	0.10-1	1-20	Agogué et al.,2004; Brinis et al., 2004; Carlucci et al., 1991; Cunliffe et al., 2008; Falkowska, 1999b; Frka et al., 2012; Gasparović et al., 2007; Guitard et al., 2007; Jarvis, 1967;Joux et al., 2006; Kuznetsova et al., 2005; Kuznetskova and Lee, 2002; Zhou and Mopper, 1997; Obernosterer et al., 2005; Saliot et al., 1991; Schaule and Patterson, 1981; Scribe et al., 1991; Zhang et al., 2013.
Pumping system: Teflon gear pump, polypropylene tubing,hydrophore, hand-held vacuum pump	particulate and dissolved organic matter, surface active substances, chromophoric dissolved organic matter, total dissolved carbohydrates, transparent exopolymeric particles, polyaromatic hydrocarbons, nutrients, pigments , ATP, algae	0.15-1	0.2-4	Estep et al., 1985; Kuznetsova et al., 2004; Ya et al., 2014; Wurl et al., 2009.
Drop-weight mechanism: Niskin bottle, glass tube, Van Dorn bottle	particulate organic carbon and nitrogen content, dissolved organic carbon, chlorophyll *a*, carbohydrates, amino acids, bacterioplankton	0.20-1	2	Carlson, 1983; Chen et al., 2013; Stolle et al., 2011; Xhoffer et al., 1992.
Rosette/carousel systems	all parameters	15-20	12-30	e.g. Measures et al., 2008a

For volatile and semi-volatile organic compounds, clear or brown glass bottles or vials with screw caps or stoppers with fluoropolymer resin liners, or similar products, can be used to provide a gas-tight seal. For inorganic compounds, such as heavy metals, polyethylene, Teflon, or pure fused silica (quartz) glass containers should be used.

Sampling tools and containers should be pre-cleaned to eliminate or minimize contamination. The method and extent of cleaning will be influenced by one's target analyte and the expected concentration ranges relative to the instrumental detection limits. For volatile organic compounds, containers should be heated at 105 °C for 3 hours and then allowed to cool in a desiccator to avoid contamination immediately before use. For semi- and non-volatile organic compounds, containers should be washed with an appropriate organic solvent such as pesticide residue analysis grade solvent, and dried immediately before use. For total dissolved and particulate organic carbon and surface active substances, borosilicate or quartz glass materials should be pre-baked at 400-500 °C for 4-8 h before use. For heavy metals plastic containers are often pre-washed with reagent grade acetone (to remove organics), then a dilute detergent ("trace-metal" compatible surfactant such as Micro) followed by soaking (or heating) in diluted nitric (1-3 M) and/or hydrochloric acid (0.5-3 M).

Sample contamination from the atmosphere should be avoided (e.g. paint and rust particles, engine exhaust, atmospheric background). To minimize contamination from the atmosphere, the surfaces of the sampling equipment in contact with the sample should be isolated from the atmosphere before and after the sampling, including storage of the equipment. Equipment blanks and recovery samples yield important quality control information that can be used to assess sample contamination and analyte losses, bearing in mind the potentially site-specific nature of airborne contamination. Concentrations of target analytes in the water may be elevated because of leaching from the sampling platform itself (e.g. polyaromatic hydrocarbons, organotin, polychlorinated biphenyls, iron, and chlorofluoroalkanes can be released from the ship during ship-based sampling). The ship's heading should be at an angle of 20 to 40 degrees to any current coming from the bow at the sampling side (typically starboard side), to minimize any influence from the ship's hull. Since the subsurface sampling equipment passes through the air-water interface, contamination from the SML is also a significant risk. Elevated concentrations of dissolved and particulate matter in the microlayer may therefore contaminate samples that will be taken at greater depths. Sample contamination from the SML can be avoided by closing the sampling equipment during passage through the sea surface and only allowing the sample intake to be exposed at the intended depth.

7.2.3. Multilayer surface sampling

The uppermost meter of the ocean surface is the layer where matter is in transit and its depth distribution is therefore influenced by various fluxes. Factors that could generate small scale vertical variability in the distributions of various analytes in the upper meter include the sea state (turbulent mixing), estuarine or river outflow (freshwater gradients), time of day (diurnal heating and cooling), occurrence of phytoplankton blooms (altered chemical gradients), etc., and these factors are likely to be more important in nearshore regions.

The large variety of depths used for sampling the subsurface (Table 1) indicates that the vertical distributions of organic and inorganic matter have often been assumed to be rather homogenous within this portion of the water column. Based on physical and chemical concepts, several theoretical classifications of the microlayer, i.e. subdivisions of the surface film into strata, exist (MacIntyre 1974, Norkrans 1980, Hardy 1982, Maki 1993). However, only a few biological, chemical, and physical experiments using multilayer sampling techniques have demonstrated that small-scale stratification may be found within the first meter below the surface (Hardy 1982). Bogorov (1966) designed a sampler for studying the distribution of microorganisms in the upper meter consisting of three pipette-like openings, each leading to a vacuum bulb which collected small volumes from 0.3, 1.0 and 5.0 cm depths. Hühnerfuss (1981b) criticized this sampler construction, arguing that the stream lines leading to a sucking tube can be difficult to maintain at constant depth under the dynamic conditions often encountered in the open sea. A multilayer sampler fixed in the frame of a double-hulled catamaran was constructed by a group at the Institute of Organic Chemistry of the University of Hamburg to investigate surface active substances in the upper meter of the ocean surface (Dr. U.Brockmann, personal communication). This floating device consisted of a tower-like cylinder (diameter ~6 cm and 30 cm length) which includes Teflon platforms forming sections of 2 cm distance (Fig. 1). Each section contained an opening with a pipette-like tube connected by a polyethylene tube. Samples were taken by parallel vacuum suction through tubes into glass bottles. Under calm sea conditions the sampler was kept by hand near the surface in front of the catamaran against the current. The upper section ended exactly at the water surface and the sucking velocity was kept low to avoid turbulent mixing.

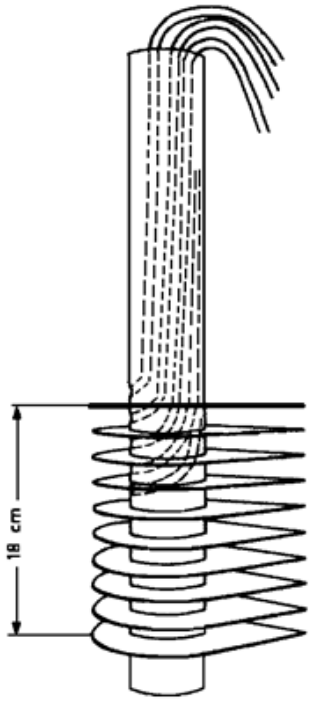

Figure 1: Scheme of multilayer sampling device with tubing for simultaneous vacuum suction constructed for the sampling of near surface water; adopted from (Brockmann, 1987).

Data describing the inhomogeneous vertical distribution of organic compounds in upper meter was presented in Danos et al. (1983). Samples from 5, 10, 20, 30, 40 and 50 cm were collected using a hand held vacuum pump attached to an autoclaved graduated high-density polyethylene siphoning tube, to investigate the distribution of nutrients, pigments and bacteria within the upper meter of fresher water. The first meter below the surface was also sampled using a simple device (easy to handle at sea) that allows sampling at various depths by Momzifkoff et al. (2004). It consists of 7 rigid Teflon tubes (5 mm internal diameter) perpendicular to a flat polypropylene floater with openings at 5, 10, 20, 30, 50, 70, 100 cm below the sea-surface. Seawater was collected with individual 50 mL syringes and quickly filtered on board through a double stack of Whatman GF/F glass fiber filters (0.7 µm pore size) for the analysis of dissolved total carbohydrates (DTCHO) and other bulk chemical parameters. Adsorption of dissolved carbohydrates on the GF/F filters was evaluated by comparing the carbohydrate concentrations retained on the top and bottom filters. Significant variability in the DTCHO concentrations at the 10 cm scale in the upper meter emphasizes how the choice of the subsurface sampling depth can affect enrichments relative to the SML. The variability in the reported DTCHO concentrations was lowest around 50 cm, suggesting that this depth was the most appropriate for use as a subsurface “reference” depth.

7.3. Hand-dip sampling and pump systems

The simplest, and perhaps the most common, method for collecting bulk subsurface water (0.2-0.5 m) to investigate SML enrichments is to “hand-dip” for samples (Table 1). As it is presented on Figure 2, the sampling person should wear shoulder-length polyethylene gloves (held up with rubber bands) and immerse a capped sample container beneath the surface. The cap is removed, and seawater is allowed to flow into the bottle (10-20% of the bottle volume). The cap is replaced, the bottle is brought out of the water, shaken, and dumped three times to rinse the bottle thoroughly. After the final rinse, the bottle is dipped

again and allowed to fill. It is important that the cap be removed (and replaced) while the bottle is under water to avoid collecting any

Figure 2: Sampling of the bulk subsurface water by “hand-dipping” for samples.

microlayer water during the rinsing and filling process. Sampling containers should be made of relatively inert materials (depending on the target analytes) such as stainless steel, glass, or synthetic polymers such as polypropylene, polyethylene, and Teflon. Subsurface hand-dipped seawater samples were collected for suspended particulate matter, particulate organic carbon, surface active substances, fatty acids, dissolved organic carbon, nutrients, dissolved amino acids and carbohydrates, and trace gases (e.g. Momzikoff et al., 2004; Yang et al., 2005, Kuznetsova et al., 2004, Gašparović et al., 2007). Subsurface water from within 1 m depth was also collected using a self-made device consisting of a glass bottle mounted on a telescopic rod that regulates sampling depth (Pinxteren et al., 2012). As in the case of hand-dip approach the bottle still needs to be opened and closed while below the surface in order to avoid contamination from the sea surface microlayer.

Various combinations of tubing and pumps are commercially available for collecting subsurface seawater samples. These sampling schemes can collect unfiltered samples, or can be adapted for *in-line* filtration using a coarse mesh (to remove larger organisms) and/or membrane filtration (using capsule filters or membrane discs). The tubing must be suitably de-contaminated prior to use, and kept clean between deployments, often by filling with an appropriate decontamination solution between uses. The pump manifold (tubing, fittings, and filters) must be flushed with 3-5 manifold volumes of seawater prior to starting sample collection. Wurl et al. (2009) used a 12-volt DC Teflon gear pump and polypropylene tubing to collect 200 ml subsurface water samples for analysis of surface active substances, total dissolved carbohydrates, chromophoric dissolved organic matter and transparent exopolymer particles. Subsurface samples for chlorophyll pigments and chemical analyses can also be collected by pumping. Specially designed seawater intake systems are reported to pump water directly in clean rooms located on deck (Gustafsson et al., 2005). Such intake

systems are often located at the prow of the ship to collect surface waters from depths of several meters. The Lamont Pumping SeaSoar (LPS) system is a combination of measurement and sampling platform towed by a research ship at speeds of 6-7 knots (Hales and Takahashi, 2002). The system allows not only *in situ* measurement of a variety of oceanographic parameters, but also collection of seawater from a depth down to 200 m through a 750 m tube to a shipboard laboratory for chemical analyses.

Landing et al. (1991) collected trace-metal clean water column samples from depths of 2-30 m from a raft moored over the center of a marine lake, Jellyfish Lake (Palau), with a 12-VDC Masterflex peristaltic pump (Cole-Parmer) with a short length of silicone tubing in the pump head and 35 m of 9.5-mm-i.d. Bevaline-IV tubing (Cole-Parmer). The volume of water in the tubing was ~2.5 L and the residence time of water in the tubing during sampling was ~2 min. The flowing sample stream was split after the pump head with Teflon fittings for collecting trace-metal samples and other samples off separate lines. Uncontaminated samples were collected for Mn, Fe, and Zn analyses. Uncontaminated samples were also collected for fluoride, chloride, sulfate, dissolved oxygen, dissolved total sulfide, alkalinity, nitrate, nitrite, ammonia, phosphate, silicate, and pH. A similar pump/manifold system (using FEP-Teflon tubing instead of Bevaline tubing) was also used to collect uncontaminated samples for dissolved and particulate inorganic Hg and monomethyl Hg (Buck et al., 2014). For very shallow samples (1 m depth), the end of the Teflon tubing was extended ~3-4 m away from the small boat by attaching it to an anodized aluminum extending pole (from a swimming pool supply store).

For subsurface sampling from a moving ship, Vink et al. (2000) and Bruland et al. (2005) describe “towed fish” systems where a hydrodynamically-optimized device (such as a bathythermograph) is hung from a boom and towed 5-10 meters outboard from the ship. Tubing is run from the nose of the device to a pump on the ship. The devices are designed to sample at 1-2 m depth while under way at up to 12 knots. Because they are deployed outside the influence of the ship’s bow wave, they are always collecting from “clean” water. When the ship is stopped on station, the devices can also be lowered to provide profiling capability. Submersible pumps have also been used for sampling subsurface waters. Friederich and Codispoti (1987) used a DC powered submersible pump attached to several hundred meters of reinforced tubing wound on a winch drum to collect continuous profiles of nutrients. This system supplied subsurface water at flow rates as high as 3-5 liters per minute.

For trace organic compounds, the sampling is challenging, as high volumes of seawater are needed (10-400 L) to pre-concentrate these compounds to above their analytical/instrumental detection limits. Sampling by pumping can be performed with compressed air Teflon pumps (although this is not suitable for subsequent analysis of fluorinated compounds). The hose is kept away from the ship's hull while the system is being rinsed, and during the collection of the subsurface samples. In situ filtration and solid-phase extraction sampling devices may minimize the risk of sample contamination during sampling. A typical in situ pump system, the Kiel In-Situ Pump (KISP), has been widely applied to the extraction of organic contaminants in seawater (Petrick et al., 1996). The pumping rate can be selected and kept constant between 1 and 200 L/h. Glass fiber or polycarbonate filters (diameter of 140 or 290 mm) are used in an all-Teflon filter holder. A modified KISP has been described for seawater sampling on-board research vessels (Ebinghaus and Xie, 2006). Additional submersible pump systems have been described. McClane pumps (Morrison et al., 2000) and the MULVFS system (Bishop et al., 1985) can both be equipped with extraction cartridges or columns to extract analytes from seawater. Similar to the KISP pumps, McClane pumps are battery operated and can be attached to a hydrocable while the MULVFS system uses a long umbilical power cable and the pumps are attached at various depths.

7.3.1. Advantages and disadvantages

The hand-dip sampling approach is a simple and low cost way to collect subsurface water samples very quickly, although for open-ocean sampling it requires leaving the research vessel in a small boat or raft, therefore adding additional time for the raft deployment and recovery. One disadvantage of hand-dipped sampling is that filtration must be done off-line. Depending on the project, this off-line filtration can only be done many minutes to hours after sample collection, potentially causing artifacts for analytes that might exchange between dissolved, colloidal, and particulate phases. Moreover, the sample volumes that are generally obtained using this method are relatively small. In comparison to the hand-dip approach, subsurface sampling via bottle attachment to a telescoping rod has the advantage that it can be performed by reaching out from the deck of a research vessel, such that it may not be necessary to leave the ship in a small boat.

Pump systems are well suited for projects where large sample volumes are required, and can easily include in-line filtration (thereby minimizing contamination and avoiding artifacts for analytes that may quickly change their phase association). Pumping has been criticized as potentially damaging to organisms, especially gelatinous zooplankton, however, with the appropriate choice of gear, damage is negligible (Beers, 1978). Depending on the free-board

height of the working deck, pulling seawater onto a ship can be problematic. Diaphragm pumps are often not self-priming and may not be able to lift water out of the ocean, and while peristaltic pumps can usually lift water to the deck of most ships, no pump can lift water to a height greater than ~10 m. Also, pumping speeds (and sampling depths) can be limited by wall friction in the tubing; large diameter tubing is required for deeper sampling and higher flow rates. The choice of tubing with walls that are rigid enough to withstand the vacuum and pressures associated with pumping is also important. The “towed fish” pump systems provide uncontaminated samples at flow rates of 1-2 liters per minute, and the flow stream can be split to run directly to filtration manifolds, ship-board sensors, and analytical systems. They are very well suited for collecting subsurface samples in a “survey” mode. They do require that a suitable boom be available for hanging the fish outside the bow wave of the ship, and the tubing running to the ship can be damaged (even severed) by towing through the water at high speeds. They therefore require frequent inspection and servicing, which can be performed while the ship is stopped on station.

When in-line extraction cartridges can be deployed (e.g. for trace organics or radionuclides), in-situ pump systems with batteries can be deployed at different depths on a hydrocable, and the pumping can be started and ended by pre-programming or remote control. Pump systems can be also deployed from moorings and are capable of providing temporally integrated samples. Deploying in-situ pumps on a hydrocable can consume a lot of ship time (8-12 h) and most ship operators will not allow simultaneous deployment of in-situ pumps with other hydrographic sampling requiring the lowering of cables and equipment. It can also be difficult to validate the extraction efficiency for various extraction cartridges, as they can be affected by the ambient concentrations of dissolved organic matter. The extraction efficiency can often be estimated by placing two (or more) extraction cartridges in sequence.

Pumps can be easily operated on board by connecting to the ship’s seawater intake systems, however these intake systems can be affected by two potential problems. Often, the intake plumbing becomes coated with bio-fouling growth. Biofilms and organisms on the walls (alive and dead) can alter the chemistry of the seawater as it passes through the plumbing to the lab. It is generally not possible to decontaminate these systems, even when the ship is in dry dock. For some analytes (trace metals in particular), the plumbing and fittings on the ship’s seawater line can be a significant source of contamination. It is also not possible to change the sampling depth for most ship’s seawater lines.

7.4. Niskin and GO-FLO samplers

The Niskin bottle (Fig. 3a) is a modification of the Nansen bottle, and was patented by Shale Niskin in 1966. Instead of a metal bottle sealed at one end, the “bottle” is a tube with stoppers at each end. Niskin bottles of different sizes (available up to a volume of 30 L) are used for sample collection for various analytes. To minimize contamination of the sample, Niskin-X samplers are made of PVC and their interior is totally free from metal parts. This bottle features a special V4A-stainless steel spring closure mounted externally (Fig. 3b). Moreover, horizontal Niskin samplers are intended for taking water samples near the bottom in lakes, streams, or in stratified water bodies. There is also special subtypes of convertible Niskin samplers which could be used either in horizontal and vertical position.

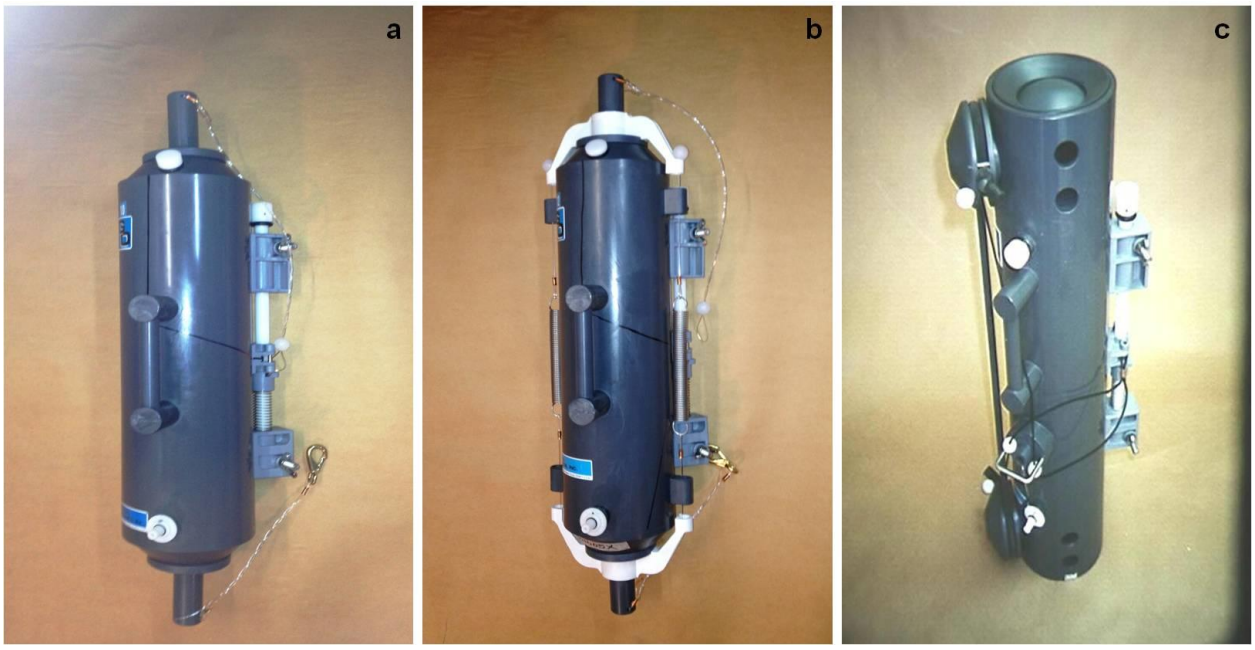

Figure 2: Niskin (a), Niskin-X (b) and GO-FLO (c) sampling bottles. General Oceanics Inc. (http://www.generaloceanics.com/) is gratefully acknowledged for providing these photos.

The GO-FLO water sampling bottle (General Oceanics, Inc.) can also be deployed on a hydrocable or a rosette (Fig. 3c). It features a close-open-close operation using rotating ball valves. It is often immersed through the air/sea interface in a closed state and opened by a pressure-activated release at ~10m depth. Upon recovery, a GO-FLO bottle can be pressurized (using any compressed gas supply to the air-relief port at the top) to force retrieved sample out of the sampling valve, and directly through a filter system if desired. This type of water sampler is available with bottle capacity between 1.7 and 60 L. Teflon-lined GO-FLO bottles were used to collect uncontaminated samples for trace elements and isotopes (TEIs) (e.g., Bruland et al., 1979). Individual GO-FLO bottles were hung on a non-

conducting Kevlar cable and triggered with plastic messengers. While highly successful, this method is time consuming and clearly too slow for global surveys.

All of these sampling bottles can be clamped to a hydrocable. Two clamps on the side of the cylinder are used to attach the bottle to a hydrocable so that it can be lowered to a pre-determined depth in the water and the bottles are held open by monofilament lanyards attached to a release mechanism. When a small weight, called a messenger, encircling the hydrocable is released down the line, it strikes the release mechanism resulting in bottle closure. A reversing thermometer may also be carried on a frame fixed to the bottle. Since there is no rotation of the bottle to fix the temperature measurement, the thermometer has a separate spring-loaded rotating mechanism of its own tripped by the messenger weight. These bottles are often either set up in a series of individual bottles on a hydrocable that trigger each other in turn as they close, or they are deployed on a rosette of as many as 24-36 bottles attached around a CTD instrument. Rosette systems are generally lowered using conducting cable (metallic or nonmetallic) and bottles are triggered to close using signal pulses from the ship.

The so-called Free Flow Water Sampler (Hydrobios) is similar in design to the Niskin bottle, but no cone or ball valve hinders the flow through the bottle, therefore offering optimal flushing characteristics. The LIMNOS sampler is a surface sampler (down to depths of 100 m) consisting of two to four 500 mL glass bottles, which are opened at the desired depth. The advantage is that the bottles can be used as storage bottles thereby avoiding possible contamination during sample transfer.

7.4.1. Advantages and disadvantages

The Niskin water sampler has several important advantages. The release mechanism allows samples to be taken at different water depths starting from the surface layer (upper meter) in a way that seals off the sample and allows it to be brought to the surface without mixing with water from different depths. Niskin samplers can be individually or serially attached on a hydrocable and activated by messenger or placed in any kind of multisampling system and activated by remote or pre-programmed command. These samplers are therefore suitable for water column profiling, and/or replicate sampling at the same depth. Niskin samplers are recommended for general purpose water sampling as they are made of inert materials and are non-contaminating for most analytes. Thus, the water collected by Niskin bottles is used for studying plankton or measuring many physico-chemical characteristics such as salinity, dissolved oxygen, nutrients, trace metals (Niskin-X bottle type) and dissolved organic and inorganic carbon. The horizontal Niskin water sampling device is ideal for sampling at the

thermocline or at other stratification horizons. One disadvantage of Niskin bottles is that they cannot be easily used for pressure filtration directly out of the bottle; the stoppers will push out if the internal pressure is higher than ~50 kPa. Another disadvantage with Niskin bottles is that they are lowered into the ocean in the open position, and could become contaminated by material in the SML (which is often enriched in trace metals, organic compounds, and particles) and/or contamination emanating from the research vessel itself. It has been reported that the black rubber tubing used for the closing mechanism and the black rubber O-rings in standard Niskin bottles are toxic to marine microplankton (Price et al., 1986). It was recommended to replace the black tubing and O-rings with silicone tubing and silicone O-rings.

The GO-FLO water sampling bottle is used whenever uncontaminated samples need to be taken, for instance for the chemical analysis of trace metals in sea water. The GO-FLO bottles are closed when they are lowered into the water column and open automatically at a depth of ~10 m. As a result, these bottles are neither contaminated on deck nor as they are lowered into the water. This avoids contamination from the SML and from the upper few meters of the water column (which may be contaminated by the research vessel or with atmospheric contaminants). Because it has no internal closure mechanism, there is no contamination from the tubing or spring that is used to close a Niskin Bottle. It has been reported that GO-FLO bottles do not seal as tightly as Niskin bottles, thus they are not recommended for trace gas sampling. One advantage to GO-FLO bottles is that they can be pressurized for filtration directly out of the bottle.

Niskin, Niskin-X, and GO-FLO bottles can be prone to an artifact, that rapidly settling particles can sink inside a closed bottle to a level below the outlet of the sampling port. This would create bias in the chemistry of particles that are recovered by direct filtration out of the bottles. Planquette and Sherrell (2012) studied this problem and recommended that a short piece of FEP-Teflon tubing be inserted between the inside of the sampling port and the opposite wall of the bottle, so that settled particles would be drawn out of the bottle. They also showed that this artifact could be further minimized by holding the bottle horizontally and gently rocking it back and forth to re-suspend any settled particles prior to sampling. Finally, tin (Sn) is often used as a catalyst when casting PVC, and since all of these bottles are made of PVC, there is a possibility that samples will be contaminated for Sn.

7.5. Rosette/carousel sampling devices

Rosette/carousel sampling devices allow the use of multiple Niskin or GO-FLO bottles for replicate and fast collection of water column profiles. Different manufacturers have different names for their products, such as rosette or carousel. It is a framework with from 3 to 36 sampling bottles (typically ranging from 1.2 - to 30 L capacity) clustered around a central cylinder (Figs. 4a and b). All presently manufactured rosettes have adaptor plates with a hole pattern to allow the bottles to snap securely in place, and to permit quick attachment or release. Rosette systems can be operated independently by pre-programming to trip based on time, temperature, pressure or other sensor output, without the need for conducting cable. Moreover those systems can be operated in conjunction with a CTD or other sensor system usually mounted underneath or in the centre. The CTD sonde is a standard instrument used to obtain continuous vertical profiles of conductivity, temperature, and pressure. The CTD data can then be used to calculate depth, salinity, density, and sound velocity. The combined signal is sent up through the conducting cable on which the CTD is lowered. This produces a continuous reading at a rate of up to 30 readings per second. Other sensors may be added to the cluster, including some that measure chemical or biological parameters, such as dissolved oxygen, hydrogen sulfide, pH, turbidity, and chlorophyll fluorescence.

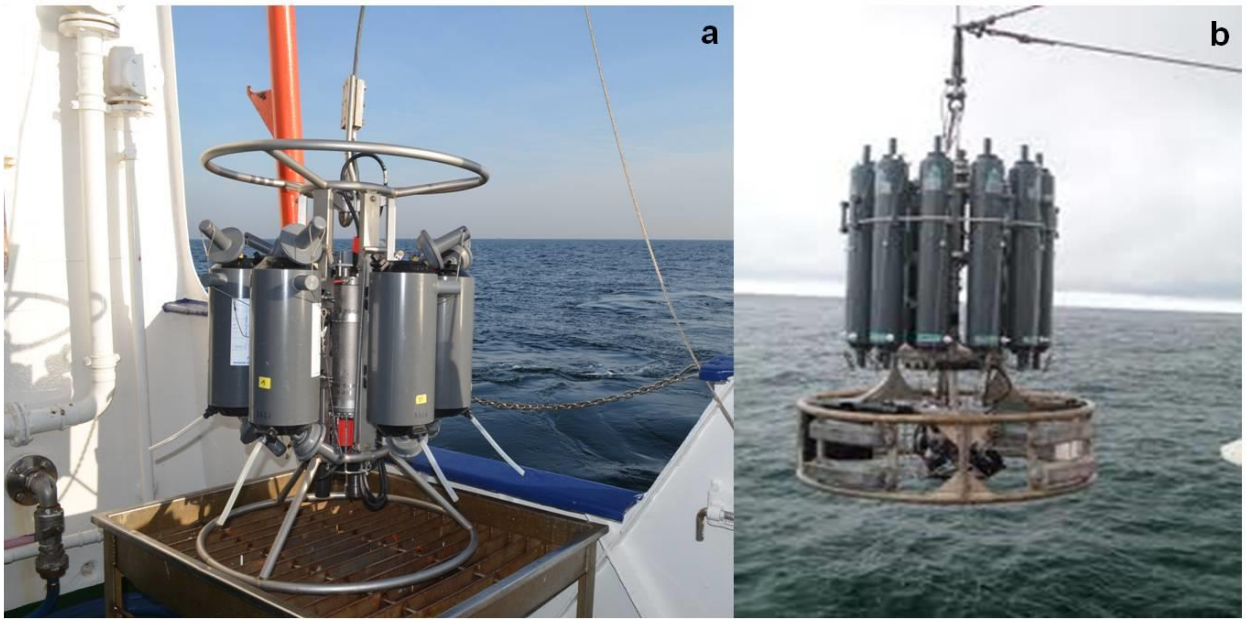

Figure 4: Rosette-based sampling system. (a) Small rosette with Niskin Bottles. (b) Large rosette with Niskin Bottles.

Early attempts at speeding up sampling for selected TEIs used coated stainless steel rosettes and conducting metal or Kevlar cables (e.g., Hunter et al., 1996; Löscher et al., 1998). In response to a need to collect water column profiles quickly for trace element

analysis for the CLIVAR/Repeat Hydrography program, Measures et al. (2008a) assembled an aluminum-frame rosette loaded with twelve 12L Teflon-lined GO-FLO bottles to collect profiles of uncontaminated seawater samples for trace element analysis. The rosette was equipped with a standard Seabird CTD and fluorometer sensor package, and was lowered on Kevlar conducting cable (coated with a polyurethane sheath) hung from a non-metallic meter-wheel. All of the components in this system are readily available commercially. Sampling was triggered while raising the rosette slowly (8-12 m/min) into clean water to avoid contamination from the rosette itself. A 12-depth profile to 1100 m can be collected in less than 60 minutes using this system. Uncontaminated samples were collected for dissolved and particulate Al, Mn, Fe, Co, Ni, Cu, Zn, Cd, and Pb (Barrett et al., 2012; Measures et al., 2008b; Milne et al., 2010) and dissolved ferrous Fe (Hansard et al., 2009).

Cutter and Bruland (2012) describe a 24-bottle rosette system similar to the rosette system described by Measures et al. (2008a) that is currently being used for the US GEOTRACES program. All of the components in this system are also readily available commercially. The main modification for the GEOTRACES system is that the CTD sensors are all housed in titanium pressure casings, eliminating the need for sacrificial anodes on the rosette frame or the sensor housings. The typical number of Zn sacrificial anodes used on most rosettes (5-10) can contaminate samples for Zn. The trace element concentrations in samples collected using this larger rosette system were compared to samples collected using MITESS “vane” samplers (Boyle et al., 2005) and also to the Dutch GEOTRACES “Titan” sampler (De Baar et al., 2008), and all three sampling systems showed no evidence of contamination for Al, Fe, Zn, or Cd. Both the MITESS vane samplers and the Dutch Titan system are custom built and are not readily available commercially.

7.5.1. Advantages and disadvantages

Multi-depth sampling devices such as rosettes allow relatively simple, precise and accurate selection and identification of the actual sampling depth in comparison to the use of a hydrocable with messengers. This means that the sample depths do not have to be set before the bottles are lowered. Most of the time a conducting cable (wire or Kevlar) is attached to the CTD and allows instantaneous uploading and real time visualization of the collected data on a computer screen. The water column profile of the downcast is often used to determine the depths at which the bottles will be closed on its way back to the surface, on the upcast, to collect the water samples. Consequently, this sampling approach significantly speeds up sampling of the water column profile. Moreover, rosettes can be used to collect samples from depths up to 6000 meters and a variety of sensors can be interfaced to meet specific scientific needs.

The rosette is not a particularly suitable device for the collection of subsurface water of importance for the study of sea surface microlayer enrichments as the sampling depth using a rosette is typically more than one meter. Moreover, because this system is deployed from a research vessel, samples from depths shallower than 15-20m can be contaminated with trace metals such as Fe and Zn. A trace-metal free rosette system may also require its own Kevlar cable and winch, and can be more costly than a regular rosette system. Due to the hydrodynamic resistance of a rosette in water, it must be weighted (usually with lead weights) to ensure that it descends more rapidly than the cable itself. It is therefore usually a heavy package that can be challenging to deploy and recover under rough conditions.

8. PHYSICAL AND IN-SITU TECHNIQUES

Christopher Zappa

8.1. Meteorological fluxes

8.1.1. Techniques

The flux determined by the micrometeorological methods assumes stationary conditions over the measurement period and knowledge of the atmospheric boundary layer stability. The inferred fluxes are critically dependent on these assumptions. The stationarity criteria for micrometeorological fluxes will be violated if there are significant horizontal gradients in the air over the area of measurements (Businger and Delaney, 1990). This requires the signal averaging duration to correspond to as much as 50 km. Islands and coastal regions as well as storm fronts may violate this assumption, although the measurements are likely reasonable at 10-km range.

The essential method for flux measurement is the eddy covariance technique which requires the use of a fast-response sonic anemometer to obtain the three turbulent components of the wind vector (u', v', w') and the sonic temperature deviation (T'). A high-speed infrared hygrometer is used to obtain Q' to arrive at the moisture flux. The velocity fluctuations in fixed-earth coordinates are obtained from the raw anemometer output by applying rotations to account for mounting geometry. The optics of the high-speed hygrometer can be contaminated by salt and sea spray (Fairall et al., 1997), and this is a particular problem for deployment on the open ocean. However, closed-path modification of the standard open-path configuration of the hygrometer has proved to be a viable method for measurement of the small-scale humidity fluctuations (e.g., during the Southern Ocean GasEx cruise (Edson et al., 2011) and in the Greenland Sea (Lauvset et al., 2011)). Covariance momentum fluxes in the streamwise and transverse directions are computed in 20-min segments from the wind components, and these are averaged together to obtain a 1-hr estimate of the wind stress. The methods employed are backed by over 10 years of experience in measurement of turbulent fluxes over the open ocean (Edson et al., 2004; Edson et al., 2011; Lauvset et al., 2011; McGillis et al., 2004; Zappa et al., 2012a).

Covariance flux estimates are subject to random sampling errors associated with atmospheric variability (Finkelstein and Sims, 2001) and other random errors caused by sensor noise and drift. In addition, particular care and consideration will be made to mount the instrumentation to minimize the effects of flow distortion on the resulting fluxes.

The corrected velocity components are used to compute the covariance fluxes of momentum, sensible heat, and water vapor. The momentum flux is described by

$$\tau = -\rho\overline{u'w'}, \quad (1)$$

where the overbar represents a time average quantity (20 minutes), ρ is the density of moist air, and u and w are the longitudinal and vertical wind velocity components, respectively. In this expression, u' and w' represent the turbulent fluctuations. The surface friction velocity can be derived from the direct covariance by

$$u_* = (-\overline{u'w'})^{1/2} \quad (2)$$

The turbulent air-sea fluxes for sensible, H_s, and latent, H_l, heat can also be measured using w' with fluctuating temperature and water vapor concentrations, giving

$$H_s = \rho c_p \overline{w'T'}, \quad (3)$$

and

$$H_l = \rho L_E \overline{w'q'}, \quad (4)$$

where c_p is the specific heat for moist air, L_E is the water latent heat of vaporization, T is the air temperature, and q is the specific humidity. The CSAT3 sonic anemometer measures temperature based on the speed of sound, which is a function of density; hence the result must be corrected for water vapor. The sensible heat flux is determined following Dupuis et al. (1997) by $\overline{w'T'} = \left(\overline{w'T_{sonic}^{'}} - 0.518T\overline{w'q'}\right)\Big/\left(1+0.518q\right)$, where T_{sonic} is the measured sonic temperature. The net heat flux, Q_{net}, is the sum of H_s, H_l, net longwave radiation, Q_{lw}, and net solar radiation, Q_{sw}. The net longwave radiation is defined as $Q_{lw} = \varepsilon_{si}\left(I_{lw} - \sigma_b SST_{skin}^4\right)$ and the net solar radiation is defined as $Q_{sw} = \left[1 - a_s\left(\tau_{es}\right)\right]I_{sw}$ where I_{lw} is the longwave irradiance measured by the pyrgeometer, ε_{si} is the spectrally integrated emissivity as a function of temperature based on Downing and Williams (1975), σ_b is the Stefan-Boltzmann constant, SST_{skin} is the ocean skin temperature, a_s is the albedo using Payne (1972) that is a function of atmospheric transmittance, τ_{es}, and I_{sw} is the shortwave irradiance measured by the pyranometer. The corresponding bulk fluxes can be calculated using the COARE 3.5 algorithm (Edson et al., 2013; Fairall et al., 2003; Fairall et al., 1996) from the mean atmospheric properties including wind speed, barometric pressure, relative humidity, and air temperature.

8.1.2. Instruments

Typical instruments are summarized in Table 1. Meteorological and direct covariance turbulent flux measurement systems can be mounted fixed towers, ships, buoys, and R/P FLIP. Direct covariance flux systems are capable of correcting for the velocity of platform

motion (Drennan et al., 1999; Edson et al., 1998). Measurement of the true vertical wind velocity is needed to compute the covariance fluxes. A three axis ultrasonic anemometer-thermometer (e.g., Vaisala model CSAT-3) and an inertial measurement unit (IMU) system of three orthogonal angular rate sensors and accelerometers or similar can be used (e.g., Crossbow model VG400MA-100). The IMU is mounted directly beneath the sonic anemometer, allowing for accurate alignment with the sonic axes in addition to ensuring that the wind and motion measurements were collocated. During experiments, the micrometeorological system is typically deployed at the end of a nominally *O*(10-m) boom. This placed the anemometer *O*(10-m) above the mean sea surface.

Table 1: Meteorological measurements.

Measurement	Methodology	Scales	Comments
Wind Stress/Airside TKE	3-D Anemometer	30-60 min avg	Wind stress and turbulent dissipation at a nominal height between 10m and 30m.
Sensible/Latent Flux	e.g., CSAT-3/Licor 7500	30-60 min avg	Turbulent fluxes at a nominal height between 10m and 30m.
Temperature / Humidity Profiles	e.g, Vaisala HMP155	30-60 min avg	Means at a nominal height between 10m and 30m.
Up and Down Solar Radiation	Pyranometer	5 min	Needed to constrain energy input to the ocean.
Up and Down Longwave Radiation	Pyrgeometer	5 min	Needed to constrain energy input to the ocean.
Cloud Base/Boundary Layer Height	Ceilometer	5 min avg	Data provides some aerosol, precipitation & PBL profile.
Total Aerosol Concentration	Optical Particle Counter	10-60 min avg	Overall fine and coarse mode particle volume (at a nominal height between 10m and 30m)

A fixed sensor package is deployed at the end of boom for mean meteorological measurements (Figure 1). The sensor package is aspirated and included a combined RH-temperature and H_2O measurement. The RH-temperature sensor is a small Vaisala model HMP45. Measurement of the mean and fluctuating water vapor for the direct covariance technique is made by a fast hygrometer (e.g., Licor model 7500 open-path NDIR sensor). Long- and short-wave radiation are measured by a pyrgeometer (e.g., Kipp and Zonen model CGR-4) and pyranometer (e.g., Kipp and Zonen model CMP-22) respectively. Barometric pressure is supplied by a Vaisala model PTB110.

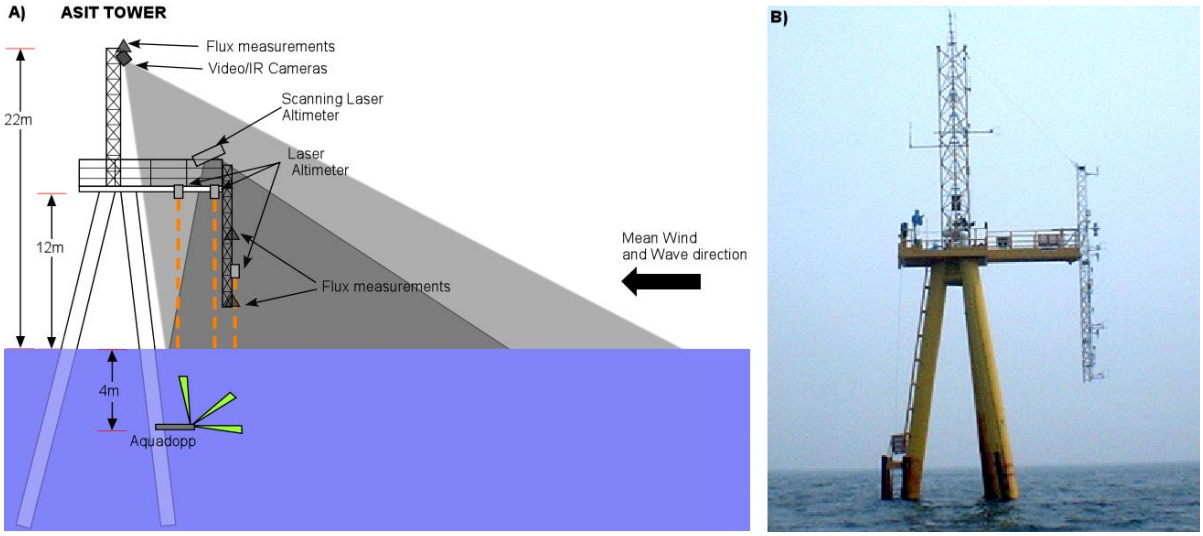

Figure 1: A) Schematic drawing of the existing and planned instrumentation on the ASIT tower. Not to scale. B) ASIT setup during CBLAST-LOW. Note the vertical mast at the end of the 10-m platform that allows for probing the wave boundary layer. This vertical mast can be lowered closer to the ocean surface. Also note that the subsurface boom exists as part of the ASIT. The Aquadopp is mounted on the existing subsurface boom away from the wake of the ASIT pilings.

8.1.3. Platforms

The Surface Processes Instrument Platform (SPIP) is a 15-foot Hobie Wave catamaran (Figure 2). Previous deployments of the SPIP have taken place in the equatorial Pacific (McGillis et al., 2004) and in the Hudson River estuary (Orton et al., 2010; Orton et al., 2010a; Orton et al., 2010b). Surface platforms similar to SPIP have been developed and deployed by Zappa (McGillis et al., 2004; Orton et al., 2010; Zappa et al., 2003; Zappa et al., 2007; Zappa et al., 2009] in various incarnations. SPIP can be used to measure the atmospheric CO_2, temperature, water vapor, and wind speed and direction very close to the air-water interface (Figure 1). SPIP has the advantage of measuring the atmospheric boundary layer near the surface with less flow distortion than from a ship. SPIP has fixed atmospheric sensors at the top of its mast roughly 3 m above the water surface. In addition, SPIP measures rain rate, solar radiation, and longwave radiation. Instrumentation on SPIP is powered by batteries and over the tethered cables from the small boat. The measurements are used to characterize the atmospheric forcing including the latent heat, sensible heat, and momentum fluxes from bulk formulae. SPIP also provides near-surface ocean measurements of

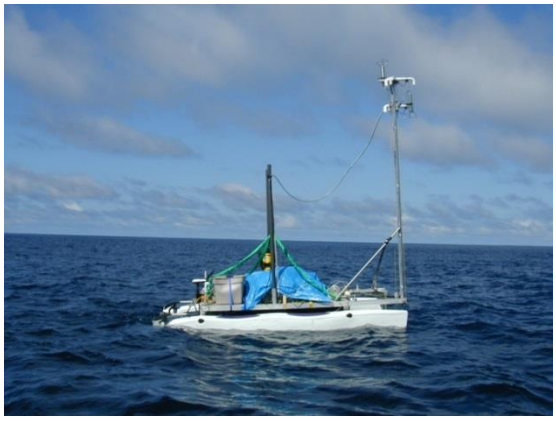

Figure 2: Surface Processes Instrument Platform (SPIP).

temperature, salinity, and turbulent kinetic energy dissipation rate and the techniques are described below.

The Air-Sea Interaction Spar (ASIS, Figure 3) buoy provides a unique opportunity to conduct novel coupled measurements of high quality air-sea exchange, ocean surface waves, and ocean and atmospheric turbulence. The ASIS is an ideal platform for near surface-layer turbulence measurements on both sides of the air-sea interface. The ASIS has been designed to reduce both the flow distortion and platform motion. As a result, it permits higher quality flux estimates than is possible from traditional research vessels and surface moorings.

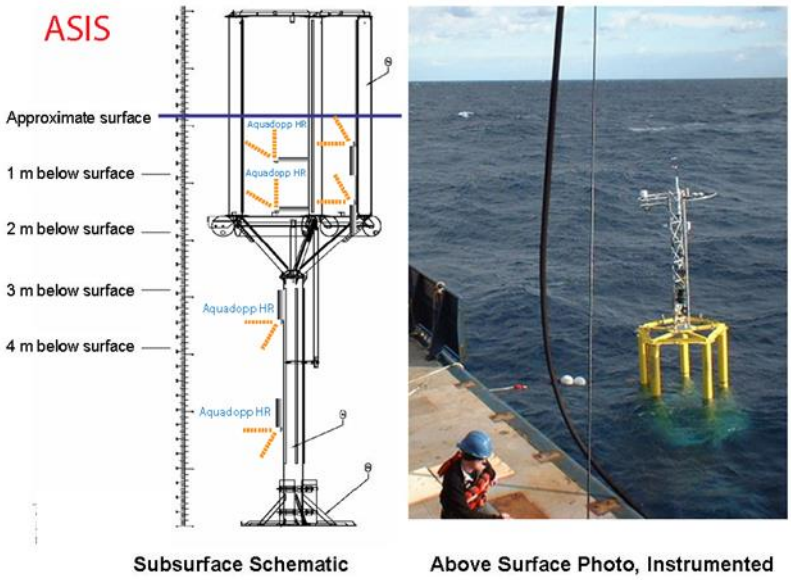

Figure 3: A) Schematic of the cage and under-water components of the ASIS buoy B) photo of the ASIS buoy being deployed from a research vessel.

We illustrate the advantage of ASIS versus ship-based measurements in Figure 4. It compares drag coefficient estimates made from ASIS and the R/V Knorr during the NSF-sponsored CLIMODE experiment. The upper two panels show the raw data and bin average values of the drag coefficient during a 10-day ASIS deployment (i.e., the measurements from both platforms are from the same period). The lower panel shows an estimate of the uncertainty from the ratio of the standard deviation of the drag coefficient divided by the mean within each wind speed bin. This uncertainty is dominated by flow distortion and incomplete motion correction for the ship-based measurements. As such, direct estimates of the fluxes from ships have to be heavily averaged to reduce this noise for parameterization studies. However, this estimate of uncertainty is clearly lower for the ASIS measurements, and our investigations have shown that a large fraction of this “uncertainty” is due to naturally-occurring variability and physical processes. This allows the direct covariance fluxes from ASIS to be used in time-series analysis for the process studies. Therefore, the use of ASIS can be central to process studies and provides an excellent means of validation

for the more heavily average ship-based measurements required in investigations aboard research vessels.

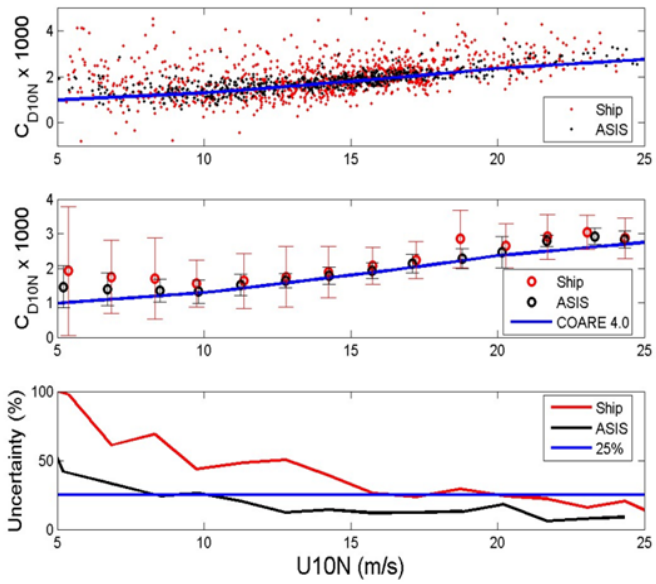

Figure 4: (Top two panels) A comparison of the drag coefficient estimates from the ASIS and Ship during CLIMODE. The blue line is a modified version of the COARE 3.0 algorithm. (Bottom panel) An estimate of the uncertainty computed from the ratio of the standard deviation to the mean in each wind speed bin shown in the middle panel. The blue line represents an uncertainty of 25%.

ASIS has been successfully deployed from the R/V Knorr during the NSF-sponsored CLIMODE experiment. Once deployed, the ASIS is allowed to drift with the mean current of the water mass through use of a subsurface drogue and not the surface wind-driven current. Ideally, it should be attempted to deploy the ASIS in such a way that the drifting spar would remain upstream of the ship within a selected water mass during a 10-15 day deployment. The position of the ASIS buoy is remotely tracked to ensure its recovery. This is done by sending its position via Iridium to home base and then emailing this position to the ship.

Ocean towers are excellent platforms to study air-sea interaction. One example is the Air-Sea Interaction Tower (ASIT, Figure 5) cabled ocean observatory located off the South coast of Martha's Vineyard, MA, USA. ASIT is part of the Martha's Vineyard Coastal Observatory (MVCO; http://www.whoi.edu/mvco) where the climatology of the wind and wave conditions span from low to moderately-high forcing during the measurement period (see Figure 6). ASIT provides a unique opportunity to conduct novel, long-duration, coupled measurements of high quality air-sea exchange, ocean surface waves, and ocean and atmospheric turbulence. The ASIT is an ideal platform for process studies related to near surface-layer turbulence measurements on both sides of the air-sea interface. The ASIT is a low-profile

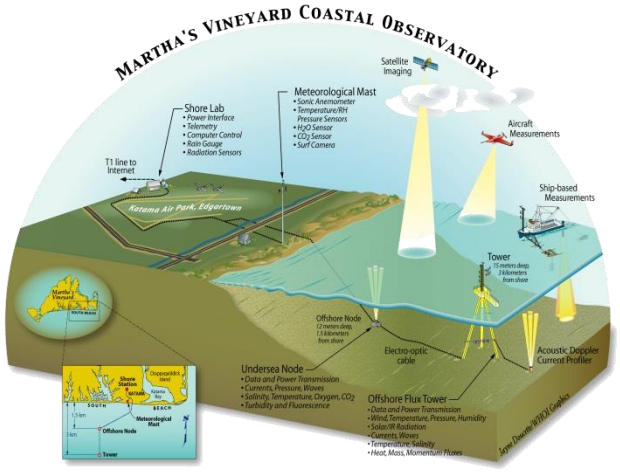

Figure 5: Location of the Martha's Vineyard Coastal Observatory.

fixed structure that has been designed to minimize the flow distortion and removes the need for motion correction. As a result, it permits higher quality flux estimates than is possible from traditional research vessels and surface moorings.

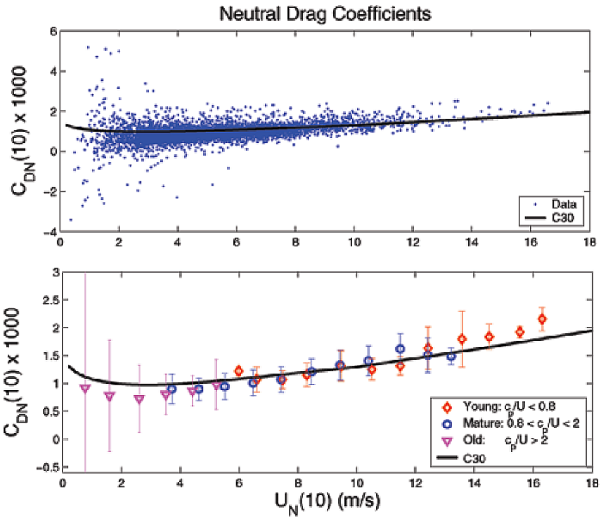

Figure 6: (top) Individual estimates of the neutral drag coefficient. The black lines labeled with C30 represents the COARE 3.0 parameterization from Fairall et al. (2003). (bottom) Bin-averaged results for subsets of the data that were measured in young, mature, and old seas as characterized by the wave age parameter cp/U. Reproduced from Edson et al. (2007).

The advantage of ASIT is illustrated by comparison of drag coefficient estimates made from ASIT and the TOGA-COARE model 3.0 during the ONR-sponsored CBLAST-LOW experiment. The transfer coefficient for momentum, that is, the drag coefficient, computed from the CBLAST-LOW dataset, shows good agreement in the mean with the COARE 3.0 algorithm (Fairall et al., 2003), particularly between 4 and 12 m s^{-1}, as shown in Figure 6. The bottom panel of Figure 6 plots the bin-averaged results for three subsets of the data that were measured in young, mature, and old sea. The drag coefficients for a range of wave ages ($0.8 < c_p/U < 2$) that includes mature seas are in good agreement with the COARE parameterization, which was developed using open ocean observations. If the COARE parameterization is correct for mature seas at all wind speeds, then the bin-averaged results indicate that the drag coefficients of the younger seas are enhanced while those of the older seas are suppressed. The figure also shows, however, that the difference between the drag coefficients for wind speed bins that have more than one wave-age category is not significant. Therefore, these results, by themselves, are not sufficient to conclude that wave age is the cause for the discrepancy. In fact, investigations have shown that a large fraction of this “discrepancy” is due to naturally-occurring variability and physical processes and not flow distortion or motion (Edson et al., 2007). This allows the direct covariance fluxes from ASIT to be used in our time-series analysis for the process studies.

8.2. Ocean wave characterization

The sea state can be measured covering the full spectrum of waves of O(0.01 - 3m) using polarimetric imaging, to moderate scales of O(1-30m) using a scanning Lidar system to a WaMoS radar to measure the large-scale directional wave spectrum of O(10-500m).

8.2.1. Polarimetric ocean wave slope sensing

The small-scale sea surface roughness is fundamental to air-sea gas exchange processes as well as to satellite-borne microwave backscatter techniques for recovering global marine winds and waves. Additionally, refining radiative-transfer modeling for light transmission through the sea surface requires a more detailed prescription of the sea surface roughness beyond the probability density function of the sea surface slope field. In this context, exciting new measurement methodologies now provide the opportunity to enhance present knowledge of sea surface roughness, especially at the microscale. Polarimetric Slope Sensing (PSS) is a passive optical remote sensing technique for recovering shape information about a water surface, in the form of a two-dimensional slope map. The PSS method uses the relationship between surface orientation and the change in polarization of reflected light to infer the instantaneous 2-dimensional slope across the field-of-view of an imaging polarimeter. For unpolarized skylight, the polarization orientation and degree of linear polarization of the reflected skylight provide sufficient information to determine the local surface slope vectors. We have demonstrated that the two-dimensional slope field of short gravity waves could be recovered accurately without interfering with the fluid dynamics of the air or water, and water surface features appear remarkably realistic.

The polarimetric slope sensing (PSS) method enables direct measurements of the time varying structure (in the form of an array of X and Y-slopes) at 60 Hz of the ocean surface at millimeter scales over a range of approximately 1 meter (Zappa et al., 2008; Zappa et al., 2012a). At these scales we can measure the time varying history of ultragravity waves. Wind forcing, currents, gravity waves and swell, and surfactant slicks modulate ultragravity waves posing a solvable inverse problem.

The PSS method recovers orientation of the surface normal vectors relative to the polarimeter coordinate system. However, in many applications a surface height map in an Earth-based coordinate system is a more desirable product. The orientation of the polarimeter relative to the Earth is found by attaching an inertial measurement unit (IMU) to the polarimeter's case. The x and y components of surface slopes are found by rotating the surface normal vectors to an Earth-based coordinate system. Figure 7 shows a typical gray-scale plot of the x and y components of the surface slope taken during the Santa Barbara Channel field experiment. Next, a height map h(x,y) is found by integrating the two-

dimensional slope fields ($s_x = \partial h/\partial x$, $s_y = \partial h/\partial y$). This produces a map of the local wave height topography of the imaged patch of the sea surface that is riding on the larger-scale dominant wave. The local mean tilts of the patch are preserved in this processing. Figure 8 shows a shaded relief of a typical reconstructed local surface height topography.

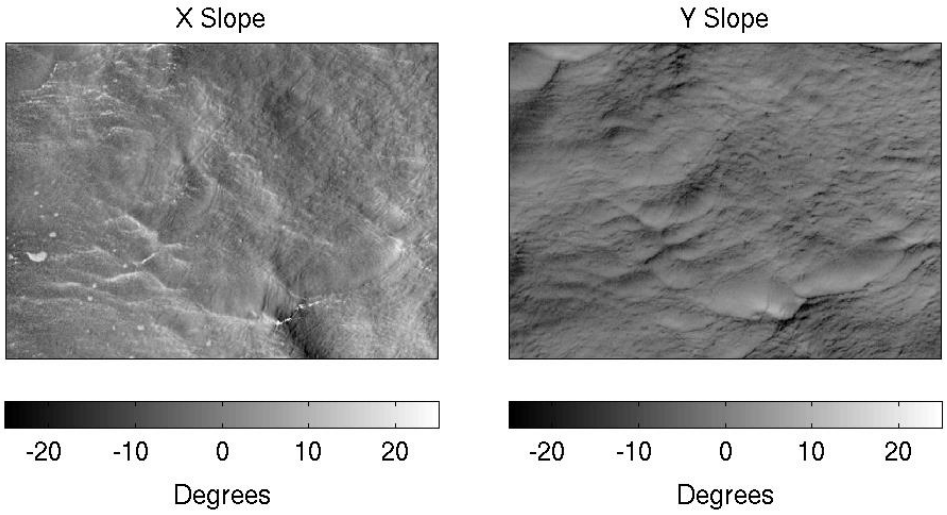

Figure 7: A typical gray-scale image of the X- (Left) and Y-Slope (Right) slope field of a small patch of sea surface during the Santa Barbara Channel experiment with a wind speed of 9.2 m s^{-1}.

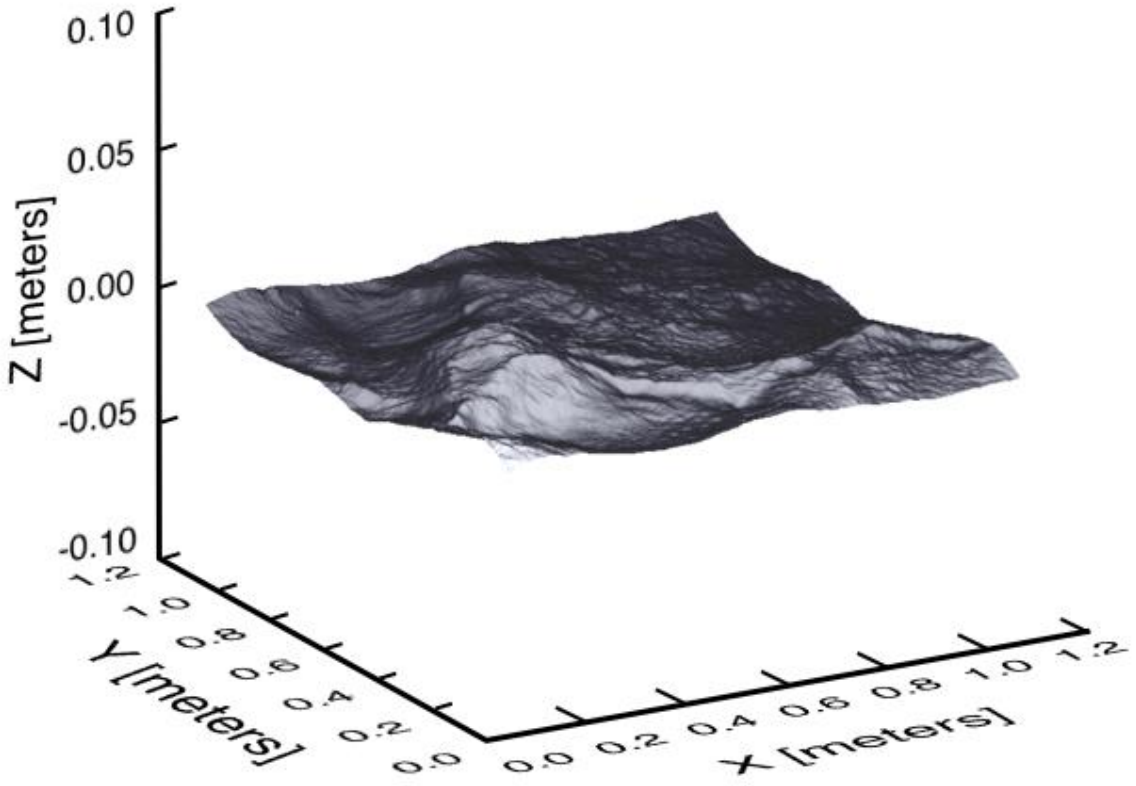

Figure 8: Representative frame from a video sequence showing a reconstructed wave train for the same data shown in Figure 7.

8.2.2. Fixed and linear scanning laser altimeters

A compact, portable wave measurement system (e.g., Riegl or SICK) can be used (Table 2); it is based on scanning Lidar technology capable of measuring the dominant sea state from ships and towers. The fixed and scanning lidars operates continuously throughout field experiments. Their data are used to obtain wave spectra and other wave statistics including significant wave height and dominant wave frequency. In addition, the orthogonal linear scanning lidar system provides spatio-temporal properties (interlaced x-z and y-z scans) of the wave height field resolved to the order of 0.5 m wavelengths. These measurements provide the phase of polarimetric, infrared and visible camera imagery (described below) of surface microstructure needed for quantifying short wave modulation with respect to the underlying dominant wind waves.

Table 2: Ocean wave characterization.

Measurement	Methodology	Scales	Expert	Comments
Waves	Riegl LD-90 Laser Altimeters	30-60 min avg	LDEO	Significant wave height. Directional wave spectra.
Waves	Riegl q240i Scanning LIDAR	λ = 0.05 to 20 m; 40-120 min avg	LDEO	High spatial resolution; wavenumber spectra.
Waves	Wave Imaging Marine Radar	λ = 15 to 600 m; 20 min avg	LDEO	Directional wave spectra; Wave frequency/length. X-band radar.
Whitecapping & Breaking Distribution	Stereo Visible/IR Imaging	40-120 min avg	LDEO	Continuous sampling.
Waves, Surface Roughness	Polarimeter	λ = 0.002 to 1 m; 40-120 min avg	LDEO	Wavenumber-Frequency Slope Spectra

The Riegl Q240i scanning Lidar provides the capability for a continuous wavenumber wave spectrum that ranges in wavelength from O(1cm to 20m) which is crucial for open ocean studies. Wave measurements are optimally performed at 10-20 m over the ocean. The Riegl Q240i scanner is deployed at the end of the boom aligned with the wind for the surface wave and wave roughness measurement. Furthermore, four Riegl LD-90 laser altimeters can be placed on the boom and directed vertically downward for redundant localized breaker disturbance fluctuations, as well as wave height measurements. These data serve to estimate the directionality in the wave field. For best practice ship-based ocean experiment, measurement of short to moderate gravity waves and actively breaking surface waves can be done using a scanning LIDAR. To locate breakers and quantify the local surface roughness in the breaking zones, the spatio-temporal synchronicity between the visible/IR cameras and the static/scanning LIDARs are used.

The Riegl model LMS-Q240i high-speed, long-range airborne laser scanner, commonly used in airborne altimetry, operates at a wavelength of 0.9 μm (near infrared), with a beam divergence of 2.7 mrad that corresponds to a footprint on the ocean surface of 2.65 cm at a range of 10-m. The manufacturer specified measurement accuracy is ± 2.0 cm with a precision of ± 0.25 cm. The system is capable of 10,000 measurements per second and a scan rate of up to 60 scans s^{-1} along a ± 40° scan. Our experience with the Q240i indicates that given the high reflectivity of wind-roughened ocean surfaces that we can easily anticipate an operation range of 10-20 m, producing a horizontal scan extent of 20-40 m. The Q240i 60-Hz linear scanning laser altimeter data independently characterize spatial and temporal properties of the wave height field resolved from O(0.05 to 20 m) wavelengths, that provides overlap with SEROSS to extend the wavenumber spectra at shorter wavelengths

8.2.3. Marine wave radar (X-Band)

Our experience indicates that given the high reflectivity of wind-roughened ocean surfaces that we can independently characterize spatial and temporal properties of the wave height field resolved from O(0.5 to 20 m) wavelengths (Zappa et al., 2012a), that provides overlap with X-band radar to extend the wavenumber spectra at shorter wavelengths. A suitable radar system consists of a commercial (e.g., WaMoS® II, Si-Tex, SEROSS), imaging marine radar, operating at X-band (9.45 GHz) and horizontal polarization. The system is capable of imaging waves, day or night, at a rate of 0.73 Hz with an image footprint radius of ~2-4 km depending on the environmental conditions (e.g. wind speeds >3 m/s) and the height of the antenna above the sea surface. These X-band systems have an extensive history, being used previously in numerical data-assimilating modeling systems (van Dongeren et al., 2008) and for wave breaking detection (Catalán et al., 2011), and open-ocean storms (Cifuentes-Lorenzen et al., 2013).

Directional ocean wave spectra, significant wave height, peak wave period, and peak wave direction can be obtained with a X-Band radar. The marine wave radar system also has the capability to resolve two-dimensional maps of surface elevation snapshots and allow for real-time measurement with the significant advantage of continuous availability of wave data in rough seas, under harsh weather conditions with limited visibility and at night. The system uses the unfiltered output from a marine coherent X-Band radar to determine wave and surface current parameters. The coherent radar offers new technology to measure surface currents and wave spectra by using a measure of the wave orbital velocity. Other systems that use backscatter intensity from standard marine radar approaches require an empirical MTF to scale spectral echo strength to wave height spectra, which is sensitive to a number of environmental parameters. Coherent marine wave radar measures directly and does not

suffer from this environmental dependence. The marine wave radar capabilities on research vessels provide directional wave spectra and individual wave state components at wavelengths of O(15 to 600)m that overlap with the scanning LIDAR for a continuous wavenumber spectra that spans wavelengths from O(0.05 to 600)m. In addition, waves can be measured using a system of laser altimeters that are both deployed from the bow of a research vessel. Cifuentes-Lorenzen et al. (2013) provides a detailed comparison of measurements from the R/V Brown during SO GasEx in 2008 made using WaMoS® II and Riegl laser altimeters. The significant wave heights range between 2 and 6 m with typically old seas and brief periods of young seas.

8.3. Ocean surface and near-surface characterization

High resolution dual LWIR and visible imaging stereographic systems will be implemented to characterize the breaking wave field and measure $\Lambda(c)$. The LWIR capability provides stereo capability to quantify white-capping and micro-breaking waves.

8.3.1. Ocean skin temperature

A longwave narrow field-of-view Heitronics model KT-15.82 LWIR radiometer (8-14 μm) is directed skyward to discriminate real from apparent ocean surface temperature variability during field experiments. During most open ocean experiments, we used the skyward radiometer at 20° zenith angle in combination with a Heitronics model KT-15.82 LWIR radiometer at 20° incidence angle to determine the skin temperature. Likewise, we deployed a second Heitronics model KT-15.85 radiometer (9.6-11.5 μm) that viewed the ocean surface at an incidence angle of 25° with the skyward radiometer at 25° zenith angle. The combination of Heitronics skyward- and downward- looking radiometers provided a continuous time series of skin temperature. We use the method outlined in Equation A2 of Appendix A of Zappa et al. (1998) to calculate the skin temperature.

8.3.2. Ocean wave breaking characterization

Recent developments (Banner et al., 2013; Gemmrich et al., 2013; Sutherland and Melville, 2013) in the spectral characterization of breaking wave properties (Phillips, 1985) in terms of spectral density of breaking crest length per unit area, $\Lambda(c)$, have added a new theoretical and observational framework that potentially adds reliable breaking wave information to routine wave forecasts (Banner and Morison, 2010). Evidence from previous experience (RaDyO (Zappa et al., 2012a); and SO GasEx (Edson et al., 2011)) strongly suggests that the actively breaking crest region (whitecap) of breaking waves is important to air-sea fluxes. The near-crest wind, sweeps over this highly fragmented, turbulent white capping region and amplifies the instabilities. The wind stress is highly sensitive to the breaking properties of the

wave field. Microbreaking generates surface roughness in the near-surface layer, while the larger whitecapping generates both surface roughness and bubble effects. A significant scientific challenge is to understand the effects of breaking processes (e.g., sharp-crestedness, bubbles and surface roughness). An example of $\Lambda(c)$ is shown in Figure 9 measured during the RaDyO experiment aboard R/P Flip.

For open ocean work, high resolution IR/visible imaging are implemented to characterize the breaking wave field and measure $\Lambda(c)$. A dual-LWIR system (Sofardir 640L) provides repeatable measurements up to 100 Hz of the water surface temperature accurate to 0.1°C with thermal resolution better than 20 mK for accurate sea surface skin temperature. The LWIR capability provides stereo capability to quantify both whitecapping and micro-breaking waves. A similar visible dual-camera system (two collocated downward-looking Imperx model Bobcat 2520 digital video cameras with a sensing array of 2500 x 2000 elements) provides stereo capability of white capping only. The visible and IR camera system are positioned at the highest possible point on the existing platform, roughly 25 m above the water line. The visible cameras view the ocean surface such that scanning Lidar is within the field-of-view (FOV). For an instrument elevation of 25 m above the water surface, the visible cameras have a resolution of 4 cm with a wide FOV of roughly O(100 m) square viewing southern azimuths of the platform in order to provide optimal imaging of all scales of whitecaps including the short whitecaps with wavelengths less than one meter for all daylight conditions. For an instrument elevation of 25 m above the water surface, the resolution for the LWIR camera is 1 cm with an image FOV of roughly O(10 m). The visible cameras are run at a frame rate of 10 Hz and the IR camera at a frame rate of 20 Hz. Each camera has an Xsens model MTi IMU that records the attitude of the camera and is used to correct for image distortion employing Holland et al. (1997).

8.3.3. Ocean surface thermography

Infrared measurements of the sea surface have been used to detect breaking waves (Jessup et al, 1997a), microscale breaking waves (Jessup et al., 1997b; Zappa et al., 2001, 2004), internal wave structures (Zappa and Jessup, 2005), the momentum flux (Garbe et al., 2007; Garbe and Heinlein, 2011) and also used to infer gas flux (Jähne and Haußecker, 1998; Garbe et al., 2004; Schimpf et al., 2004; Asher et al., 2004). In thermographic techniques, an infrared camera is used for visualizing thermal patterns directly at the interface.

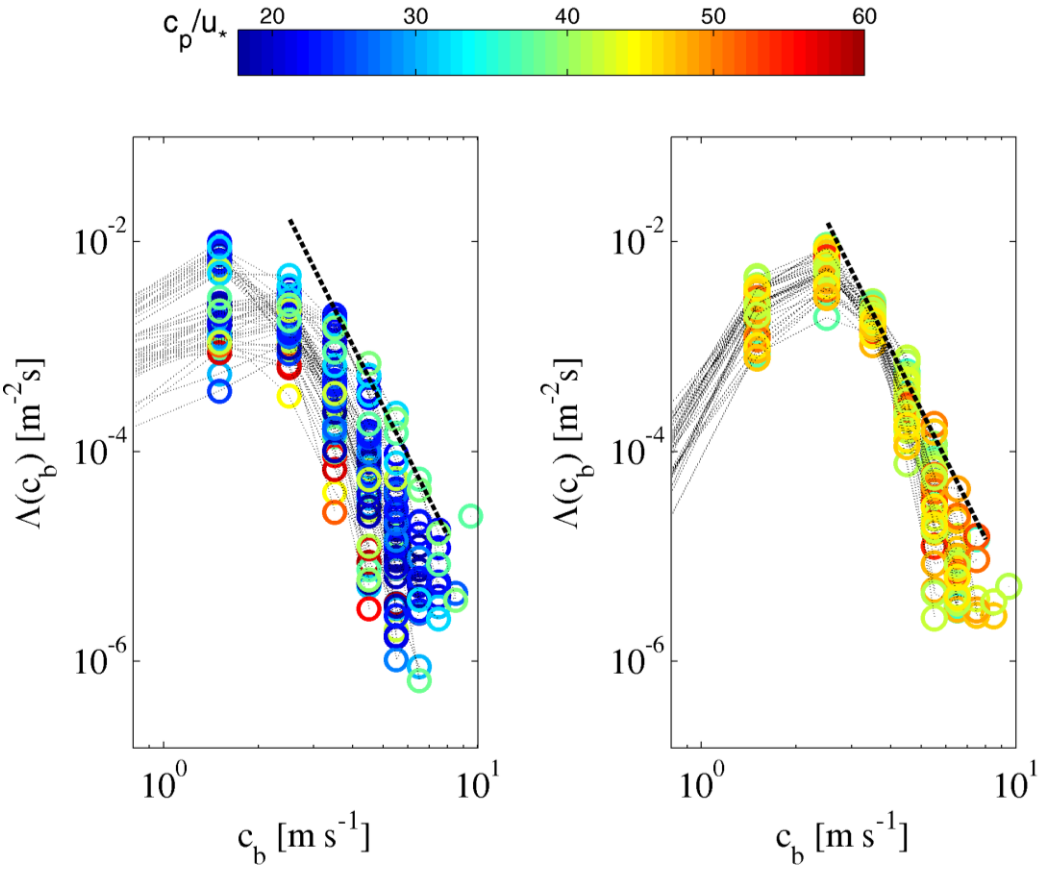

Figure 9: Breaking crest length distributions during the Santa Barbara Channel (left) and Hawaii (right) experiments. Note that the wave age (cp/u*) shows young wind seas in Santa Barbara Channel compared to old wind seas south of Hawaii. The dashed line represents the c_b^{-6} dependence predicted by Phillips (1985).

Generally, midwave (sensitive spectral range: 3-5 μm) or longwave (sensitive spectral range: 8-10μm) thermal imagers are used. In these spectral ranges, the penetration depth of the radiation is _ 20μm. Thermographic techniques are distinguished in active and passive techniques. In passive techniques, visualized temperature fluctuations occur from a natural net heat flux at the interface. For active techniques, a heat source such as a laser is used for imposing an external heat flux.

One such active thermographic technique is the active controlled heat flux method proposed by Jähne (1989). Haußecker and Jähne (1995) used an IR-camera to track a small patch at the water surface heated up by a short pulse of a CO_2 laser. The temporal temperature decay of the patch is fitted based on solving the diffusive transport equation including the surface renewal model (Higbie, 1935; Danckwerts, 1951) as a first-order process. The time constant of the decay is identified with the surface renewal time scale and the heat transfer

rate is calculated. A further method for the analysis of the decay curves was proposed by (Atmane et al, 2004), whereas the diffusive transport is combined with a Monte Carlo simulation of the renewal process based on the surface penetration model (Harriott, 1962). Zappa et al. (2004) and Asher et al. (2004) measured a scaling factor of roughly 2.5 between the gas and heat transfer velocity when they applied the active controlled flux technique. Following Asher et al. (2004), the surface penetration theory provides a more accurate conceptual model for air-sea gas exchange which is supported by the work of Jessup et al. (2009) who found evidence for complete and partial surface renewal at an air-water interface. Passive techniques are used successfully to estimate the temperature difference across the thermal skin layer (Garbe et al., 2004; Jessup et al., 2009). Passive thermographic techniques have also been used to investigate the features of near surface turbulence (Handler et al., 2012; Handler et al., 2001; Melville et al., 1998; Veron et al., 2008; Veron et al., 2009; Veron et al., 2011).

Recent measurements during RainEx II and III (Zappa et al., 2009) have demonstrated the importance of surface mixing in precipitating events. Evidence from our experience strongly suggests that the rain-induced turbulence is important to near surface salinity dilution (Zappa et al., 2007; Zappa et al., 2009). Figure 10 shows snapshots of infrared imagery of the Biosphere 2 ocean at successive times over the course of a 40 mm hr^{-1} rain. The temperature variation over the image is approximately 1 °C. Warmer regions appear light and cooler regions are dark. The first image in Figure 10a is a snapshot before a rain event. At this time, the surface is cooler than the water below. The temperature variations reveal small structures created by buoyancy-driven circulation. A look at the movie of infrared imagery also reveals small drift motions caused by the wave field as well as the underlying near-surface current. Figure 10b captures the onset of rain. Airborne rain is observed as black (cool), very fine objects. As rain impacts the water surface, small localized light (warm) patches are generated. The warm patches are caused by energetic mixing disrupting the thin, cool surface layer of O(1 mm). Warm water is entrained from below. An individual raindrop causes a disruption of the surface aqueous boundary layer. At this point, the buoyancy-driven background circulation is still apparent. Figure 10c demonstrates that the spatial extent of individual drops eventually will affect the entire ocean surface. Each injected raindrop is seen to influence spatial scales of O(10cm) or less. This scale is comparable to small breaking waves. As the cumulative number of drops increases with time, more of the surface is disrupted by rain. This process significantly enhances mixing. Figure 10d shows that the turbulent disruptions of the TBL by raindrops have reached a level of steady-state saturation. Comparing Figure 10a and 10d, it is clear that the surface mixing due to rain is complete in its spatial extent. The turbulence due to the raindrops now

dominates over the buoyancy-driven circulation that dominated previous to the inception of rain. The raindrops are ubiquitous, and the uniform surface mixing and subsequent air-water gas exchange are comparable to other seemingly more energetic processes such as wave breaking.

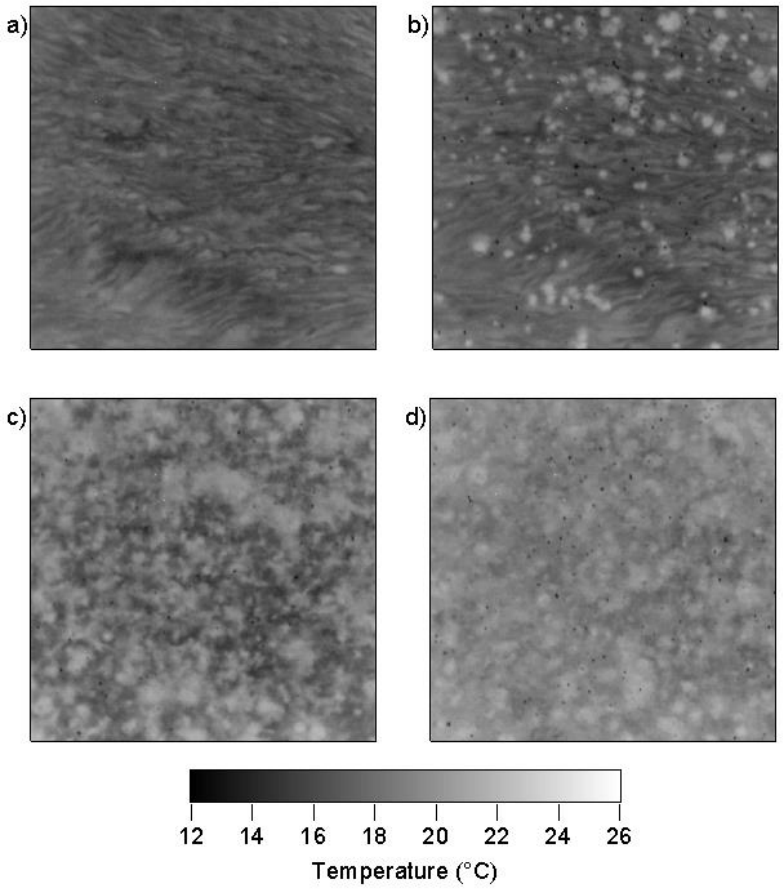

Figure 10: Snapshots of infrared imagery during the course of 40 mm hr^{-1}. The image size is 2 x 2 m and the temperature variability is 1 °C. a) The Biosphere 2 ocean before the rain began. b) The onset of rain (black dots in the image) produces localized mixing of the TBL to produce warm patches of water. c) Rain continues to mix the aqueous surface boundary layer. d) Fully developed rain causing the surface of the ocean to be intensely mixed.

A dual-LWIR system (e.g. Sofardir 640L) provides repeatable measurements up to 100 Hz of the water surface temperature accurate to 0.1°C with thermal resolution better than 20 mK for accurate sea surface skin temperature. The LWIR capability provides stereo capability to quantify both surface temperature and surface topography. A similar visible dual-camera system (two collocated downward-looking Imperx model Bobcat 2520 digital video cameras with a sensing array of 2500 x 2000 elements) provides stereo capability of the ocean surface only.

8.3.4. Ocean near-surface turbulence

Here, we propose to directly measure ε coupled with novel measurements of breaking-related properties. In steady flow with isotropic, fully-developed turbulence, kinetic energy is transferred from the mean flow to large eddies, then on to smaller eddies, and is finally dissipated by viscosity. Under these conditions, the TKE dissipation rate can be estimated

by the magnitude of the wavenumber spectrum in the inertial subrange. The inertial dissipation method is used to determine TKE dissipation rate from

$$S = A\frac{18}{55}\varepsilon^{2/3}\kappa^{-5/3} \quad (5)$$

where S is the wavenumber spectrum of the turbulent velocity, k is the wavenumber, and A is taken to be 1.5. Measurements of the turbulent dissipation rate, ε, will be made in the ocean according to the model for the inertial subrange of the kinetic energy spectrum in (5) using a pulse-to-pulse coherent Doppler sonar, the Nortek model Aquadopp HR profiler or similar device. The Aquadopp HRs operate at a transmit frequency of 1 or 2 MHz and has specialized firmware that allows for a high-resolution mode with bin sizes capable of 13 mm. It measures velocity profiles from which direct wavenumber spectra can be derived to capture the inertial-dissipation range. The Aquadopp is used to measure ε directly from the wavenumber spectrum in (5) (Veron and Melville, 1999). The ability to directly measure the wavenumber spectrum (i.e., a velocity snapshot is measured) mitigates the contaminating influences of unsteady flow, and platform motion if any. This technique has been used in previous upper ocean experiments (e.g., Gemmrich and Farmer, 2004). The Aquadopp HR profilers have a custom sensor head with 3 beams; two orthogonal beams in a plane that is orthogonal to the cylindrical axis and a third beam that is directed upward 45° to this plane and 45° between the two horizontal orthogonal beams. The two orthogonal beams of the Aquadopp HR profiler measures the along-beam velocity over a profile of 1.38 m with 2.6-cm bins. The well-known "range-velocity" ambiguity relationship for this instrument setup leads to a velocity ambiguity of roughly ±15 cm s^{-1}.

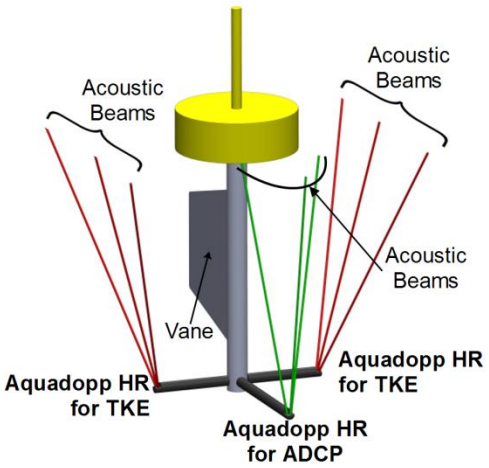

Figure 11: Schematic of SPIP-2 with three Aquadopp HR profilers. One 1 MHz sensor for measuring the profile of 3D current and two 2 MHz for measuring the TKE dissipation rates in the near surface. SPIP-2 is vaned into the current.

The next generation SPIP-2 is a spar buoy that will be used to measure the TKE and momentum fluxes in the near-surface ocean (Figure 11). SPIP has the advantage of measuring the near-surface ocean boundary layer with less flow distortion than from a ship or mooring (Prytherch et al., 2013). SPIP-2 provides near-surface ocean measurements of temperature, salinity, and turbulent kinetic energy dissipation rate. CTDs (e.g., Seabird Microcat pumped recorders model SBE37SMP) measure discrete profiles of temperature and conductivity within the top 2 m. The measurements of TKE and ε are made using an Acoustic Doppler Velocimeter (ADV; e.g., Nortek model Vector) and a pulse-to-pulse

coherent sonar (e.g., Aquadopp HR profiler) aboard the SPIP-2 platform. Multiple Aquadopp HR profilers are deployed to determine a profile of subsurface vertical velocity and TKE dissipation rates. Instruments are mounted to measure along-beam velocity over a 1-2 m profile with 1.7-2.6 cm bins. Several instruments are mounted to the buoy upward-looking at approximately 1-2 m depth to determine near surface turbulence, relative currents and bubble characteristics. A Nortek Vector (ADV) measures 3-axis velocity at a single point (1 cm^3) (Zappa et al., 2007). This instrument uses backscatter from particles in the water to make its measurement. The measurement is made at a sampling frequency of 25 Hz continuously. The Nortek 2 MHz Aquadopp HR profilers measure along-beam velocity over a profile of 1 m with 1.7 cm bins. This allows determinations of the wave-number spectra for velocity, which in turn enables estimates of the turbulent kinetic energy dissipation rate. Vertically-oriented beams provide depth-integrated estimates of ε and horizontally-oriented beams (at 30 cm and 60 cm) provide discrete depth estimates of ε. A profile is sampled at 8 Hz for 3 minutes every 10 minutes.

We have successfully made turbulence measurements from the WHOI Mooring during the NSF-sponsored VOCALS experiment under ocean conditions in Zappa et al. (2012b) for subsurface oceanic TKE dissipation at 6-m depth (Figure 12).

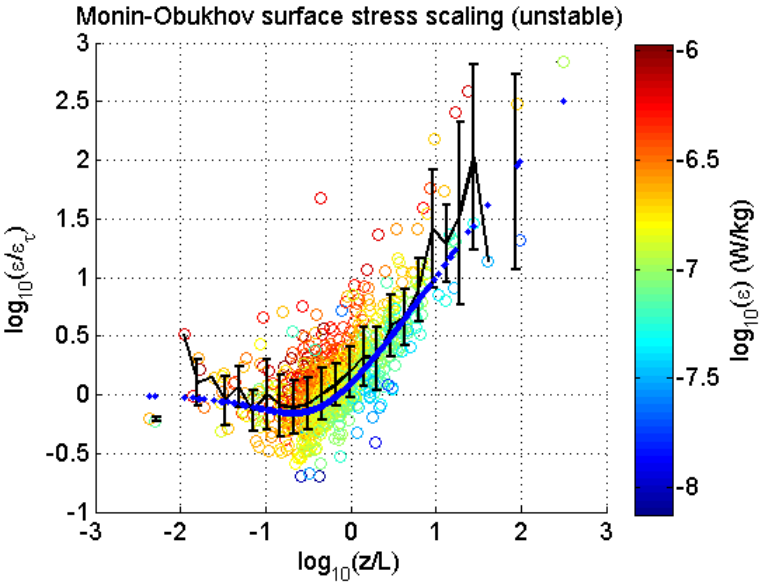

Figure 12: Stress-scaled oceanic TKE dissipation rates using MO similarity for unstable conditions during the VOCALS STRATUS mooring measurements from October 2008 through January 2010 due west of Arica Chile at 85 W 20 S. The colored open circles are the data, the black trace shows the bin-averaged data with σ bounds, and the blue trace is the air-side MOS scaling predicted by Edson and Fairall (1998).

The measurements in Figure 12 show agreement with a parameterization that assumes a balance between production and dissipation, indicating that the transport terms cancel at this depth. However, just beneath the ocean surface, it has been shown that the TKE dissipation rate deviates from the classic law-of-the-wall behavior (e.g., Anis and Moum, 1995; Terray et al., 1996; Drennan et al., 1996) showing a relative enhancement in the presence of wave breaking. This region of the near-surface ocean where waves strongly influence the

exchange of energy and momentum is known as the Wave Boundary Layer (WBL). The wave-induced exchange is believed to have the greatest impact on the shear production and pressure transport terms (Craig and Banner, 1994; Edson and Fairall, 1998).

8.4. Additional platforms and sensors

8.4.1. Saildrone

Traditionally, large ships have been used to take ocean measurements. However, these ships are very expensive to operate. Unmanned vehicles, such as gliders and drifting buoys, have been deployed recently with promising results, yet they are very slow (~1 knot) and often require a ship to deliver them to their start location. Saildrone shown in Figure 13 redefines the world of ocean monitoring by going further, faster and more cost effectively than other unmanned vehicles technologies.

Figure 13: Picture of Saildrone. Length: 19 ft. Width: 7 ft. Height: 20 ft above water surface. Draft: 6 ft below water surface. Average speed: 3-5 knots. Maximum speed: 14 knots. Payload power available: 5-10 W. Deployment duration: 6-8 Months.

Saildrone uses basic sailing principles, but combines state-of-the-art carbon fiber composites with ultra-efficient aero- and hydro-dynamics to create an incredibly robust and efficient sailing machine. The Saildrone is powered by a solid, freely rotating wing that is controlled by a tail. While delicate in appearance, Saildrone is engineered to be fully submerged and rolled in extreme waves. The Saildrone's hydrodynamic design is a hybrid, combining the best features of mono- and multi-hulls. The result is a fully self-righting platform that also benefits from high righting moments for speed and wave piercing capabilities to reduce pitching and energy absorption from waves.

Saildrone has two payload bays and external payload attachments, configurable to serve varied mission requirements. Total payload weight capacity is roughly 100 kg, and can be expanded with larger craft as required. Various power options and sampling solutions are offered depending on the mission specific tasks. For the first time, a significant payload can be transported from a conventional dock to any specified part of the world's oceans at speeds comparable to that of ships, but at a fraction of the cost. The payload can be deployed or carried aboard the Saildrone, sampling as it sails and sending data back to base station via satellite.

8.4.2. Wave Glider from Liquid Robotics

The Wave Glider SV3 (as well as the SV2) was developed by Liquid Robotics and is the world's first hybrid wave and solar propelled unmanned ocean robot. The SV3 shown in Figure 14 incorporates the latest advancements in energy harvesting technology and its innovative propulsion and energy systems help customers explore portions of the world's oceans in which it was previously too challenging or costly to operate. The SV3 features technologies such as real-time onboard processing of large data sets, a flexible power and storage system designed for "power hungry" sensors, and an adaptable operating system designed for intelligent autonomy to enable coordinated fleet operations. Operating individually or in fleets, the Wave Glider SV3 enables 24/7/365, all-weather operations at a daily cost of up to 90 percent less than today's data collection alternatives, while complementing and improving the efficiency of ships, buoys, satellites and aircraft.

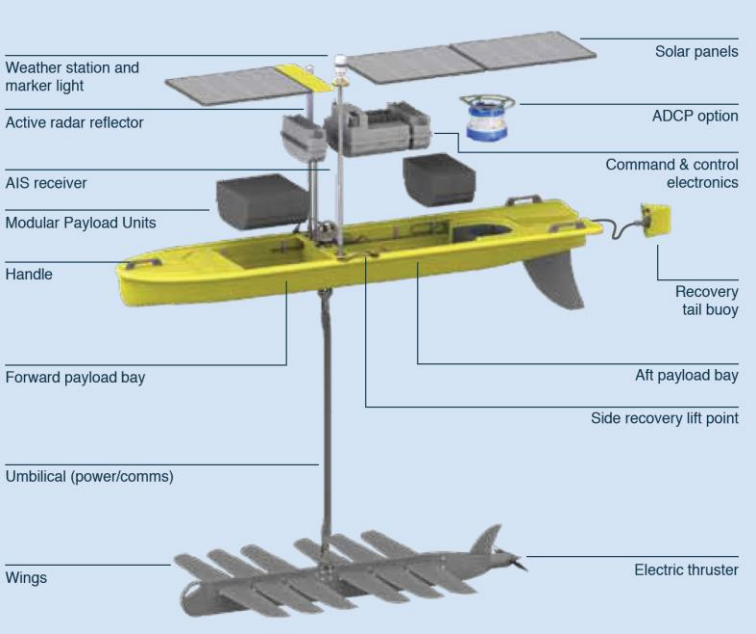

Figure 14: Schematic of Wave Glider SV3.

8.4.3. Air-Sea Interaction Profiler (ASIP)

The Air-Sea Interaction Profiler (ASIP; Ward et al. 2014) shown in Figure 15 is an autonomous vertically-moving profiling platform that is equipped with a suite of sensors that make measurements of the physical properties of the ocean from a maximum depth of 100m up to the air-sea interface. The sensor payload on ASIP also includes microstructure sensors (two shear probes and a thermistor); a slow response accurate thermometer; a pair of conductivity sensors; pressure for a record of depth; PAR for measurements of light absorption in the water column. Other non–environmental sensors are acceleration, rate, and heading for determination of vehicle motion. ASIP is ~ 2.5m in length and weighs

approximately 100kg. The sensors are located at the top of ASIP and are protected by a guard.

Profiling is accomplished with three thrusters that submerge the positively buoyant instrument to a maximum depth of 100 m. Once the pre-programmed depth is reached, the thrusters turn off and ASIP ascends to the surface at about 0.5 m s^{-1} acquiring data along this path. Once the surface is reached, ASIP gets its location with the GPS engine and transmits this with the iridium modem. Power is provided with rechargeable lithium-ion batteries, supplying 1000 Whr, allowing approximately 300 profiles. ASIP will provide periodic updates on its location via iridium SBD.

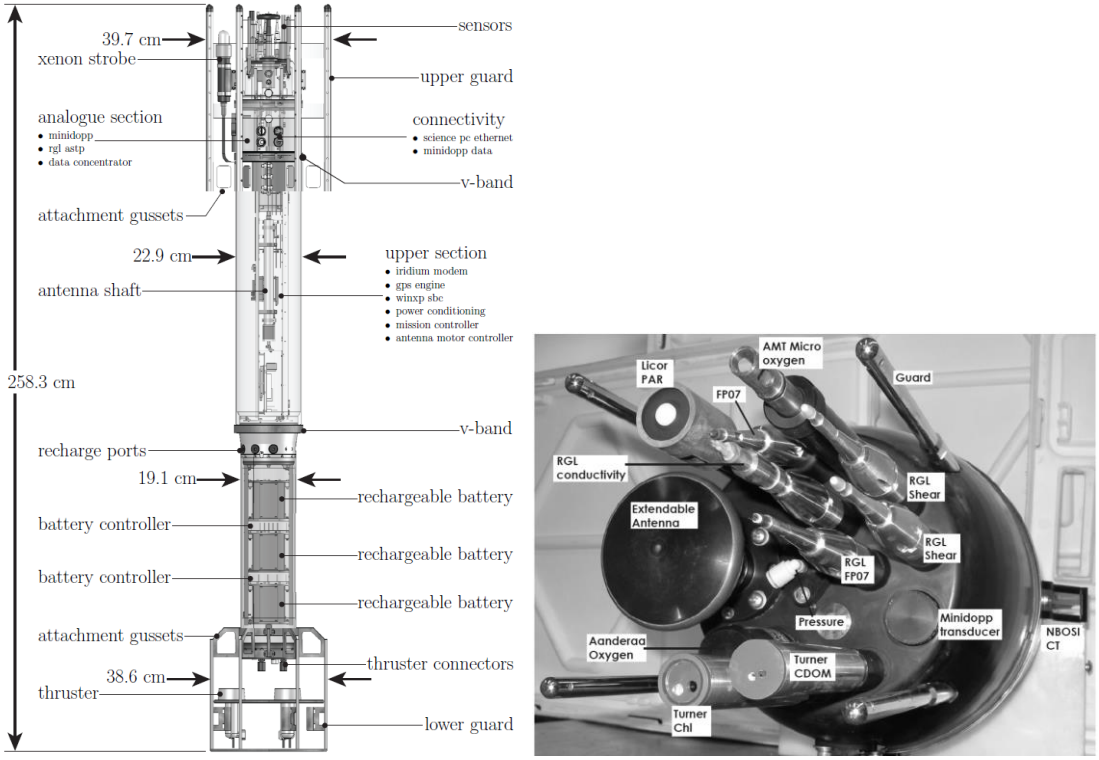

Figure 15: Schematic of ASIP (Left). Sensors on ASIP (Right).

9. DESCRIPTIVE INDICATORS FOR SURFACE CONDITIONS

Anja Engel, Kristian Lass, Oliver Wurl and Mohd Talib Latif

9.1. How to describe and differentiate slick conditions

Organic compounds in the SML may change the appearance of the sea surface as they attenuate capillary waves, i.e. small ripple waves typically having wave lengths less than a few centimeters. Through this capillary wave damping effect surface films can become visible as slicks such as in the presence of oils (Fig. 1). Mesoscale gyres and fronts, phenomena at the sea surface leading to slick formation, can also be identified as areas of abrupt changes (maximum gradients) in sea surface temperature. Natural slicks are often observed at low wind speeds (<6 m s^{-1}) typically having wider areal coverage for longer time in coastal seas compared to the open-ocean (Romano, 1996).

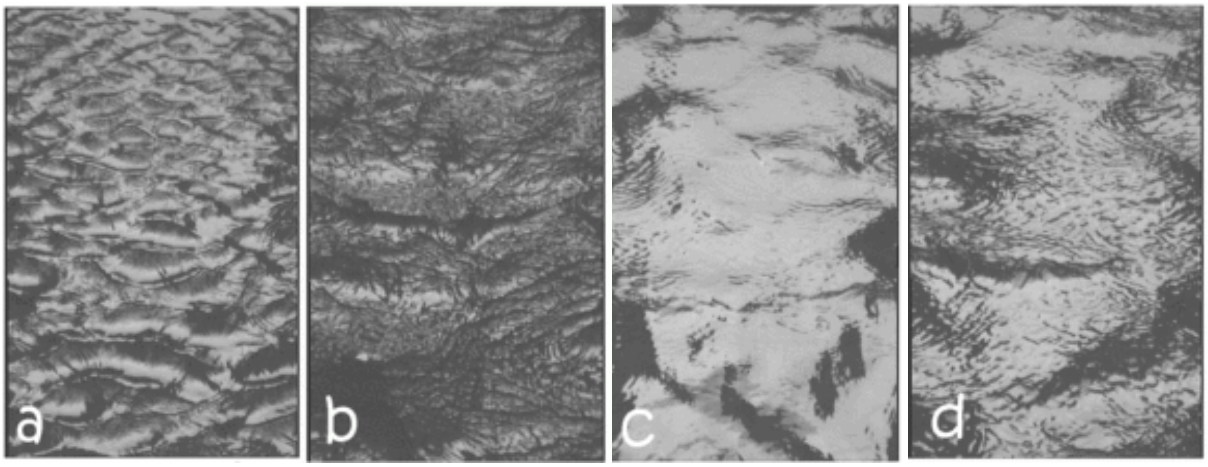

Figure 1: Video images of bound and free windwaves; a: 5 m/s, slick-free; b: 9 m/s, slick-free; c: 9 m/s, oleyl alcohol slick; d: 9 m/s, palmitic acid methyl ester slick (pictures M. Gade ZMAW, Hamburg, Germany)

It is sometimes difficult to distinguish natural slicks from anthropogenic pollutions, e.g. from petroleum products, since both types of films attenuate capillary waves. This prompted the Intergovernmental Oceanographic commission IOC (1985) to recommend considering the ambient wind conditions when characterizing film types. Since natural slicks will be readily dispersed at winds >6 m s^{-1}, slicks visible at the sea surface under stronger wind conditions should be assumed to originate from oil pollution. Visible slicks oriented along narrow bands containing seaweeds or floating microalgae, however, should not be considered as oil slicks as they can indicate Langmuir-type convergence circulations. Likewise under relatively calm wind conditions, visible sea-surface patterns in which capillary waves are virtually absent can indicate the presence of natural slicks originating from accumulations of biologically produced surfactants. The absence of ripples in the slick area produces a light reflection

pattern where the sun glitter appears brighter or darker than the surrounding slick-free area, depending on the viewing angle and the position of the sun. It has been observed that slicks become strikingly apparent during rain, as the circular ripples caused by raindrops are rapidly damped out in slick areas (Blanchard 1963).In order to minimize confusion of natural slicks with oil slicks, additional criteria may be used, such as the presence of an oily smell, tar or dark oil residues.

9.2. Defining microlayer enrichment

The relative concentration of a substance A in the SML is compared to the underlying water (ULW) is defined by the enrichment factor (EF) by:

$$EF_A = [A]_{SML} / [A]_{ULW}$$

where [A] is the concentration of a given parameter in the SML or ULW (GESAMP, 1995).Because the concentration of a component is normalized to its values in the underlying water, EF for different components can be readily compared. Enrichment of a component is indicated by EF>1, depletion by EF<1. Typically, concentrations of substances vary even within the upper meters of ULW. Enrichment factors of microbial components have been demonstrated to depend on the depth where the ULW sample is taken (Agogue et al., 2004). It is therefore recommended that reference depth be recorded and clearly indicated when calculating the EF. Many authors have used depths between 20 and 50 cm below the surface as characteristic of the ULW. EF can be reported as individual, maximum, minimum or median values.

Different SML sampling methods, e.g. glass plate, rotating drum, Garrett screen, yield different SML samples and hence refer to different SML depths (see chapter 2-4). In order to compare accumulations of components within the SML between different methods, these differing SML depths can be taken account of by calculating the surface excess concentration (SE) (Hunter and Liss, 1981):

$$SE= ([A]_{SML}-[A]_{ULW})\ 1000\ d$$

where A_{SML} and A_{ULW} are the concentrations (i.e. in gdm^{-3} or mol dm^{-3}) of the component in the SML and ULW, respectively and d (m) is the typical method-related sampling thickness of the SML (see chapter 2-4). The results indicate the excess concentration through a cross-section (m^2) of the surface. However, since the SE yields an absolute value, it is not recommended for comparison between different components.

9.3. Standardization of descriptive physical, chemical, and biological indicators

Description of the physical environment includes standard oceanographic measurements such as salinity, and temperature (°C).The upper few millimeters of the sea surface are characterized by a distinct temperature (the 'skin' temperature) relative to the ULW immediately below; the topmost few millimeters are typically cooler by several tenths of degree (Schlüssel et al., 1990). This results from the exchange of heat and moisture with the atmosphere as well as the emission of infrared radiation. The exchange of heat within slicks is probably very different from that in non-slick areas due to the diffusion-limited transport across the sea surface. Therefore, data on the temperature gradient between the sea surface and underlying water can be very useful for characterizing the sea surfaces. An array of micro-thermistors is a straightforward way to determine temperature gradients, even though measuring the actual SML temperature is not feasible under field conditions. Ascending thermo microprofilers (i.e. SkinDeEP, Ward et al., 2004) are not suitable for routine measurements, although smaller profilers are now commercially available but with limited resolution (~ 1mm), i.e. Self-Contained Autonomous Micro Profiler (SCAMP, Precision Measurement Engineering, Inc.), MSS Profiler (Sun & Sea Technology GmbH), VMP 250 (Rockland Scientific). On larger scales, remote sensing technology provides data on the sea-surface skin temperature (SST) in layers of 0.5 to 1mm thickness depending on the radiometer technology (Donan et al., 2002). Differences between satellite-derived skin and bulk temperature are obtained by algorithms developed from *in-situ* data (Schlüssel et al., 1990)

Damping of capillary waves is an important physical property of surface films that is linked to the reduction of surface tension by surface active substances (surfactants) that are a component of the SML. Clean seawater of salinity 35 and temperature 10°C has a surface tension of 75 x 10^{-3} N m^{-1} (Hunter and Liss, 1981). The film pressure (N m^{-1}) exerted by surfactant in the SML can reduce the surface tension. It has been suggested that effective damping of capillary waves requires film pressures of at least 1 N m^{-1} (Hunter and Liss, 1981). This is the lower detection limit for natural film pressures when determined with the oil drop technique (Adam, 1937). Early measurements of surface pressure ranged between <1-2.5 N m^{-1} for non-slick and between 1-24 N m^{-1} for slick conditions (Hunter and Liss, 1977).A well-established instrument for characterizing the surface pressure behavior of a film is a Langmuir trough equipped with a Wilhelmy balance. It is described in a large number of standard textbooks (for example, Dörfler, 2002). This device basically consists of a flat Teflon trough and movable barriers for the purpose of compressing the surface film. Although the name suggests otherwise, the device is based on studies originally carried out by Agnes Pockels (Pockels, 1891). The film pressure is determined by measuring the force

exerted on a small metal or paper plate (the “Wilhelmy plate”) hanging vertically into the water surface (Fig. 2). This technique allows the determination of surface pressures with sensitivities less than 0.1 Nm^{-1}, according to equipment specifications. The actual trough containing the liquid sub-phase is usually lined with Teflon or a comparable hydrophobic material, which is also used as a material for the movable barriers. The barriers close tightly with the trough to prevent the evasion of surfactant material through the opening between trough wall and barrier. Moving the barriers alters the water surface area available to the film surfactant and thus changes the compression state of the film. Recording the surface pressure as a function of surface area thus leads to valuable information regarding the density of film-forming molecules, average molecular weight etc. (Frka et al., 2012).

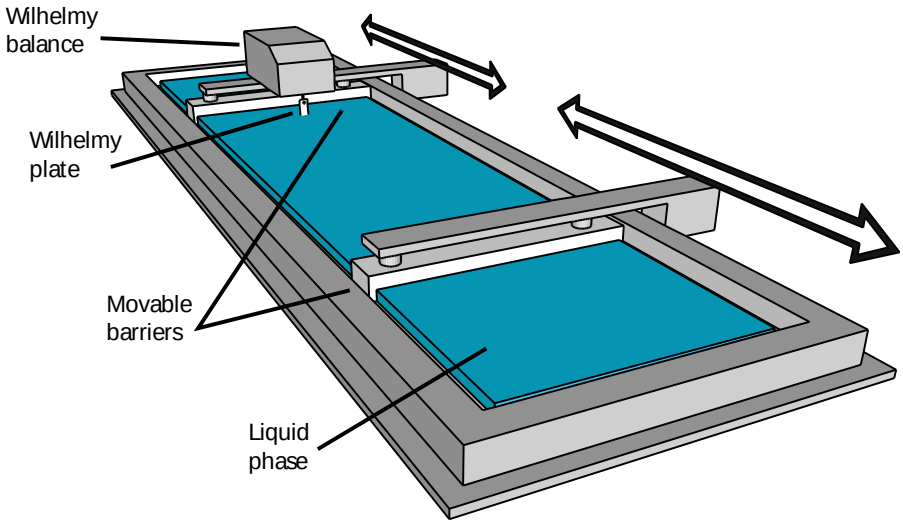

Figure 2: Principle sketch of a Langmuir trough. The Wilhelmy balance measures the surface tension, or the surface pressure, respectively, by means of measuring the force exerted to the Wilhelmy plate or a piece of filter paper. (Drawing: Courtesy of Joscha Kleber, with labeling added.)

Such “compression isotherms”, if they are part of studies of well-defined monolayers, usually are normalized to give the area per molecule. With such a complex mixture as a natural surface film this is not a feasible approach, as has been recognized in a number of Langmuir trough SML studies (e. g. Frew and Nelson, 1992, Frka et al., 2012).One possible way to state the layer compression in such experiments at least independent of size and geometry of the trough used would be to give compression ratios A/A_0 instead of just surface areas. Previous studies have normalized isotherms to an area-per-molecule or area-per-surfactant mass-scaling using either specific assumptions or theoretical models relating to the layer composition (Barger and Means, 1985, Pogorzelski and Kogut, 2003), or data from separate analytical methods (Frew and Nelson, 1992). Standardization in these studies depends entirely on the parameter chosen for standardization, which is naturally not commonly

available. Inter-comparison of data normalized by such procedures thus remains at least challenging, especially in light of the fact that *in situ* as well as laboratory studies exist with samples subject to different treatments (expansion or compression to different areas, filtration, extraction/re-spreading etc.) that influence layer density in the instrument. If such a treatment has been performed, the experimenter could facilitate inter-comparison by providing an estimate of the layer density change induced by the sample treatment. A successful practiced approach is to compare with a standard surfactant, such as Triton X-100 (Wurl et al., 2009, Frka et al., 2012).

Since the absolute amount of a chemical or biological component may depend on the SML sampling device and procedure used, normalization of components can create a common basis for better comparison of data between studies. For studies of organic components such as carbohydrates, amino acids, lipids, or gel particles, normalization to a bulk organic carbon, nitrogen or phosphorus pool like TOC/N/P, DOC/N/P or POC/N/P is recommended, depending on the total sample volume available. Organic element analysis is described in detail in analytical textbooks (Grasshoff et al., 1999; Wurl and Sin, 2008). For biological studies it might also be appropriate to normalize to components indicative of autotrophic biomass (e.g. Chl a [µg L^{-1}]) or cell abundance. Additional information on abundances of planktonic prokaryotes and protists (heterotrophic and autotrophic) can be retrieved even from small sample volumes (i.e. 5 - 50 mL depending on the trophic state) using epifluorescence microscopy or flow cytometry. Protocols for theses analyses are also described elsewhere (e.g. JGOFS Protocols 1996; Gasol and Del Giorgio, 2000). Concerning the rapid development and decreasing costs of molecular biological techniques the application of these to study bacterioneuston structure and function might be of increasing importance.

9.4. Reporting meteorological data

Meteorological conditions affect the formation and persistence of the SML and slicks, i.e. through wind dispersion, evaporation, and UV- and light-controlled microbial and photo catalytic processes. It is therefore recommended to report meteorological data as accurately as possible, including water and air temperatures (°C), cloud coverage (%) and precipitation type (rain, snow, hail) and intensity. Ambient wind speed (m s^{-1}) and if available wind history can help explain slick formation and/or assist in differentiating between slick types. Wave high should also be recorded. Sea state can be classified by appearance, for example by using the Beaufort Scale, where the Beaufort scale number (v) can be related to wind speed (m s^{-1}) by $v = 0.836\ B^{3/2}$.

Most importantly, the coverage of the ocean by SML and slicks is related to wind speed, and these usually persist up to wind speeds of ~6 m s^{-1} (Romano 1996). As wind influences the distribution and intensity of surface films, it consequently affects the amount of surfactants in atmospheric aerosols (Roslan et al. 2009) produced by wave breaking. At high wind speeds typically above 7 to 10 $ms^{-1}$the surface film disappears from the sea surface because of entrainment into the underlying waterby wave breaking. Furthermore, after the passage of storms when the wind has calmed down, enhanced coverage of the sea surface with biogenic slicks is often observed. The amount of surface-active material released by plankton into the water increases on the sea surface during high wind speed periods, because the substances accumulate on air bubbles generated by breaking waves and are being transported upward by turbulence and rising air bubbles (Liss, 1975; Wurl et al. 2011).

UV and solar radiation can become detrimental or stimulatory factors in the existence of slicks and the SML (Carlucci et al. 1985). High intensity of UV radiation reduces the capability of biogenic sources to produce SML surfactants. On the other hand high intensity solar radiation can lead to the production ofsmaller molecular weight proteins and lipids, giving rise to a biological slick of low average molecular weight. Suitable intensities of solar and UV radiation combined with high temperature can promote the growth of phytoplankton and increase the concentration of organic matter (Marić et al. 2013). A study by Latif and Brimblecombe (2004) showed the concentration of surfactants from high molecular weight molecules to first increase and subsequently decrease due to high UV intensity and oxidation. A study of SML sample storage by Schneider-Zapp et al. (2013) showed that SML samples can be sensitive to light intensity. Cloud cover will reduce the intensity of UV radiation and thereby affect slicks arising from biogenic sources. Therefore, the recording of UV- and light intensities is recommended for all studies of the sea surface. Raindrops are expected to interfere with SML and slick integrity. It is well reported by seafarers than rain calms the sea (Tsimplis, 1992). A study by Alsalahi et al. (2014) showed a higher concentration of the surfactants during the wet season than during the dry season in tropical region. Lim et al (2007) observed a high enrichment of particulates in the SML after heavy rainfall events, and suggested a wash-out effect from the atmosphere. It was also suggested that rain drops have a damping effect through producing wavelets, contributing freshwater to the sea surface, changing the temperature and, therefore the viscosity, and finally creating laminar vortex rings (Tsimplis, 1992). Rainfall events also affect river run-off and hence the transport of terrestrial organic matter that potentially supports slick formation, into coastal waters. This phenomenon usually happens in the areas influence by river and run-off water intrusion such as within the estuarine areas. It is recommended that any rainfall events prior or during observations of the SML are duly recorded.

REFERENCES

Adam, N.K., 1937. A rapid method for determining the lowering of tension of exposed water surfaces, with some observations on the surface tension of the sea and inland waters. Proc. Royal Soc. Lond., Series B, Biol. Sci., 122, 134-139.

Agogué, H., Casamayor, E.O., Joux, F., Obernosterer, I., Dupuy, C., Lantoine, F., Catala, P., Weinbauer, M.G., Reinthaler, T., Herndl, G.J., Lebaron, P., 2004. Comparison of samplers for the biological characterization of the sea surface microlayer. Limnol. Oceanogr.: Methods 2, 213–225.

Alsalahi, M.A., Latif, M.T., Ali, M.M. et al., 2014. Distribution of surfactants along the estuarine area of Selangor River, Malaysia. Mar. Pollut. Bull. 80, 344-350.

Albright, L.J., 1980. Photosynthetic activities of phytoneuston and phytoplankton. Can. J. Microbiol. 26:389–392.

Alpers, W., Espedal, H.A., 2004. Oils and surfactants. In: Synthetic Aperture Radar Marine User's Manual, Jackson, C.R., Apel, J.R. Eds. Washington, D. C.: National Oceanic and Atmospheric Administration, pp. 263–275.

Anis, A., Moum, J.N., 1995. Surface wave-turbulence interactions: Scaling e(z) near the sea surface, J. Phys. Oceanogr. 25, 2025-2045.

Ashmole, N., 1988. Insect dispersal on Tenerife, Canary Islands: high altitude fallout and seaward drift. Arctic Alpine Res. 20,1–12

Barger, W.R., Daniel, W.H., Garrett, W.D., 1974. Surface chemical properties of banded sea slicks. Deep–Sea Res. 21, 83–89.

Barger, W. R., & Means, J. C., 1985. Clues to the structure of marine organic material from the study of physical properties of surface films. Marine and Estuarine Geochemistry, Lewis Publishers, Chelsea Michigan, p 47-67.

Barrett, P.M., Resing, J.A., Buck, N.J., Buck, C.S., Landing, W.M., Measures, C.I., 2012. The trace element composition of suspended particulate matter in the upper 1000m of the eastern North Atlantic Ocean: A16N. Mar. Chem. 142-144,41-53.

Bartlett M, Haedrich R (1968) Neuston Nets and South Atlantic Larval Blue Marlin (Makaira Nigricans). Copeia 1968, 469–474.

Beers, J.R., 1978. About microzooplankton. In: Phytoplankton Manual. Sournia, A. (ed). UNESCO, Paris, pp. 288-296.

Bieri, R, Newbury, T.K., 1966. BOOBY II, a quantitative neuston sampler for use from small boats. Pub. Seto Mar. Biolog. Lab. 13, 405–410.

Bishop, J.K.B., Schupack, D., Sherrell, R.M., Conte, M., 1985. A multiple-unit large-volume in-situ filtration system for sampling oceanic particulate matter in mesoscale environments. Adv. Chem. Series 209, 155-175.

Blanchard, D.C., 1963. The electrification of the atmosphere by particles from bubbles in the sea. Prog. Oceanogr. 1, 73-112.

Bock, E.J., Frew, N.M. 1993. Static and dynamic–response of natural multicomponent oceanic surface-films to compression and dilation – laboratory and field observations. J. Geophy. Res. Oceans 98, 14599–14617.

Bogorov, L.V., 1966. Procedure for studying the quantitative distribution of microorganisms in the surface layers of a water body. Bull. Mosk. Obshchest. Inspyt. Prir. Otd. Biol. 71, 75-78.

Boyle, E.A., Bergquist, B.A., Kayser, R.A., 2005. Iron, manganese, and lead at Hawaii Ocean Time-series Station ALOHA: temporal variability and an intermediate water hydrothermal plume. Geochim. Cosmochim. Acta 69, 933-952.

Brinis, A., Méjanelle, L., Momzikoff, A., Gondry, G., Fillaux, J., Point, V., Saliot, A., 2004. Phospholipid ester-linked fatty acids composition of size-fractionated particles at the top ocean surface. Org. Geochem. 35, 1275-1287.

Brockmann, U., 1987. Nordsse, meerechemische Arbeiten auf der Valdivia. Nachr. Chem. Tech. Lab. 35, 9-15.

Brown, D.M., Cheng, L., 1981. New net for sampling the ocean surface. Mar. Ecol. Prog. Ser. 5, 224–227.

Bruland, K.W., Franks, R.P., Knauer, G.A., Martin, J.H., 1979. Sampling and analytical methods for the determination of Cu, Cd, Zn, and Ni at the nanogram per liter level in seawater. Anal. Chim. Acta 105, 233-245.

Bruland, K.W., Rue, E.L., Smith, G.J., DiTullio, G.R., 2005. Iron, macronutrients and diatom blooms in the Peru upwelling regime: brown and blue waters of Peru. Mar. Chem. 93, 81-103.

Buck, C.S., Bowman, B., Gill, G., Hammerschmidt, C., Landing, W.M., 2014. The partitioning, speciation, and flux of mercury in Gulf of Mexico estuaries. 2014 Ocean Sciences Meeting, Honolulu, HI. Abstract 209.

Burchard, H., Bolding, K., Villarreal, M.R., 1999. GOTM—a general ocean turbulence model. Theory, applications and test cases.Rep., In Vol. EUR18745, European Commission Report.

Burchard, H., Craig, P.D., Gemmrich, J.R., Haren, H.v., Mathieu, P.-P., Meier, H.E.M., Smith, W.A.M.N., Prandke, A.H., Rippeth, T.P., Skyllingstad, E.D., Smyth, W.D., Welsh, D.J.S., Wijesekera, H.W., 2008. Observational and numerical modeling methods for quantifying coastal ocean turbulence and mixing, Progr. Oceanogr. 76, 399-442.

Businger, J.A., Delaney, A.C., 1990. Chemical sensor resolution required for measuring surface fluxes by three common micrometeorological techniques. J. Atmos. Chem. 10, 399-410.

Caccia, M., Bono, R., Bruzzone, G., Spirandelli, E., Veruggio, G., Stortini, A.M., Capodaglio, G., 2005 Sampling sea surfaces with SESAMO: an autonomous craft for the study of sea-air interactions. IEEE Robot. Autom. Mag. 12(3), 98-105.

Cada, G.F., Loar, J.M., 1982. Relative effectiveness of two ichthyoplankton sampling techniques. J Fish. Res. Board Can. 39, 811–814.

Calleja, M.L., Duarte, C.M., Navarro, N., Agustí, S., 2005. Control of air–sea CO_2 disequilibria in the subtropical NE Atlantic by planktonic metabolism under the ocean skin. Geophys. Res. Lett. 32, L08606.

Carlson, D.J., 1982. A field evaluation of plate and screen microlayer sampling techniques, Mar. Chem., 11, 189–208.

Carlson, D.J., 1983. Dissolved organic materials in surface microlayers: Temporal and spatial variability and relation to sea state. Limnol. Oceanogr 28, 415-431.

Carlucci, A.F., Craven, D.B., Henrichs, S.M., 1985. Surface-film microheterotrophs: amino acid metabolism and solar radiation effects on their activities. Mar. Biol. 85, 13-22.

Carlucci, A.F., Craven, D.H., Wolgast, D.M., 1991. Microbial populations in surface films and subsurface waters: amino acid metabolism and growth. Mar Biol. 108, 329-339.

Champalbert. G., 1977. Variations locales de la répartition verticale et de l“abondance de l”hyponeuston en fonction des situations météorologiques. Cahiers de Biologie Marine XVIII, 243–255.

Chen, Y., Yang, G.-P., Wu, G.-W., Gao, X.-C., Xia, Q.-Y., 2013. Concentration and characterization of dissolved organic matter in the surface microlayer and subsurface water of the Bohai Sea, China. Cont. Shelf Res. 52,97-107.

Cifuentes-Lorenzen, A., J. B. Edson, C. J. Zappa, and L. Bariteau, 2013. A multi-sensor comparison of ocean wave frequency spectra from a research vessel during the Southern Ocean Gas Exchange Experiment, J. Atmos. Oceanic Tech., 30, 2907-2925.

Cincinelli, A., Stortini, A.M., Perugini, M., Checchini, L., Lepri, L., 2001. Organic pollutants in sea-surface microlayer and aerosol in the coastal environment of Leghorn – (Tyrrhenian Sea). Mar. Chem. 76(1-2), 77-98.

Craig, P. D., Banner, M.L., 1994. Modeling wave-enhanced turbulence in the ocean surface layer, J. Phys. Oceanogr. 24, 2546–2559.

Crow, S.A., Ahearn, D.G., Cook, W.L., Bourquin, A.W., 1975. Densities of bacteria and fungi in coastal surface films as determined by membrane-adsorption procedure. Limnol. Oceanogr. 20, 602–605.

Cunliffe, M., Schäfer, H., Harrison, E., Cleave, S., Upstill-Goddard, R., Murrell, J.C., 2008. Phylogenetic and functional gene analysis of the bacterial and archaeal communities associated with the surface microlayer of an estuary. ISME 2, 776-789.

Cunliffe, M., Murrell, J.C., 2009. The sea surface microlayer is a gelatinous biofilm. ISME 3, 1001-1003.

Cunliffe, M., Harrison, E., Salter, M., Schäfer, H., Upstill-Goddard, R.C., Murrell, J.C., 2009a. Comparison and validation of sampling strategies for the molecular microbial analysis of surface microlayers. Aquat. Microb. Ecol. 57, 69-7.

Cunliffe, M., Harrison, E., Salter, M., Schafer, H., Upstill-Goddard, R.C., Murrell, J.C., 2009. Comparison and validation of sampling strategies for the molecular microbial ecological analysis of surface microlayers. Aquat. Microb. Ecol. 57, 69–77.

Cunliffe, M., Upstill-Goddard, R.C., Murrell, J.C., 2011. Microbiology of aquatic surface microlayers. FEMS Microbiol. Rev. 35, 233-246.

Cunliffe, M., Engel, A., Frka, S., Gašparovic, B., Guitart, C., Murrell, J. C., Salter, M., Stolle, C., Upstill-Goddard, R., Wurl, O., 2013. What is the sea surface microlayer? Towards a unified physical, chemical and biological paradigm of the air-ocean interface. Prog. Oceanogr. 109, 104-116.

Cutter, G.A., Bruland, K.W., 2012. Rapid and noncontaminating sampling system for trace elements in global ocean surveys. Limnol. Oceanogr.-Meth. 10, 425-436.

Danos, S.C., Maki, J.S., Remsen, C.C. 1983. Stratification of microorganisms and nutrients in the surface microlayer of small freshwater ponds. Hydrobiol. 98, 193–202.

Daumas, R.A., Laborde, P.L., Marty, J.C. Saliot, A., 1976. Influence of sampling method on the chemical composition of water surface film. Limnol. Oceanogr. 21, 319-326.

David, P.M., 1965. The neuston net. A device for sampling the surface fauna of the ocean. J. Mar. Biol. Assoc. UK 45, 313–320.

De Baar, H.J.W., Timmermans, K.R., Laana, P., De Porto, H.H., Ober, S., Blom, J.J., Bakker, M.C., Schilling, J., Sarthou, G., Smit, M.G., Klunder, M., 2008. Titan: a new facility for ultraclean sampling of trace elements and isotopes in the deep oceans in the international Geotraces program. Mar. Chem. 11, 4-21.

de Boyer Montégut, C., Mignot, J., Lazar, A., Cravatte, S., 2007 Control of salinity on the mixed layer depth in the world ocean: 1. General description. J. Geophys. Res., 112(C06011), doi:10.1029/2006JC003953.

Dickey, T., Banner, M.L., Bhandari, P., Boyd, T., Carvalho, L., Chang, G., et al., 2012. Introduction to special section on recent advances in the study of optical variability in the near-surface and upper ocean. J. Geophys. Res. 117, C00H20.

Dietz, A.S., Albright, L.J., Tuominen, T. 1976. Heterotrophical activities of bacterioneuston and bacterioplankton. Can. J. Microbiol. 22, 1699–1709.

DiGiacomo, P.M., Washburn L., Holt, B., Burton, H. Jones, C., 2004. Coastal pollution hazards in southern California observed by SAR imagery: stormwater plumes, wastewater plumes, and natural hydrocarbon seeps. Mar. Pollut. Bull. 49, 1013–1024.

Dörfler H.-D., 2002. Grenzflächen und kolloid-disperse Systeme. Springer, Berlin.

Donan, C.J., Minnett, P.J., Gentemann, C., Nightingale, T.J., Barton, I.J., Ward, B., Murray, M.J., 2002. Toward improved validation of satellite sea surface skin temperature measurements for climate research. J. Climate 15, 353-369.

Doyle, M.J., Rugen, W.C., Brodeur, R.D., 1994. Neustonic ichthyoplankton in the western Gulf of Alaska during spring. Fish. B-NOAA 93, 231–253.

Drennan, W.M., Donelan, M.A., Terray, E.A., Katsaros, K.B., 1996. Oceanic Turbulence Dissipation Measurements in SWADE. J. Phys. Oceanogr. 26, 808-815.

Ebinghaus, R., Xie, Z., 2006. Occurrence and air/sea-exchange of novel organic pollutants in the marine environment. J. Phys. IV France 139, 211-237.

Ebling, A.M.; Landing, W.M., 2014. Residence times of trace metals in the sea surface microlayer. 2014 Ocean Sciences Meeting, Honolulu, HI, Abstract 204.

Edson, J.B., Fairall, C.W., 1998. Similarity relationships in the marine atmospheric surface layer for terms in TKE and scalar variance budgets. J. Atmos. Sci. 55, 2311-2328.

Edson, J.B., Hinton, A.A., Prada, K.E., Hare, J.E., Fairall, C.W., 1998. Direct covariance flux estimates from mobile platforms at sea. J. Atmos. Oceanic Tech. 15, 547 - 562.

Edson, J. B., V. Jampana, R. A. Weller, S. Bigorre, A. J. Plueddemann, C. W. Fairall, S. Miller, L. Mahrt, D. Vickers, and H. Hersbach, 2013. On the exchange of momentum over the open ocean, J. Phys. Oceanogr., 43, 1589-1610.

Ekau, W., Westhaus-Ekau, P., 1996, Ichthyoplankton distribution and community structure. In: Ekau, W., Knoppers, B. (eds), JOPS-II: Sedimentation processes and Productivity in the Continental Shelf Waters off East and Northeast Brazil. und Produktivität in den Gewässern des Kontinentalschelfs vor Ost- und Nordostbrasilien. Cruise Report and First Results, BMFT 03F0144A.

Estep, K.W., Maki, J.S., Danos, S.C., Remsen, C.C., 1985. The retrieval of material from the surface micro layer with screen and plate samplers and its implications for partitioning of material within the micro layer. Freshwater Biol. 15, 15-19.

Fairall, C. W., E. F. Bradley, J. E. Hare, A. A. Grachev, and J. B. Edson, 2003. Bulk parameterization of air-sea fluxes: Updates and verification for the COARE algorithm, J. Climate, 16, 571-591.

Fairall, C. W., E. F. Bradley, D. P. Rogers, J. B. Edson, and G. S. Young, 1996. Bulk parameterization of air-sea fluxes for Tropical Ocean Global Atmosphere Coupled Ocean Atmosphere Response Experiment, J. Geophys. Res., 101(C2), 3747-3764.

Falkowska, L., 1999a. Sea surface microlayer: a field evaluation of teflon plate, glass plate and screen sampling techniques. Part 1. Thickness of microlayer samples and relation to wind speed. Oceanol. Acta 41, 211–221.

Falkowska, L., 1999b. Sea surface microlayer: a field evaluation of teflon plate, glass plate and screen sampling techniques. Part 2. Dissolved and suspended matter. Oceanol. Acta 41, 223–240.

Flores, A.A., Cruz, J., Paula, J., 2002. Temporal and spatial patterns of settlement of brachyuran crab megalopae at a rocky coast in Central Portugal. Mar. Ecol. Prog. Ser. 229, 207–220.

Franklin, M.P., McDonald, I.R., Bourne, D.G., Owens, N.J.P., Upstill-Goddard, R.C., Murrell, J.C., 2005. Bacterial diversity in the bacterioneuston (sea surface microlayer): the bacterioneuston through the looking glass. Environ. Microbiol. 7, 723–736.

Frew, N.M., Nelson, R.K., 1992a. Isolation of marine microlayer film surfactants for ex–situ study of their surface physical and chemical properties. J. Geophys. Res. 97, 5281–5290.

Frew N.M., Nelson R.K., 1992b. Scaling of marine microlayer film surface pressure-area isotherms using chemical attributes. J. Geophys. Res. 97, 5291-5300.

Frew, N.M., Nelson, R.K., 1999. Spatial mapping of sea surface microlayer surfactant concentration and composition. In: Stein, T.I. (ed) Proceedings of the 1999 International Geoscience and Remote Sensing Symposium, IEEE Publications, Piscataway, pp. 1472-1474.

Friederich, G.E., Codispoti, L.A., 1987. An analysis of continuous vertical nutrient profiles taken during a cold-anomaly off Peru. Deep-Sea Res. Part A 34, 1049-1065.

Frka S., Pogorzelski S., Kozarac Z. and Ćosović B., 2012. Physicochemical signatures of naturals films from middle Adriatic stations. J. Phys. Chem. A 116, 6552-6559.

García–Flor, N, Guitart, C., Bodineau, L., Dachs, J., Bayona, J.M., Albaigés, J., 2005a. Comparison of sampling devices for the determination of polychlorinated biphenyls in the sea surface microlayer. Mar. Environ. Res. 59, 255–275.

García-Flor, N., Guitart, C., Abalos, M., Dachs, J., Bayona, J.M., Albaigés, J., 2005b. Enrichment of organochlorine contaminants in the sea surface microlayer in the NW Mediterranean. An organic carbon driven process. Mar. Chem. 96, 331–346.

Garrett, W.D., 1965. Collection of slick-forming materials from the sea surface. Limnol. Oceanogr. 10, 602–605.

Garrett, W.D., 1974. Comments on "Laboratory comparisons of four surface microlayer samplers". Limnol. Oceanogr. 19, 166-167.

Garrett, W.D., Duce, R.A., 1980. Surface microlayer samplers. In: Dobson F, Hasse L, Davis R (eds) Air–sea interaction. Plenum, New York, p 471–490.

Gasol, J.M., Del Giorgio, P.A., 2000. Using flow cytometry for counting natural planktonic bacteria and understanding the structure of planktonic bacterial communities. Sci. Mar. 64 (2), 197-224.

Gašparović, B., Plavšić, M., Ćosović, B., Saliot, A., 2007. Organic matter characterization in the sea surface microlayers in the subarctic Norwegian fjords region. Mar. Chem. 105, 1-14.

GESAMP, 1995. The Sea-Surface Microlayer and its Role in Global Change. Reports and Studies No. 59. WMO.

Gever, J.R, Mabury, S.A., Crosby, D.G., 1993. Rice field surface microlayers: Collection, composition and pesticide enrichment Environ. Toxic. Chem. 115, 1676-1682.

Grasshoff, K., Kremling, K., Ehrhardt, M. (eds.), 1999. Methods of seawater analysis", 3rd edition, Verlag Chemie, Weinheim, Germany

Godfrey, J.S., Lindstrom, E.J., 1989, The heat budget of the equatorial Western Pacific surface mixed layer. J. Geophys. Res. 94(C6), 8007-8017.

Guitart, C., García-Flor, N., Dachs, J., Bayona, J.M., Albaigés, J., 2004. Evaluation of sampling devices for the determination of polycyclic aromatic hydrocarbons in surface microlayer coastal waters. Mar. Pollut. Bull. 48, 961–968.

Guitart, C., García-Flor, N., Bayona, J.M., Albaigés, J., 2007. Occurrence and fate of polycyclic aromatic hydrocarbons in the coastal surface microlayer. Mar. Pollut. Bull. 54, 186–194.

Gustafsson, O., Andersson, P., Axelman, J., Bucheli, T., Komp, P., McLachlan, M., Sobek, A., Thorngren, J.O., 2005. Observations of the PCB distribution within and in-between ice, snow, ice-rafted debris, ice-interstitial water, and seawater in the Barents Sea marginal ice zone and the North Pole area. Sci Total Environ. 342, 261-279.

Hales, B., Takahashi, T., 2002. The Pumping SeaSoar: A high-resolution seawater sampling platform. J. Atmos. Ocean Tech. 19,1096-1104.

Hamilton, B., Dean, C., Kurata, N., Vella, K., Soloviev, A., Tartar, A., Shivji, M., Perrie, W., Lehner, S., 2014. Surfactants and surfactant associated bacteria in the sea surface microlayer. IGARSS 2014. Quebec City, Canada. Oral paper.

Handler, R. A., I. Savelyev, and M. Lindsey, 2012. Infrared imagery of streak formation in a breaking wave Phys. Fluids, 24, 1070–6631.

Handler, R. A., G. B. Smith, and R. I. Leighton, 2001. The thermal structure of an air-water interface at low wind speeds, Tellus, 53A, 233-244.

Hansard, S.P., Landing, W.M., Measures, C.I., Voelker, B.M. 2009. Dissolved iron(II) in the Pacific Ocean: Measurements from the PO2 and P16N CLIVAR/CO2 repeat hydrography expeditions. Deep Sea Res. I 56, 1117-1129.

Hardy, J.T., 1982. The sea surface microlayer: biology, chemistry and anthropogenic enrichment. Prog. Oceanogr. 11, 307-328.

Hardy, J.T., Apts, C.W., 1984. The sea-surface microlayer - Phytoneuston productivity and effects of atmospheric particulate matter. Mar. Biol. 82, 293–300.

Hardy, J.T., Apts, C.W., Crecelius, E.A., Bloom, N.S., 1985. Sea-surface microlayer metals enrichments in an urban and rural bay. Est. Coast. Shelf Sci. 20, 99-312.

Hardy, J.T., 1997. Biological effects of chemicals in the sea-surface microlayer. In: The sea surface and global change. P.S. Liss and R.A. Duce, Cambridge University Press, 339-370.

Harvey, G.W., 1966. Microlayer collection from the sea surface: A new method and initial results. Limnol. Oceanogr. 11, 608-613.

Harvey, G.W., Burzell, L.A., 1972. A simple microlayer method for small samples. Limnol. Oceanogr. 11, 156–157.

Hatcher, R.F., Parker, B.C., 1974a. Laboratory comparisons of four surface microlayer samplers. Limnol. Oceanogr. 19, 162–165.

Hatcher, R.F., Parker, B.C. 1974b. Microbiological and chemical enrichment of freshwater-surface microlayers relative to the bulk-subsurface water. Can. J. Microbiol. 20, 1051-1057.

Hempel, G., Weikert, H., 1972. The neuston of the subtropical and boreal North-eastern Atlantic Ocean. A review. Mar. Biol. 13, 70–88.

Henocq, C., Boutin, J., Petitcolin, F., Reverdin, G., Arnault, S., Lattes, P., 2010. Vertical variability of near-surface salinity in the tropics: Consequences for L-band radiometer calibration and validation. J. Atmos. Oceanic Technol. 27, 192-209.

Henrichs, S.M., Williams, P.M., 1985. Dissolved and particulate amino acids and carbohydrates in the sea surface microlayer. Mar Chem 17, 141-163.

Holland, K.T., Holman, R.A., Lippmann, T.C., Stanley, J., Plant, N., 1997. Practical use of video imagery in nearshore oceanographic field studies. IEEE J. Ocean. Eng. 22(1), 81-92.

Hühnerfuss, H., 1981a. On the problem of sea surface film sampling: a comparison of 21 microlayer-, 2 multilayer-, and 4 selected subsurface-samplers – Part 1. Sonderduck aus Meerestechnik 12, 137–142.

Hühnerfuss, H., 1981b. On the problem of sea surface film sampling: a comparison of 21 microlayer-, 2 multilayer-, and 4 selected subsurface-samplers – Part 2. Sonderduck aus Meerestechnik 12, 170–173.

Hunter K.A., Liss P.S., 1977. The input of organic material to the oceans: air—sea interactions and the organic chemical composition of the sea surface. Mar. Chem. 5, 361-379.

Hunter K.A., Liss P.S., 1981. Organic sea surface films. In: Marine organic chemistry. E. K. Duursma and R. Dawson (eds.), Elsevier-Amsterdam, 259-298.

Hunter, C., Gordon, R.M., Fitzwater, S.E., Coale, K.H. 1996. A rosette system for the collection of trace metal clean seawater. Limnol. Oceanogr. 41, 1367-1372.

IOC, International Oceanographic Commission, 1985. Procedure for sampling the sea-surface microlayer. Report no. 15, UNESCO, Paris.

International A. Standard Specification for Woven Wire Test Sieve Cloth and Test Sieves. 2009.

Jarvis, N.L., 1967. Adsorption of surface active material at the air–sea interface. Limnol. Oceanogr. 12, 213–221.

Jarvis, N.L., Garrett, W.D., Scheiman, M.A., Timmons, C.O., 1967. Surface chemical characterization of surface active material in seawater. Linmol. Oceanogr. 12, 88–96.

John, H.-C., Mohrholz, V., Lutjeharms, J., 2001. Cross-front hydrography and fish larval distribution at the Angola–Benguela Frontal Zone. J. Mar. Sys. 28, 91–111.

Joux, F., Agogue, H., Obernosterer, I., Dupuy, C., Reinthaler, T., Herndl, G.J., Lebaron, P., 2006. Microbial community structure in the sea surface microlayer at two contrasting coastal sites in the northwestern Mediterranean Sea. Aquat. Microb. Ecol. 42:91-104.

Kattner, G., Nagel, K., Brockmann, U.H., Hammer, K.D., Eberlein, K., 1983. Composition of natural surface films in the North Sea. In: North Sea Dynamics. Sündermann, J., Lenz, W. (eds.). Springer, Berlin, pp. 662-670.

King, L.R., Smith, B.A., Kellogg, R.L., Perry, E.S., 1981. Comparison of ichthyoplankton collected with a pump and stationary plankton net in a power plant discharge canal. In: Issues associated with impact assessment. L.D. Jensen, ed., Proceedings of the Fifth National Workshop on Entrainment and Impingement. E.A. Communications, Melville, N.Y., p 267-275.

Kjelleberg, S., Stenstrom, T.A., Odham, G., 1979. Comparative study of different hydrophobic devices for sampling lipid surface films and adherent microorganisms. Mar. Biol. 53, 21–25.

Knap, A.H., Burns, K.A., Dawson, R., Ehrhardt, M., Palmork, K.H. 1986. Dissolved/dispersed hydrocarbons, tar balls and the surface microlayer: experiences from and IOC/UNEP Workshop in Bermuda. Mar. Pollut. Bull. 17, 313–319.

Kurata, N., Vella, K., Tartar, A., Matt, S., Shivji, M., Perrie, W., Soloviev, A., 2012. Surfactant-associated bacteria in the sea surface microlayer and their effect on remote sensing technology. AGU Fall Meeting 2012. San Francisco.

Kuznetsova, M.R., Lee, C. 2001. Enhanced extracellular enzymatic hydrolysis in the sea surface microlayer. Mar. Chem. 73, 319–322.

Kuznetsova, M., Lee, C., Aller, J., Frew, N.M., 2004. Enrichment of amino acids in the sea-surface microlayers at coastal and open ocean sites in the north Atlantic ocean. Limnol. Oceanogr. 49, 1605-1619.

Kuznetsova, M., Lee, C., Aller, J., 2005. Characterization of the proteinaceous matter in marine aerosols. Mar. Chem. 96, 359-377.

Landing, W.M., Burnett, W.C., Lyons, W.B., Orem, W.H., 1991. Nutrient cycling and the biogeochemistry of manganese, iron, and zinc in Jellyfish Lake, Palau. Limnol. Oceanogr. 36, 515-525.

Laß, K., Kleber, J., Friedrichs, G., 2010. Vibrational sum–frequency generation as a probe for composition, chemical reactivity, and film formation dynamics of the sea surface nanolayer. Limnol. Oceanogr. Meth. 8, 216–228.

Latif, M.T., Brimblecombe, P., 2004. Surfactants in atmospheric aerosols. Environ. Sci. Technol. 38, 6501-6506.

Leal, M.C., Sá, C., Nordez, S., Brotas, V., Paula, J., 2009. Distribution and vertical dynamics of planktonic communities at Sofala Bank, Mozambique. Estuar. Coastal Shelf S. 84, 605-616.

Leal, M.C., Pereira, T.C., Brotas, V., Paula, J., 2010. Vertical migration of gold-spot herring (Herklotsichthys quadrimaculatus) larvae on Sofala Bank, Mozambique. Western Indian Ocean J. Mar. Sci. 9, 175-183.

Lechtenfeld, O.J., Koch, B.P., Gašparović, B., Frka, S., Witt, M., Kattner, G., 2013. The influence of salinity on the molecular and optical properties of surface microlayers in a karstic estuary. Mar. Chem. 150, 25-38.

Lessa, R.P., Mafalda, P., Advincula, R., Lucchesi, R.B., Bezerra, J.L., Vaske, T., Hellebrandt, D., 1999. Distribution and abundance of ichthyoneuston at seamounts and islands off North-Eastern Brazil. Arch. Fish. Mar. Res. 47, 239–252.

Levich, V.G., 1962. Physicochemical hydrodynamics. Prentice Hall International.

Lindroos, A., Szabo, H.M., Nikinmaa, M., Leskinen, P., 2011. Comparison of sea surface microlayer and subsurface water bacterial communities in the Baltic Sea. Aquat. Microb. Ecol. 65, 29-42.

Lindsay, J.A., Radle, E.R., Wang, J.C.S., 1978. A supplemental sampling method for estuarine ichthyoplankton with emphasis on the atherinidae. Estuaries 1, 61–64.

Liss, P.S., Duce, R.A., 1997. The Sea Surface and Global Change, Cambridge: Univ. Press.

Lim, L., Wurl, O., Karuppiah, S., Obbard, J.P., 2007. Atmospheric wet deposition of PAHs to the sea-surface microlayer. Mar. Pollut. Bull. 54, 1212-1219.

Loeb, G.I., Neihof, R.A., 1975. Marine conditioning films. In: Applied Chemistry of Protein Interfaces. R.E. Baier (ed). ACS Adv. Chem. Ser., p. 319–335.

Loeb, G.I., Neihof, R.A., 1977. Adsorption of an organic film at the platinum–sea water interface. J. Mar. Res. 35, 283–291.

Löscher, B.M., De Jong, J.T.M., De Baar, H.J.W., 1998. The distribution and preferential uptake of cadmium at 6°W in the Southern Ocean. Mar. Chem. 62, 259-286.

MacIntyre, F., 1974. The top millimeter of the ocean. Scientif. Am. 230, 62-77.

Mackie, P.R., Whittle, K.J., Hardy, R., 1974. Hydrocarbons in the marine environment: I. n–alkanes in the firth of clyde. Estuar. Coastal Mar. Sci. 2, 359–374.

Maki, J.S., 1993. The air-water interface as an “extreme” environment, In: Aquatic Microbiology: An Ecological Approach. T.E. Ford (ed.), Cambridge Blackwell Scientific Publications, Inc, p. 409-439.

Manley, J.E., 1997. Development of the autonomous surface craft ”ACES”. In: Proc. of Oceans’97. Vol. 2. pp. 827–832.

Manley, J.E., Marsh, A., Cornforth, W., Wiseman, C., 2000. Evolution of the autonomous surface craft AutoCat. In: Proc. of Oceans’00. Vol. 1. pp. 403–408.

Marić, D., Frka, S., Godrijan, J., Tomažić, I., Penezić, A., Djakovac, T., Vojvodić, V., Precali, R., Gašparović, B., 2013. Organic matter production during late summer-winter period in a temperate sea. Cont. Shelf Res. 55, 52-65.

McGillis, W.R., Edson, J.B., Zappa, C.J., Ware, J.D., McKenna, S.P., Terray, E.A., Hare, J.E., Fairall, C.W., Drennan, W., Donelan, M., DeGrandpre, M.D., Wanninkhof, R., Feely, R.A., 2004. Air-sea CO_2 exchange in the equatorial Pacific. J. Geophys. Res. 109, doi:10.1029/2003JC002256.

Measures, C.I., Landing, W.M., Brown, M.T., Buck, C.S., 2008a. A commercially available rosette system for trace metal–clean sampling. Limnol. Oceanogr.-Meth. 6, 384-394.

Measures, C.I., Landing, W.M., Brown, M.T., Buck, C.S., 2008b. High-resolution Al and Fe data from the Atlantic Ocean CLIVAR-CO2 Repeat Hydrography A16N transect: Extensive linkages between atmospheric dust and upper ocean geochemistry. Global Biogeochem. Cycles 22, GB1005.

Melville, W. K., R. Shear, and F. Veron, 1998. Laboratory measurements of the generation and evolution of Langmuir circulations, Journal of Fluid Mechanics, 364, 31-58.

Miller, J.M., 1973. A quantitative push-net system for transect studies of larval fish and macrozooplankton. Limnol. Oceanogr. 18, 175–178.

Milne, A., Landing, W., Bizimis, M., Morton, P., 2010. Determination of Mn, Fe, Co, Ni, Cu, Zn, Cd and Pb in seawater using high resolution magnetic sector inductively coupled mass spectrometry (HR-ICP-MS). Anal. Chim. Acta 665, 200-207.

Momzikoff, A., Brinis, A., Dallot, S., Gondry, G., Saliot, A., Lebaron, P., 2004. Field study of the chemical characterization of the upper ocean surface using various samplers. Limnol. Oceanogr.- Meth. 2, 374–386.

Morrison, A.T., Billings, J.D., Doherty, K.W., 2000. The McLane WTS-LV: a large volume, high accuracy, oceanographic sampling pump. OCEANS 2000 MTS/IEEE Conference and Exhibition 2, 847-852.

Moum, J.N., Szoeke, S.P.d., Smyth, W.D., Edson, J.B., DeWitt, H.L., Moulin, A.J., Thompson, E.J., Zappa, C.J., Rutledge, S.A., Johnson, R.H., Fairall, C.W., 2014. Air-sea interactions from the westerly wind bursts during the November 2011 MJO in the Indian Ocean. Bull. Amer. Meteor. Soc. doi:10.1175/BAMS-D-1112-00225.00221.

Münster, U., Heikkinen, E., Knulst, J., 1997. Nutrient composition, microbial biomass and activity at the air-water interface of small boreal forest lakes. Hydrobiol. 363, 261-270.

Murakami, M., Nishikoori, H., Sakai, H., Oguma, K., Takada, H., Takizawa, S., 2013. Formation of perfluorinated surfactants from precursors by indigenous microorganisms in groundwater. Chemosphere. 93, 140-145.

Naumann, E., 1917. Über das Neuston des Süßwassers. Biol. Zentralblatt 37, 98–106.

Neihof, R.A., Loeb, G.I., 1972. Surface charge of particulate matter in seawater. Limnol. Oceanogr. 17, 7–16.

Neihof, R.A., Loeb, G.I., 1974. Dissolved organic matter in seawater and the electric charge of immersed surface. J. Mar. Res. 32, 5–12.

Norkrans, B., 1980. Surface microlayers in aquatic environments. Adv. Microbiol. Ecol. 4, 51-85.

Obernosterer, I., Catala, P., Reinthaler, T., Herndl, G.J., Lebaron, P., 2005. Enhanced heterotrophic activity in the surface microlayer of the Mediterranean Sea. Aquat. Microb. Ecol. 39, 293-302.

Orellana, M.V., Matrai, P.A., Leck, C., Rauschenberg, C.D., Lee, A.M., Coz, E., 2011. Marine microgels as a source of cloud condensation nuclei in the high Arctic. PNAS 108, 13612–13617.

Orton, P.M., Zappa, C.J., McGillis, W.R., 2010. An autonomous self-orienting catamaran (SOCa) for measuring air-water fluxes and forcing, paper presented at The 6th International Symposium on Gas Transfer at Water Surfaces, Kyoto University Press, Kyoto, Japan.

Petrick, G., Schulz-Bull, D.E., Martens, V., Scholz, K., Duinker, J.C., 1996. An in-situ filtration/extraction system for the recovery of trace organics in solution and on particles – tested in deep ocean water. Mar. Chem. 54, 97-105.

Pinxteren, V.M., Müller, C., Iinuma, Y., Stolle, C., Herrmann, H., 2012. Chemical characterization of dissolved organic compounds from coastal sea surface microlayers (Baltic Sea, Germany). Environ. Sci. Tech. 46, 10455-10462.

Planquette, H., Sherrell, R.M., 2012. Sampling for particulate trace element determination using water sampling bottles: methodology and comparison to in situ pumps. Limnol. Oceanogr. Meth. 10, 367-388.

Pogorzelski, S.J., Kogut A.D., 2003. Structural and thermodynamic signatures of marine microlayer surfactant films. J. Sea Res. 49, 347-356.

Price, J.F., Weller, R.A., Pinkel, R. 1986. Diurnal cycling: observations and models of the upper ocean response to diurnal heating, cooling, and wind mixing. J. Geophys. Res. 91(C7), 8411-8427.

Price, N.M., Harrison, P.J., Landry, M.R., Azam, F., Hall, K.J.F., 1986. Toxic effects of latex and tygon tubing on marine phytoplancton, zooplankton and bacteria. Mar. Ecol. Prog. Ser. 34, 41-49.

Prytherch, J., Farrar, J.T., Weller, R.A., 2013. Moored surface buoy observations of the diurnal warm layer. J. Geophys. Res. Oceans 118, doi:10.1002/jgrc.20360.

Queiroga, H., Cruz, T., Santos dos, A., Dubert, J., González-Gordillo, J.I., Paula, J., Peliz, Á., Santos, A.M.P., 2007. Oceanographic and behavioural processes affecting invertebrate larval dispersal and supply in the western Iberia upwelling ecosystem. Prog. Oceanogr. 74, 174–191.

Quinn, P.K., Bates, T.S., 2011. The case against climate regulation via oceanic phytoplankton sulphur emissions. Nature 480, 51–56.

Pockels, A., 1891. Surface Tension. Nature 43, 437-439.

Reinthaler, T., Sintes, E., Herndl, G.J. 2008. Dissolved organic matter and bacterial production and respiration in the sea–surface microlayer of the open Atlantic and the western Mediterranean Sea. Limnol. Oceanogr. 53, 122-136.

Romano, J.C., 1996. Sea-surface slick occurrence in the open sea (Mediterranean, Red Sea, Indian Ocean) in relation to wind speed. Deep Sea Res. 43, 411-423

Roslan, R.N., Hanif, N.M., Othman, M.R. et al., 2009. Surfactants in the sea-surface microlayer and their contribution to atmospheric aerosols around coastal areas of the Malaysian peninsula. Mar. Pollut. Bull. 60, 1584-1590.

Russell, L.M., Hawkins, L.N., Frossard, A.A., Quinn, P.K., Bates, T.S., 2010. Carbohydrate-like composition of submicron atmospheric particles and their production from ocean bubble bursting. PNAS 107, 6652–6657.

Santos, A.M.P., 2006. Vertical distribution of the European sardine (Sardina pilchardus) larvae and its implications for their survival. J. Plankton Res. 28, 523–532.

Salter, M.E., Upstill-Goddard, R.C., Nightingale, P.D., Archer, S.D., Blomquist, B., Ho, T., Huebert, B., Schlosser, P., Yang, M., 2011. Impact of an artificial surfactant release on air–sea gas exchange during DOGEE II. J. Geophys. Res. 116, C11016.

Schaule, B.K., Patterson, C.C., 1981. Lead concentrations in the northeast pacific-Evidence for global anthropogenic perturbations. Earth Planet. Sci. Lett. 54, 97-116.

Schlüssel, P., Emery, W.J., Grassl, H., Mammen, T., 1990. On the Bulk-skin temperature difference and its impact on satellite remote sensing of sea surface temperature. J. Geophys. Res. 95 (C8), 13341-13356.

Schneider–Zapp, K., Salter, M.E., Mann, P.J., Upstill–Goddard, R.C. 2013. Technical Note: Comparison of storage strategies for surface microlayer samples. Biogeosci. 10, 4927–4936.

Scribe, P., Fillaux, J., Laureillard, J., Denant, V., Saliot, A., 1991. Fatty acids as biomarkers of planktonic inputs in the stratified estuary of the Krka River, Adriatic Sea: relationship with pigments. Mar. Chem. 32, 299-312.

Shinki, M., Wendeberg, M., Vagle, S., Cullen, J.T., Hore, D.K., 2012. Characterization of adsorbed microlayer thickness on an oceanic glass plate sampler. Limnol. Oceanogr. Meth. 10, 728-735.

Sieburth, J.McN., 1979. Sea Microbes. Oxford University Press, New York.

Skjoldal, H.R., Wiebe, P.H., Postel, L., Knutsen, T., Kaartvedt, S., Sameoto, D.D. (2013) Intercomparison of zooplankton (net) sampling systems: Results from the ICES/GLOBEC sea-going workshop. Prog. Oceanogr. 108, 1–42

Smith, P.E., Counts, R.C., Clutter, R.I., 1968. Changes in filtering efficiency of plankton nets due to clogging under tow. ICES J. Mar. Sci. 32, 232–248.

Smith, S.L., Madhupratap, M., 2005. Mesozooplankton of the Arabian Sea: Patterns influenced by seasons, upwelling, and oxygen concentrations. Prog. Oceanogr. 65, 214–239.

Stadler, D., Schomaker, K., 1977. Beschreibung zweier Probennehmer für die Entnahme von Mikroschichtproben aus der Meeresoberfläche für die Analyse auf chlorierte Kohlenwasserstoffe. Ocean Dynam. 30, 60–67.

Stolle, C., Nagel, K., Labrenz, M., Jürgens, K., 2009. Bacterial activity in the sea-surface microlayer: in situ investigations in the Baltic Sea and the influence of sampling devices. Aquat. Microb. Ecol. 58, 67-78.

Stolle, S., Labrenz, M., Meeske, C., Jürgens, J., 2011. Bacterioneuston Community Structure in the Southern Baltic Sea and Its Dependence on Meteorological Conditions. App. Env. Microb. 77, 3726-3733.

Terray, E.A., Donelan, M.A., Agrawal, Y.C., Drennan, W.N., Kahma, K.K., Williams, I.A.J., Hwang, P.A., Kitaigorodskii, S.A., 1996. Estimates of kinetic energy dissipation under surface waves, J. Phys. Oceanogr. 26, 792-807.

Tsimplis, M.N., 1992. The effect of rain in calming the sea. J. Phys. Oceanogr. 22, 404-412.

Tsyban, A.V., 1971. Marine bacterioneuston. J. Oceanogr. Soc. Japan 27, 56–66.

Turk, D., Zappa, C.J., Meinen, C.S., Christian, J., Ho, D.T., Dickson, A.G., McGillis, W.R., 2010. Rain impacts on CO_2 exchange in the western equatorial Pacific. Geophys. Res. Lett. 37(L23610), doi:10.1029/2010GL045520.

Turner, S.M., Liss, P.S., 1985. Measurements of various sulphur gases in a coastal marine environment. J. Atmos. Chem. 2, 223–232.

UNESCO-IOC, 1975. Report of the CICAR Ichthyoplankton Workshop, Mexico City, 17-24 July 1974. UNESCO Tech. Pap. Mar. Sci. 20, 1–47.

Upstill-Goddard, R.C., Frost, T., Henry, G.R., Franklin, M., Murrell, J.C., Owens, N.J.P., 2003. Bacterioneuston control of air–water methane exchange determined with a laboratory gas exchange tank. Global Biogeochem. Cycles 17, 19.11–19.15.

Upstill-Goddard, R.C., 2006. Air–sea gas exchange in the coastal zone. Estuar. Coastal Shelf S. 70, 388-404.

Van Vleet E.S., Williams, P.M., 1980. Sampling sea surface films: a laboratory evaluation of techniques and collecting materials. Limnol. Oceanogr. 25, 764-770.

Veron, F., W. K. Melville, and L. Lenain, 2008. Infrared techniques for measuring ocean surface processes, J. Atmos. Oceanogr. Technol., 25(2), 307-326.

Veron, F., W. K. Melville, and L. Lenain, 2009. Measurements of ocean surface turbulence and wave–turbulence interactions, Journal of Physical Oceanography, 39(DOI: 10.1175/2009JPO4019.1), 2310-2323.

Veron, F., W. K. Melville, and L. Lenain, 2011. Small scale surface turbulence and its effect on air-sea heat fluxes, J. Phys. Oceanogr., 41(1), 205-220.

Vink, S., Boyle, E.A., Measures, C.I., Yuan, J., 2000. Automated high resolution determination of the trace elements iron and aluminium in the surface ocean using a towed fish coupled to flow injection analysis. Deep Sea Res. Part I 47, 1141-1156.

Ward, B., Wanninkhof, R., Minnett, P.J., Head, M.J., 2004. SkinDeEP: A profiling instrument for upper-decameter sea surface measurements. J. Atmos. Oceanic Technol. 21, 207-222.

Ward, B., T. Fristedt, A. H. Callaghan, G. Sutherland, X. Sanchez, J. Vialard, and A. ten Doeschate, 2014. The Air-Sea Interaction Profiler (ASIP): An Autonomous Upwardly Rising Profiler for Microstructure Measurements in the Upper Ocean, Journal of Atmospheric and Oceanic Technology, doi:10.1175/JTECH-D-14-00010.1.

Wiebe, P.H., Benfield, M.C., 2003. From the Hensen net toward four-dimensional biological oceanography. Prog. Oceanogr. 56, 7–136.

Wurl, O., Obbard, J.P., 2004. A review of pollutants in the sea-surface microlayer (SML): a unique habitat for marine organisms. Mar. Pollut. Bull. 48,1016–1030.

Wurl, O., Obbard, J.P., 2005. Chlorinated pesticides and PCBs in the sea-surface microlayer and seawater samples of Singapore. Mar. Pollut. Bull. 50, 1233-1243.

Wurl, O., Holmes, M., 2008. The gelatinous nature of the sea-surface microlayer. Mar. Chem. 110, 89-

Wurl, O., 2009. Sampling and sample treatments. In: Practical Guidelines for the Analysis of Seawater. Wurl, O. (ed.). CRC Press, Boca Raton, pp. 329-349.

Wurl, O., Sin, T.M., 2009. Analysis of dissolved and particulate organic carbon with the HTCO technique. In: Practical Guidelines for the Analysis of Seawater. Wurl, O. (ed.). CRC Press, Boca Raton, pp. 329-349.

Wurl O., Miller L., Röttgers R., Vagle S., 2009. The distribution and fate of surface-active substances in the sea-surface microlayer and water column. Mar. Chem. 115, 1-9.

Wurl, O., Wurl, E., Miller, L., Johnson, K., Vagle, S., 2011a. Formation and global distribution of sea-surface microlayers. Biogeosci. 8, 121-135.

Wurl, O., Miller, L., Vagle, S., 2011b. Production and fate of transparent exopolymer particles in the ocean. J. Geophys. Res. Oceans 116, C00H13.

Xhoffer, C., Wouters, G., Van Grieken, R., 1992. Characterization of individual particles in the North Sea surface microlayer and underlying seawater: comparison with atmospheric particles. Environ. Sci. Technol. 26, 2151-2162.

Ya, M.-L., Wang, X.-H., Wu, Y.-L., Ye, C.-X., Li, Y.-Y. 2014. Enrichment and partitioning of polycyclic aromatic hydrocarbons in the sea surface microlayer and subsurface water along the coast of Xiamen Island, China. Mar. Poll. Bull. 78, 110-117.

Yang, G.P., Tsunogai, S., 2005. Biogeochemistry of DMS and DMSP in the surface microlayer of the western North Pacific. Deep-Sea Res I. 52, 553-567.

Yang, G.P., Watanabe, S., Tsunogai, S., 2001. Distribution and cycling of dimethylsulfide in surface microlayer and subsurface seawater. Mar. Chem. 76, 137–153.

Zaitsev, Y.P., 1971. Marine neustonology. Jerusalem, Israel Program for Scientific Translations. Available from the U.S. Dept. of Commerce, National Technical Information Service, Springfield, VA, 173-204.

Zaitsev, Y.P., 1997. Neuston of Seas and Oceans. In: The sea surface and global change. P.S. Liss and R.A. Duce (eds), Cambridge University Press, 371-382

Zaitsev, Yu. P., 1959. K metodike sbora pelagicheskoi ikry i lichinok ryb v raionakh morya, ne podverzhennykh znachitel'nomu opresneniyu (Methods of collecting pelagic eggs and larvae of fishes in marine areas not considerably freshened). Zoologicheskii Zhurnal 38(9), 1426 (cited from Zaitsev 1971).

Zaitsev, Yu. P., 1962. Orudiya i metody izucheniya giponeistona (Tools and methods in hyponeuston research). Voprosy Ekologii 104, 107 (cited from Zaitsev 1971).

Zaitsev, Yu. P., 1964. Giponeiston Chernogo morya i ego znachenie (The Black Sea hyponeuston and its significance). Doctoral thesis. Odessa. 1964 (cited from Zaitsev 1971).

Zappa, C.J., Raymond, P.A., Terray, E., McGillis, W.R., 2003. Variation in surface turbulence and the gas transfer velocity over a tidal cycle in a macro-tidal estuary. Estuaries 26(6), 1401-1415.

Zappa, C.J., Asher, W.E., Jessup, A.T., Klinke, J., Long, S.R., 2004. Microbreaking and the enhancement of air-water transfer velocity. J. Geophys. Res. 109(C08S16), doi:10.1029/2003JC001897.

Zappa, C.J., Jessup, A.T., 2005. High resolution airborne infrared measurements of ocean skin temperature. Geosci. Remote Sens. Lett. 2(2), doi:10.1109/LGRS.2004.841629.

Zappa, C.J., McGillis, W.R., Raymond, P.A., Edson, J.B., Hintsa, E.J., Zemmelink, H.J., Dacey, J.W.H., Ho, D.T., 2007. Environmental turbulent mixing controls on the air-water gas exchange in marine and aquatic systems. Geophys. Res. Lett. 34(L10601), doi:10.1029/ 2006GL028790.

Zappa, C.J., Banner, M.L., Schultz, H., Corrada-Emmanuel, A., Wolff, L.B., Yalcin, J., 2008. Retrieval of short ocean wave slope using polarimetric imaging. Meas. Sci. Technol. 19(055503), doi:10.1088/0957-0233/1019/1085/055503.

Zappa, C.J., Ho, D.T., McGillis, W.R., Banner, M.L., Dacey, J.W.H., Bliven, L.F., Ma, B., Nystuen, J., 2009. Rain-induced turbulence and air-sea gas transfer. J. Geophys. Res. Oceans 114(C07009), doi:10.1029/2008JC005008.

Zappa, C.J., Banner, M.L., Gemmrich, J.R., Schultz, H., Morison, R.P., LeBel, D.A., Dickey, T., 2012a. An overview of sea state conditions and air-sea fluxes during RaDyO. J. Geophys. Res. – Oceans 117(C00H19), doi:10.1029/2011JC007336.

Zappa, C.J., Farrar, J.T., Weller, R.A., Straneo, F., Moffat, C.F., 2012b. Observations of upper-ocean turbulence during the VOCALS experiment, Abstract 12420, paper presented at 2012 Ocean Sciences Meeting, AGU, Salt Lake City, UT, 20-25 February.

Zhang, Z., Liu, L., Liu, C., Cai, W., 2003. Studies on the sea surface microlayer II. The layer of sudden change of physical and chemical properties. J. Coll. Interface Sci. 264, 148–159.

Zhang, Y.-P., Yang, G.-P., Lu, X.-L., Ding, H.-B., Zhang, H.-H., 2013. Distributions of dissolved monosaccharides and polysaccharides in the surface microlayer and surface water of the Jiaozhou Bay and its adjacent area. Cont. Shelf Res. 63, 85-93.

Zhou, X., Mopper, K., 1997. Photochemical production of low-molecular-weight carbonyl compounds in seawater and surface microlayer and their air-sea exchange. Mar. Chem. 56, 201-213.